GEOMAR REPORT

GEOMAR

Helmholtz-Zentrum für Ozeanforschung Kiel

RV SONNE
Fahrtbericht / Cruise Report
SO237 Vema-TRANSIT

Bathymetry of the Vema-Fracture Zone
and Puerto Rico TRench and Abyssal AtlaNtic BiodiverSITy Study

Las Palmas (Spain) - Santo Domingo (Dom. Rep.)
14.12.14 - 26.01.15

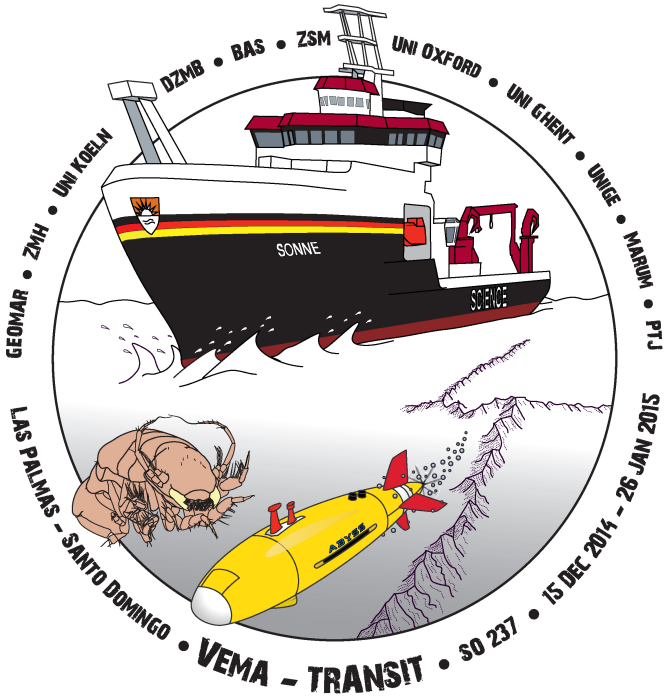

Berichte aus dem GEOMAR
Helmholtz-Zentrum für Ozeanforschung Kiel

Nr. 23 (N. Ser.)

März 2015

GEOMAR

Helmholtz-Zentrum für Ozeanforschung Kiel

RV SONNE
Fahrtbericht / Cruise Report
SO237 Vema-TRANSIT

Bathymetry of the Vema-Fracture Zone
and Puerto Rico TRench and Abyssal AtlaNtic BiodiverSITy Study

Las Palmas (Spain) - Santo Domingo (Dom. Rep.)
14.12.14 - 26.01.15

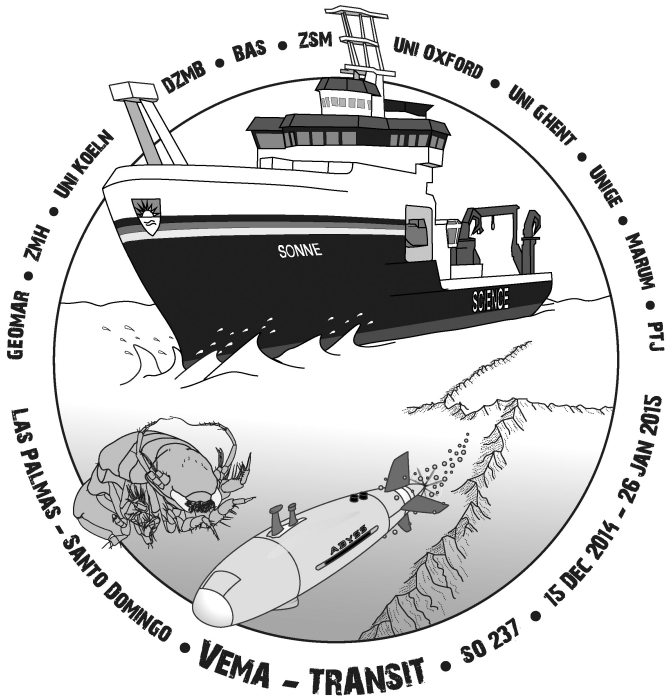

Berichte aus dem GEOMAR
Helmholtz-Zentrum für Ozeanforschung Kiel

Nr. 23 (N. Ser.)

März 2015

ISSN Nr.: 2193-8113

GEOMAR
Helmholtz-Zentrum für Ozeanforschung Kiel

Das GEOMAR Helmholtz-Zentrum für Ozeanforschung Kiel ist Mitglied der Helmholtz-Gemeinschaft Deutscher Forschungszentren e.V.

The GEOMAR Helmholtz Centre for Ocean Research Kiel is a member of the Helmholtz Association of German Research Centres

Herausgeber / Editor:
Colin W. Devey and shipboard scientific party

GEOMAR Report
ISSN Nr. 2193-8113, DOI 10.3289/GEOMAR_REP_NS_23_2015

Helmholtz-Zentrum für Ozeanforschung Kiel / Helmholtz Centre for Ocean Research Kiel
GEOMAR
Dienstgebäude Westufer / West Shore Building
Düsternbrooker Weg 20
D-24105 Kiel
Germany

Helmholtz-Zentrum für Ozeanforschung Kiel / Helmholtz Centre for Ocean Research Kiel
GEOMAR
Dienstgebäude Ostufer / East Shore Building
Wischhofstr. 1-3
D-24148 Kiel
Germany

Tel.: +49 431 600-0
Fax: +49 431 600-2805
www.geomar.de

CONTENTS

1. CRUISE SUMMARY/ZUSAMMENFASSUNG

1.1 German/Deutsch

Die abyssalen Tiefseeebenen stellen > 60% der Erdoberfläche dar, dennoch sind sie kaum erforscht. Wir wissen sehr wenig über das Leben am Meeresboden und darüber wie Hydrosphäre, Biosphäre und Lithosphäre in diesem riesigen Lebensraum interagieren. Im Atlantik charakterisieren vor allem Transformstörungen und Bruchzonen die Bathymetrie des Meeresbodens. Während der SO-237 Expedition wurde einer der größten Bruchzonen des Atlantiks, der "Vema Fracture Zone", untersucht. Die Zusammensetzung der benthischen Gemeinschaften entlang dieses longitudinalen Transektes wurde mittels Greifern und geschleppten Geräten beprobt, die der Megafauna mittels photographischer AUV-Kartierung erfasst. Mit den Ergebnissen soll die Hypothese getestet werden, ob der Mittelatlantische Rücken eine tektonische Isolationsbarriere für die benthischen Arten der abyssalen Tiefseeebenen (westlich und östlich) darstellt. Der Puerto Rico Graben ist sehr viel tiefer als der umgebende West Atlantik. Daher wurden auch dort Proben genommen um zu untersuchen, ob sich die Biodiversität der hadalen Meio-, Makro- und Megafauna durch Isolation von der des abyssalen Atlantiks unterscheidet. Die gewonnenen Daten liefern wertvolle Informationen für den geplanten SFB Transregio " Maturing oceanic plates: Earth's hidden reactors " und stellen die erste vollständige hochaufgelöste bathymetrische Daten entlang einer Bruchzone dar.

1.2 English/Englisch

The abyssal seafloor makes up > 60% of our planet´s surface, it is nevertheless largely unexplored. We know very little about how the processes which created it have varied through time, about life on the deep seafloor or about how the hydrosphere, biosphere and lithosphere interact over this vast area. In the Atlantic, transform faults and fracture zones characterize most of the seafloor bathymetry and the volcanic and tectonic process which create and modify the crust can be deduced from their bathymetric signature. During the cruise SO-237 we surveyed and sampled the entire length of one of the major offsets of the Mid-Atlantic Ridge, the Vema Fracture Zone, looking at a history of plate creation and modification over 120Ma. Variations in benthic communities along this transect will be investigated using samples recovered from corers and towed gear as well as detailed photographic mapping of the benthic megafauna using AUV. The results will be used to test the hypothesis that the Mid-Atlantic Ridge serves as a barrier limiting benthic species distribution in the abyssal basins on both sides of the ridge. The Puerto Rico Trench is much deeper than the surrounding abyssal West Atlantic and so we also took samples there to determine whether the biodiversity of its hadal meio-, macro-, and megabenthic fauna differs from that of the abyssal Atlantic due to isolation of the trench. The cruise yielded important information for the Transregio proposal "Maturing oceanic plates: Earth's hidden reactors" and has provided the first high-resolution bathymetric survey along an entire fracture zone trace and one of the world's best surveyed seafloor features.

2. PARTICIPANTS

2.1 Principle Investigators / leitende WissenschaftlerInnen

Prof. Dr. Colin W. Devey, Geomar Helmholtz Centre for Ocean Research Kiel, Wischhofstr. 1-3, 24148 Kiel, Germany

Prof. Dr. Angelika Brandt, Zoological Museum, University of Hamburg, Martin-Luther-King-Platz 3, 20146 Hamburg, Germany

Prof. Dr. Hartmut Arndt, Zoological Institute, University of Cologne, Zuelpicherstr. 47b, 50674 Köln, Germany

2.2 Scientific party / wissenschaftliche FahrtteilnehmerInnen

Name	Discipline	Institution
Devey, Colin, Prof. Dr.	Marine Geology / Chief Scientist	GEOMAR
Arndt, Hartmut, Prof. Dr.	Marine Microbiology	U. Köln
Augustin, Nico, Dr.	Marine Geology/Bathymetry	GEOMAR
Bober, Simon	Macrofauna	U. HH
Borges, Valeska	Meiofauna	U. HH
Brandt, Angelika, Prof. Dr.	Meiofauna	U. HH
Brenke, Nils, Dr.	EBS Technics	U. HH
Brix-Elsig, Saskia, Dr.	Macrofauna/Isopoda	DZMB, HH
Elsner, Nikolaus	Macrofauna/Isopoda	U. HH
Frutos, Inmaculada, Dr.	Macrofauna/Isopoda	U. HH
Guggolz, Theresa	Macrofauna/Polychaeta	U. HH
Heitland, Nele	Macrofauna/Isopoda	U. HH

Jeuck, Alexandra	Protists/Nanoflagellates	U. Köln
Klischies, Meike	Marine Geology/Bathymetry	GEOMAR
Köhler, Janna	Oceanography	U. HB
Lejzerovicz, Franck	Protists/Foraminifera	U. Geneva
Lins, Lidia	Nematodes	U. Ghent
Linse, Katrin	Macrofauna/Mollusca	BAS
Malytina, Marina	Macrofauna/Isopoda	IBM
Metz, Dirk	Marine Geology/Bathymetry	Oxon
Minzlaff, Ulrike	Macrofauna/Biochemistry	IHF
Praße, Dennis	Microbiology	U. Köln
Palgan, Dominik	Marine Geology/Petrology	GEOMAR
Riehl, Torben	Macrofauna/Isopoda	U. HH
Rothenbeck, Marcel	AUV-Leitung	GEOMAR
Schmidt, Christina	Meiofauna	DZMB, WHV
Schmidt, Christopher	Marine Geology/Pore waters	GEOMAR
Schoenle, Alexandra	Protists/Nanoflagellates	U. Köln
Schultze, Gudrun	Biology Team	PTJ
Schwabe, Enrico	Macrofauna/Mollusca	ZSM Munich
Springer, Tanya	Biology/Data management	U. HH
Steinführer, Anja	AUV-Navigation	GEOMAR
Triebe, Lars	AUV-Technik	GEOMAR
Voltski, Ivan	Protists/Foraminifera	U. Geneva
Walter, Thomas	Öffentlichkeitsarbeit	U. HH.
Wenzlaff, Emanuel	AUV-Technik	GEOMAR
Yeo, Isobel	Marine Geology/Bathymetry	GEOMAR
Zinnkann, Ann-Christine	Macrofauna/Biochemistry	U. HH
Zoeller, Khalhela	Marine Geology/Petrology	U. Ottawa

GEOMAR:	Helmholtz Centre for Ocean Research, Kiel, Germany
U. HH:	Universität Hamburg, Centrum für Naturkunde, Zoologisches Museum Hamburg.
IHF:	Institute for Hydrobiology and Fisheries Research, Hamburg
U. HB:	Institute of Environmental Physics, University of Bremen, Germany
BAS:	British Antarctic Survey, Cambridge, UK
U. Ottawa:	University of Ottawa, Canada
Oxon:	Department of Earth Sciences, University of Oxford, UK
PTJ:	Projektträger Jülich, Warnemünde, Germany
ZSM Munich:	Zoologische Stattssammlung München, Munich, Germany
U. Köln:	Institute of Zoology, University of Cologne, Germany
U. Geneva:	Department of Genetics and Evolution, University of Geneva,Switzerland
DZMB WHV:	German Centre for Marine Biodiversity Research, Senckenberg am Meer, Wilhelmshaven
DZMB HH:	German Centre for Marine Biodiversity Research, Senckenberg am Meer, Hamburg

U. Ghent:	Marine Biology Department, University of Ghent, Belgium
IMB:	A.V. Zhirmunsky Institute of Marine Biology FEB RAS, Vladivostok, Russia

3. NARRATIVE OF THE CRUISE / ABLAUF DER FORSCHUNGSFAHRT

(C. Devey)

The brand new research vessel "Sonne" left Las Palmas for her maiden scientific voyage on 14th December 2014 for a 4-day transit to the working area south of the Cape Verde islands. On Thursday 18.12.14 we left the Cape Verde EEZ and the first scientific data were collected with the ship´s multibeam echo-sounder. The seafloor sampling began on Friday 19.12.14 with successful deployments of the sediment gravity core, the multi-corer and the epibenthos sled. In parallel the deep-diving autonomous underwater vehicle ABYSS was deployed to map the seafloor in high resolution. Following a successful dredge haul in the night from Saturday 20.12.14 to 21.12.14, Sonne then began the first long mapping transect with over 4 days of multibeam measurements, providing the first-ever seafloor maps of the crust between 25° and 31°W along the Vema Fracture Zone. In the afternoon of 25.12.14 the AUV was again deployed, followed by the usual sequence of 3 Multi-corers, a gravity core, two epibenthos-sled deployments and a dredge. The return of the AUV on 27.12. with evidence of an Eh-anomaly 80m above the seafloor led us to carry out one extra gravity core at the position. There then followed the second large mapping block, covering the region 31° - 37°W. On 01.01.15 at 15:00 the first station work at 37°W began with biological sampling as the wind was too strong (Beaufort 7) to deploy the AUV. Following three successful MUC deployments the weather had improved to such an extent that we were able to deploy the AUV for its first photographic mission - this returned 9000 pictures after a 16 hour dive, showing large clumps of sunken Sargassum algae on the seafloor at 5300m. The following epibenthos sleds also contained large amounts of sargassum debris. There then followed a long mapping transit towards the active transform fault region, which we arrived at in the early morning of 06.01.15. During this mapping transit we deployed two APEX floats at 38 and 42°W. Upon arrival in the transform region, preparations began for extensive AUV diving with the deployment of two LBL transponders. During the calibration phase for these transponders the weather worsened significantly and the first AUV deployment in the region where Cannat et al. (1991) found evidence of seafloor clam beds had to be delayed. We completed 6 MUC deployments (3 empty, probably as a result of the poor weather conditions), two EBS, two gravity corers (one empty) and a CTD tow-yo whilst waiting for an improvement in the weather. When this had not materialized by 08.01.15 we continued the mapping transit westward, releasing two more YPEX floats at 45° and 48°W.

The first station on the west of the spreading axis was reached on 11.01.15. The AUV was deployed to map an area of seafloor for the filming of a subsequent EBS deployment. During the AUV dive the EBS was deployed for its first haul. This deployment led to the sled becoming stuck on the bottom, after several hours maneouvring the sled was freed and came to the surface full of round Mn-nodules. A second deployment returned benthic fauna and Mn-crusts. Due to difficulties with the first EBS haul the AUV photo-mapping did not see the EBS trace but did return with 8500 pictures of the seafloor. Three MUC deployments were successful, as was a

gravity corer. The dredge had no bites and returned empty. Late on 12.01.15 we continued the mapping westward and arrived at the second station west of the spreading axis on 13.01.15 in the early evening. Due to shortage of time (caused by the sampling problems during bad weather at the spreading axis) it was decided to only perform EBS and MUC sediment sampling and to try to make a photo-survey of the EBS track using the AUV. This was all successfully achieved and on 15.01.15 we began the 82 hour transit to the Puerto Rico trough at full speed. Details of all sampling areas along the Vema Fracture Zone are shown in Figure 3-1 and Figure 3-2.

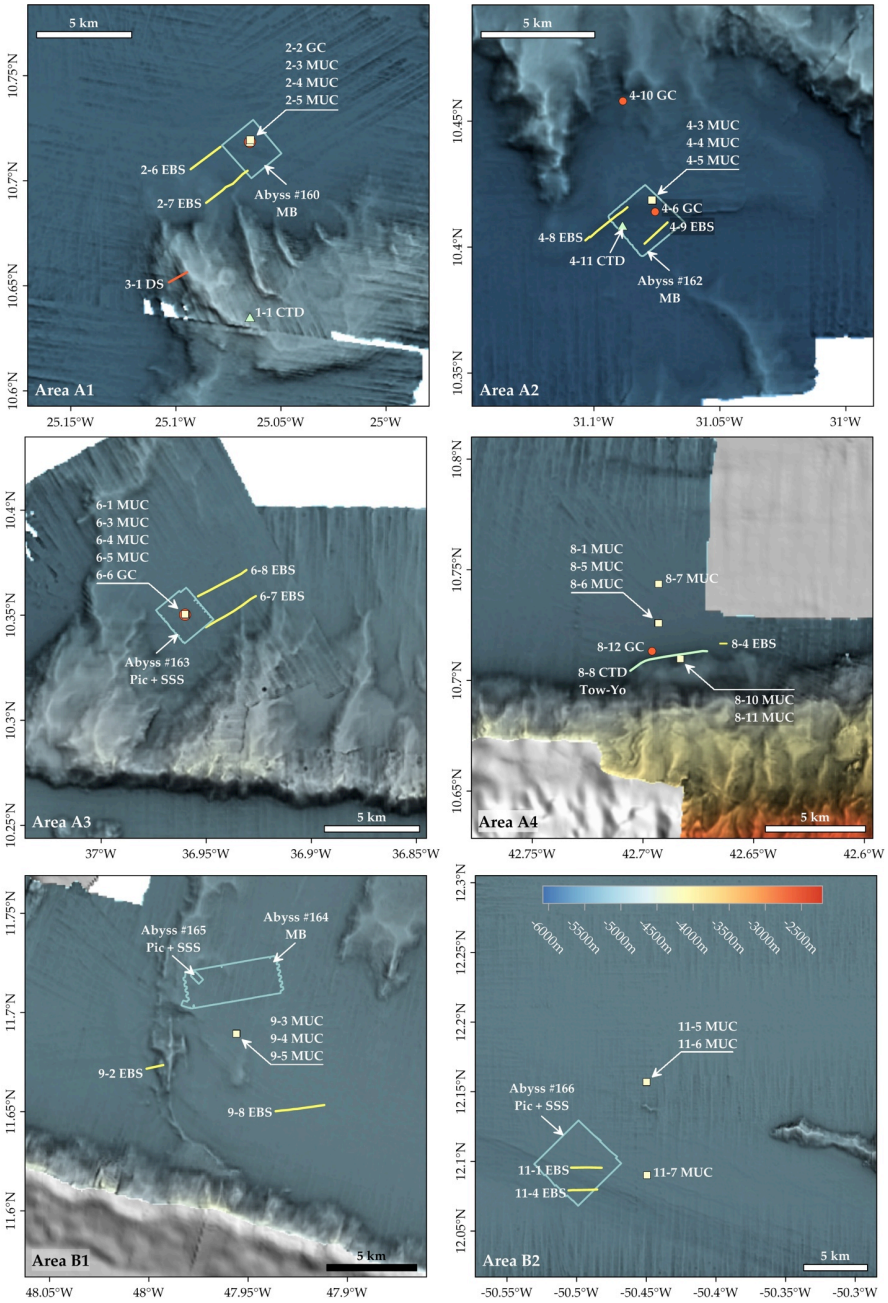

Figure 3-1: Maps of the areas of biological sampling and AUV deployment.

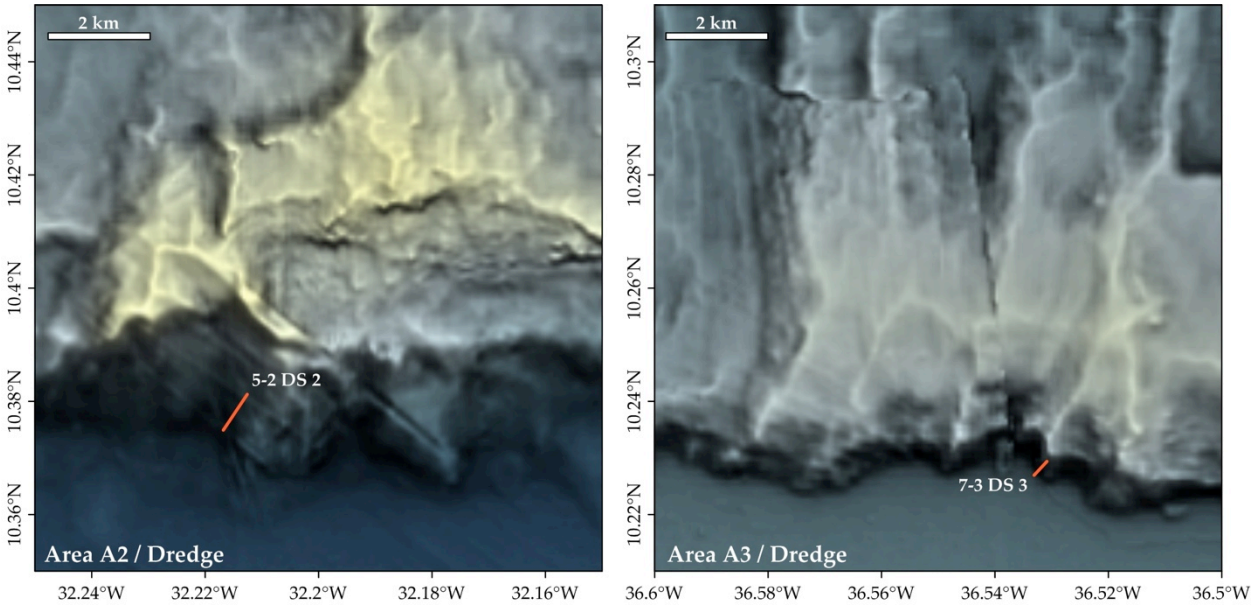

Figure 3-2: Maps of the dredge stations conducted away from the biological sampling spots.

This transit occurred with no major incidents, we arrived on station for the first MUC deployment in 8350m water depth at 20:00 on 18.01.15. At 8290m wire length (60m above bottom) problems with a pulley in the wire system (bolts in the axle had worked loose and broken) meant the station had to be abandoned and the MUC returned to deck at 0,3 m/s (7,5 hours!). The problem was solved within 3 hours by the engineers and the MUC was attempted once more. After 6 hours waiting, it returned empty. Another attempt was similarly fruitless but did return evidence for a very soft and sticky bottom sediment, which we were then able to sample with a subsequent MUC lowered extremely slowly into the sediment. We were able to recover 3 full MUCs then at this station and also deployed the EBS twice at depths of around 8350m, on the first deployment using the full working length of cable available on the ship (11.000m). During this deployment it became clear that the friction winch was at the limit of its lifting capacity and that it began to stall at around 100kN. For this reason, in consultation with the Captain and Chief Engineer, it was decided not to risk dredging at these depths as almost no tension at the seafloor would be available. The second deep station in the Puerto Rico Trough was completed on the evening of 23.01.15 and the ship moved to shallower water (ca. 5000m) for MUC and EBS deployments. These were completed at 15:00 on 25.01.15 at which time the ship began an 17-hour transit to Santo Domingo. The ship tied up in Santo Domingo on 26.01.15 at 08:00.

During the cruise there was a lot of interest from the media and public in the new ship and our work aboard. We carried out many telephone interviews for press and radio and also ran a blog (at www.oceanblogs.net/so-237/). The response to this public outreach effort was large, with many comments and questions appearing on the blog.

4. AIMS OF THE CRUISE / ZIELSETZUNG DER FORSCHUNGSFAHRT

The aim of the Vema-TRANSIT expedition was to survey and sample the Vema Fracture Zone, spanning a whole ocean basin in terms of benthic ecology and a history of plate creation and modification over 120Ma. The cruise had several major goals:

1. Generate a high-resolution map of the entire length of the eastern Vema Fracture Zone and adjacent seafloor to determine crustal structure now and in the past.
2. Determine whether the abyssal microprotists, meio-, macro-, and megabenthic assemblages differ in the western and eastern Atlantic because the topography of the Mid-Atlantic Ridge isolates the fauna on both sides of the ridge.
3. Determine whether the biodiversity of the microprotists, meio-, macro-, and megabenthic hadal fauna of the Puerto Rico Trench differs from that of the abyssal West Atlantic due to depth isolation in the trench.
4. Characterize the zoogrography of the most abundant species along the Vema-TRANSIT and in the Puerto Rico Trench.
5. Perform detailed photographic mapping of the small-scale distribution of benthic megafauna using AUV.
6. Analyze sediments and pore water from seeps detected on the cruise. Multicorer and gravity corer deployments are planned for areas with evidence for chemosymbiotic biota.
7. Measure the intensity of turbulent mixing in the near-bottom waters over a full tidal sequence.

5. AGENDA OF THE CRUISE / PROGRAMM DER FORSCHUNGSFAHRT

All of the goals listed in Chapter 4 were achieved. Some modifications to the working program were necessary during the cruise for the following reasons:

a. The water depths in the Vema Fracture Zone, at around 5800m, were deeper than expected from satellite altimetry so that station times which had been calculated based on 5000m depth in fact were closer to those for 6000m. Time was saved in the working plan by concentrating the mapping effort on the better exposed eastern section of the fracture zone
b. Problems with the US State Dept. server RATS, over which all applications to work in the US EEZ must be made, meant that we moved the Puerto Rico Trough stations to the Dominican Republic area of the Trough. Permission to work in Dominican Republic waters was granted on 02.01.15 thanks to the intense support of the Germany Embasssy staff in Santo Domingo.
c. The microstructure probe was damaged during the first recovery of the AUV and could not be deployed on the subsequent dives. Thanks to the enormous efforts of the WTD on board, the probe was repaired early in 2015.

6. SETTING OF THE WORKING AREA / BESCHREIBUNG DES ARBEITSGEBIETES

The working area can be divided into two main regions, the Vema Fracture Zone and the Puerto Rico trough. Their geographical relationship to one another is visible from Figure 6-1.

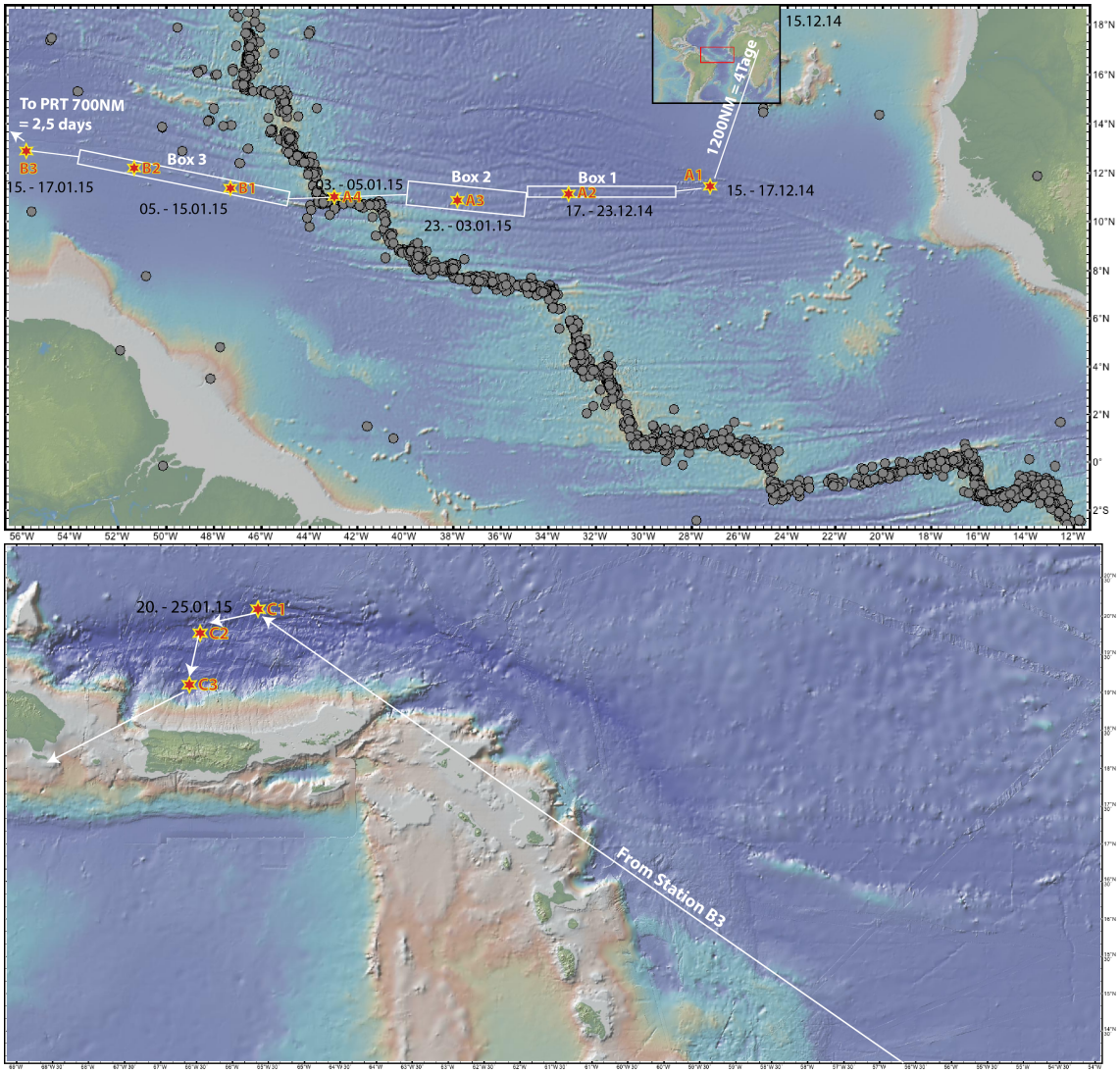

Figure 6-1: The planned cruise track for SO-237, showing the Vema Fracture Zone (upper panel) and the Puerto Rico Trench (lower panel).

The Vema Fracture Zone is the trace of the Vema Transform Fault on the Atlantic seafloor.It is one of the longest fracture zone traces in the Atlantic and covers crustal ages up to >100Ma. Along the walls of the Farcture Zone, crust is exposed representing seafloor ages covering this range. The Puerto Rico Trench is a Transfrom Fault and/or subduction zone segment to the north of the Caribbean arc. It is a relatively young structure which exposes Atlantic lithosphere created over 100Ma ago, providing the possibility to sample crust similar to that seen on the Vema Fracture Zone.

7. WORK DEATILS AND FIRST RESULTS / BESCHREIBUNG DER ARBEITEN IM DETAIL EINSCHLIEßLICH ERSTER ERGEBNISSE

7.1 Near-surface sampling

7.1.1 *Sargassum* community: Do floating algae fuel the deep-sea ecosystems?

(E. Schwabe, H. Arndt, A. Jeuck, U. Minzlaff, D. Prausse, A. Schoenle)

The Sargasso Sea, located within the North Atlantic Subtropical Gyre, is at its southern edge, influenced and defined by the westward directed North Equatorial Current and the north-westward directed Antilles Current. It is a unique ecosystem comprising the accumulated holopelagic brown algae *Sargassum natans* and *S. fluitans* (Laffoley et al. 2011). *Sargassum* patches tentatively identified as *S. fluitans* of varying dimensions, ranging from individual branches to floating mates of several meters, could always be observed during our VEMA Transit expedition, which was conducted within the range of the above mentioned southern boundary system. Being not in the main focus of our expedition, interest on these floating systems was raised due to the detection of isolated branches of *Sargassum* on the seafloor in abyssal and hadal depths.

The importance of organic material either as food source or as habitat for sessile taxa on the ocean's deep-sea floor was highlighted by several authors (e.g. Moore 1963; Grassle and Morse-Porteous 1987). Usually the origin of such organic material is not well-defined, but in the present case we have the possibility to compare the community structures of the surface algae with the material we collected from the underlying abyss and hadal.

We collected *Sargassum* from the surface at each benthic station by means of buckets or by fishing (Table 7-1). Per station we selected a volume of 570 cm³ for a final detailed analysis of meio- and macrofauna. Additional material was used for biochemistry studies (see Section 7.2.7) and for the analysis of unicellular organisms. Prior to fixation of the selected volume in pure 96% ethanol the algae were preliminary examined for mobile micro- and macrofauna.

Observed species were photo-documented (see, e.g., Figure 7-1) and fixed. At a later stage the samples will be examined more precisely in the involved institutes.

Preliminary results of as so far studied volumes indicated the presence of epibiotic bryozoans (genus *Membranipora*), the annelid worm *Spirorbis* sp. at all sampled stations. Associated vagile fauna varied among the stations. The associated gastropod *Litiopa melanostoma* was found at all stations except for SO5/008. However, juveniles and veliger stages of this species were found at the two easternmost stations only. SO5/008 was the only station where we detected two crabs *Portunus sayi* and *Hippolyte* spp. The shrimp was found with heavy infections by bopyrid isopods. The random occurrence of the shrimp *Latreutes fucorum*, the polychaete *Platynereis dumerilli*, the turbellarian *Planocera* cf. *pellucida* and the nudibranch gastropod *Scyllaea pelagica* fits well with the observations of previous studies (e.g. Weis 1968, Fine 1970, Stoner and Greening 1984, Huffard et al. 2014). Among protists associated with floating *Sargassum*, we found representatives of nearly all phylogenetic groups of protists

including bodonids, euglenids, choanoflagellates, ciliates, chrysomonads, bicosoecids, amoebae, foraminiferans, cercozoans, ancyromonads, thaumatomonads and apusozoans.

The vagile macrofauna is obviously unable to survive the sinking of algae to such enormous depths. However, the horizontal distribution of individual taxa might be of interest, especially under the aspect of amphi-atlantic distribution patterns and the resulting question whether a species endures long distance drifting and may contribute to local fauna, as Yeatman (1962) exemplarily demonstrated for harpacticoid copepods. To answer this question we are going to conduct genetic studies on potential guest species among the associated community. In addition, we carried out experiments on the pressure tolerance of the protist community and found several species to survive hydrostatic pressures of up to 400 bar (see Section 7.3.3). Further experiments will be carried out at the University of Cologne by the protistological group.

The vertical distribution of organic matter and the relevance for deep-sea communities will be studied by a comparative analysis of EBS collected deep-sea samples and the floating surface algae, with special focus on the composition of stable isotopes (13 C and 15 N) and fatty acids of the obtained algae and tissue samples of benthic consumers. Earlier observations (e.g. Smith and Hessler 1987, Grassle and Morse-Porteous 1987) already indicated the influence of *Sargassum* on benthic communities by demonstrating an increase of diversity in *Sargassum*-enhanced environments.

Table 7-1: Station data of collected holopelagic Sargassum*. Grey rows indicate stations sampled by means of a bucket and may also contain loosely associated fauna, remaining caught by fishing gear.*

Station	Date	UTC Time	Lat (N)	Long (W)	Water Temp. (°C)	Salinity (‰)	Air Temp. (°C)	Wind direction (deg)	Windspeed (m/s)
SO5/002	19.12.2014	11:32	10°43.118'	25°3.893'	26.5	35.38	25.6	54.7	10.2
SO5/004	26.12.2014	12:16	10°25.114'	31°4.617'	26.8	35.75	26	58.8	6
SO5/004	28.12.2014	16:58	10°24.481'	31°5.318'	27	35.71	25.7	48.5	8.1
SO5/006	03.01.2015	14:54	10°14.161'	36°31.615'	26.5	35.81	25.5	56	10.7
SO5/008	08.01.2015	19:10	10°42.645'	42°41.893'	26.1	35.42	25.8	67.1	12.4
SO5/009	12.01.2015	00:51	11°41.357'	47°57.334'	26.6	35.48	24.6	39.9	13.2
SO5/012	19.01.2015	00:54	19°43.400'	67°8.010'	27	35.58	25.3	15.2	5.9

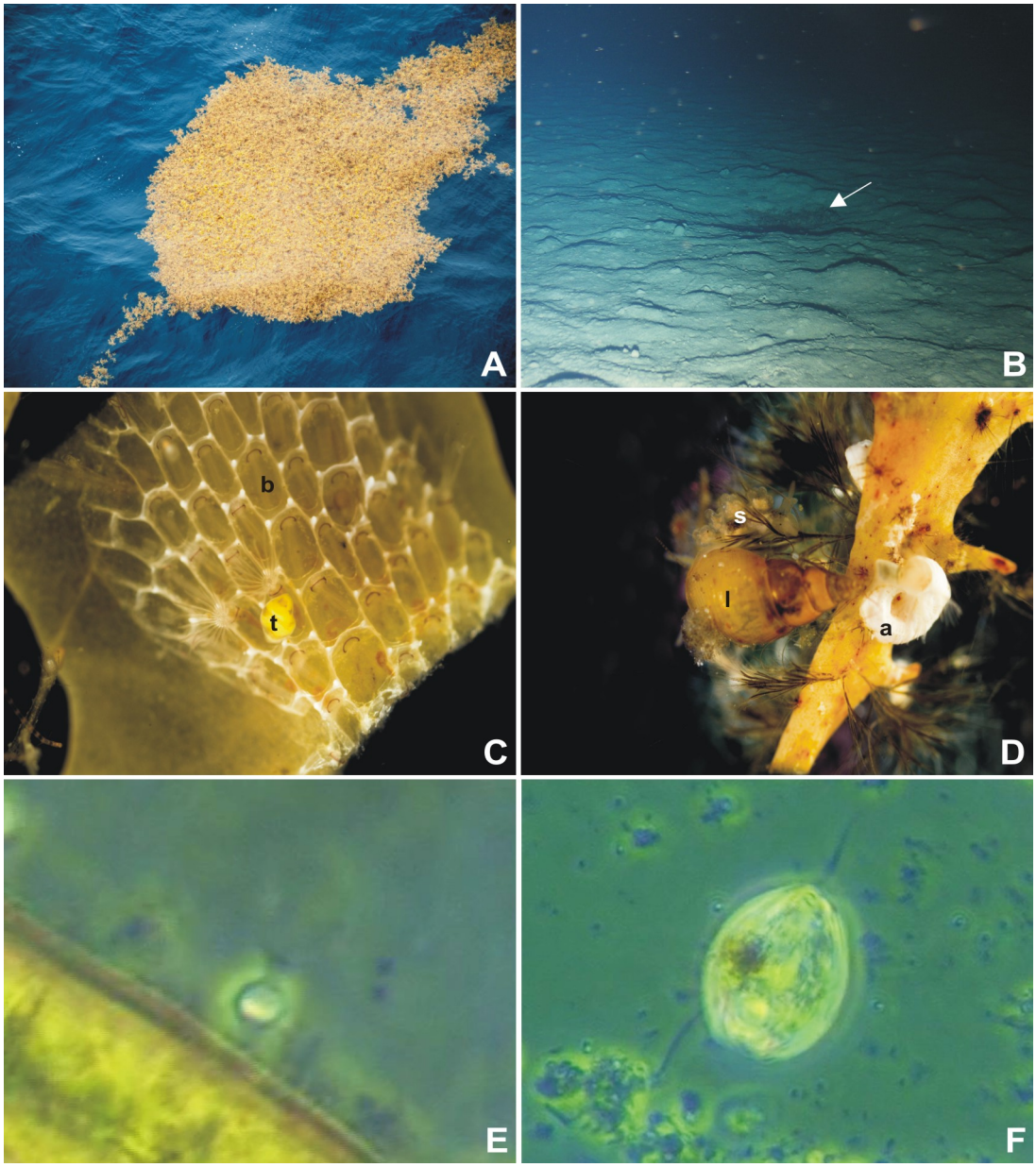

Figure 7-1: A) Floating Sargassum *between Stations SO5/002 and 004, B) accumulated* Sargassum *at seafloor during the EBS station 6-8 (10°22.66'N, 36°55.35'W, 5127 m), C) the mobile turbellarian* Planocera *cf.* pellucida *(t) on the epibiotic bryozoan* Membranipora *sp. (b) at St. SO5/002, D) the epibiotic annelid worm* Spirorbis *sp. (a) and the two gastropods* Litiopa melanostoma *(l) and* Scyllaea pelagica *(s) from the first algae sample at St. SO5/004, E) choanoflagellate* Salpingoeca *from St. SO5/002, F) heterotrophic euglenide flagellate from St. SO5/002. All images not scaled. Photo credits: A, C, D Torben Riehl (Hamburg), B Nils Brenke (Wilhelmshaven).*

7.2 Epibenthos Sled deployments

7.2.1 Camera-epibenthic sledge deployment and preliminary results

(Brandt, A., Bober, S., Brix, Frutos, I., S. Guggolz, T., Heitland, N., Linse, K., Malyutina, M., Minzlaff, U., Riehl, T., Schwabe, E., Zinkann, A.-C.)

7.2.1.1 Objectives:

One of the major objectives for the benthic fauna was to study abundance and species richness (species composition, structure and biodiversity) of the macrofauna at the different abyssal stations across an east-west transect across the Atlantic following the Vema Fracture transform fault crossing the Mid Atlantic Ridge. We were interested to investigate whether the Mid Atlantic Ridge isolates the benthic fauna in the eastern and western abyssal basins. The Vema Fracture transform crossing the Mid Atlantic Ridge could serve as a passage for the migration of organisms from one side of the Mid Atlantic Ridge to the other.

As the Puerto Rico Trench is much deeper than the surrounding abyssal West Atlantic, we also wanted to determine whether the biodiversity of its hadal meio-, macro-, and megabenthic fauna differs from that of the abyssal Atlantic, potentially due to a depth isolation of the trench.

In order to test these hypotheses, we were aimed to

- determine whether the abyssal meio-, macro-, and megabenthic assemblages differ in the western from the eastern Atlantic
- determine whether the biodiversity of the meio-, macro-, and megabenthic hadal fauna of the Puerto Rico Trench differs from that of the abyssal West Atlantic.
- characterize the zoogeography of the most abundant species along the Vema-TRANSIT and in the Puerto Rico Trench.
- analyze on the phylogenetic positions of selected taxa in the Atlantic Ocean abyss and hadal.

Community analyses will be used to describe similarities and differences of selected faunal assemblages and how these assemblages differ with regard to structure and diversity on both sides of the Mid Atlantic Ridge. We plan to compare Bivalvia and Polychaeta which reproduce via larvae and thus have a much better dispersal potential than brooding peracarid crustaceans, such as Isopoda which potentially have a reduced gene flow (Brandt et al., 2007). Within the Isopoda we will analyze a family burrowing in the sediment, the Macrostylidae, as well as a family with swimming capabilities, the Munnopsidae, with regard to their species turnover and population connectivity across the Atlantic Ocean along the Vema Fracture Zone. Statistic and multivariate methods will help to identify if and how far the abyssal communities on both sides of the MAR differ from each other. Linking genetic variability with environmental parameters, such as topographic barriers, depth, geothermal activity, and rock formation, and geographic distance, will provide fascinating clues on speciation processes in the deep sea. Putting hadal species into a phylogenetic and population-genetic context will provide ideas about the age and origin of hadal assemblages as well as their vulnerability. New

species occurring in abundance shall be described and made available for future scientific work in these areas. The new data from the Vema-Fracture Zone shall be compared at species level with the existing global data on the zoogeography of the species which were sampled with the same gear using standardized sampling approaches (e.g. Brandt et al., 2005; Brix et al. 2007; Brenke et al., 2005; Raupach et al., 2007).

7.2.1.2 Work at sea:

A camera-epibenthic sledge (C-EBS, see Figure 7-2) especially designed for sampling small epifauna of a few mm to one cm of size at any depth and on any substrate was used (Brandt et al., 2013, 2015). It has been successfully deployed 17 times at 9 stations (see Station List).

In a cool room and on deck, the complete samples were transferred into pre-cooled 96% ethanol and kept at least for 48 h in -20°C for DNA studies or, the second deployment per area, into formalin (4%).

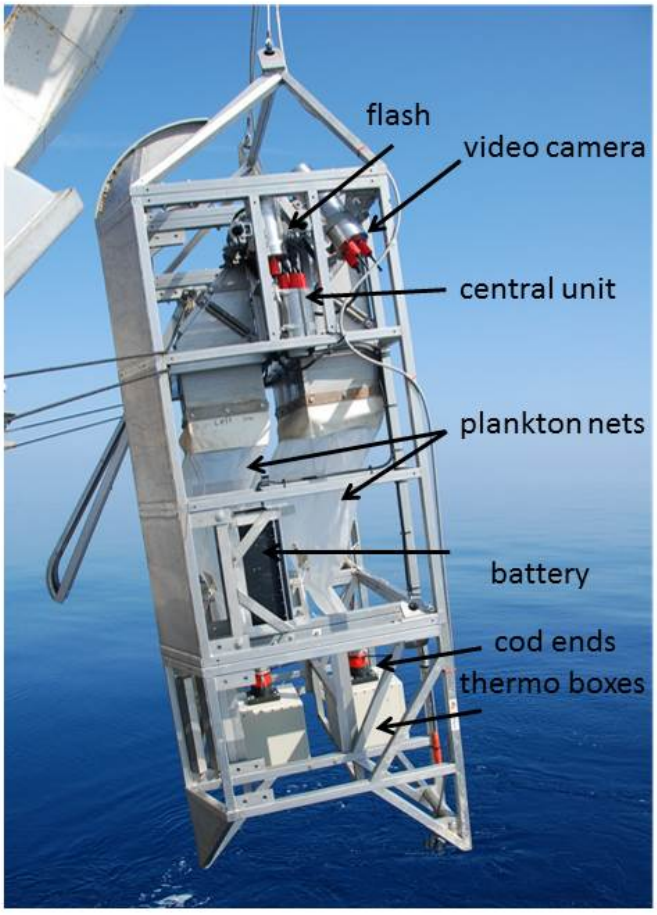

Figure 7-2: C-EBS (after Brandt et al., 2013).

7.2.1.3 Preliminary results:

On board of RV *Sonne* the supranet and epinet catches from six stations (11 C-EBS hauls) were sorted to higher taxon (class/order) level. The stations in the Puerto Rico Trench could not yet be sorted, as the fixation and expedition time available prior to

arrival in Santo Domingo was too short. From these samples, 10,363 individuals representing 17 major macrobenthic taxa were sorted out (Table 7-2; Figure 7-3 and Figure 7-4). Station 4-8 yielded the highest number of individuals (2467), station 9-2 the lowest (94) number of individuals. Crustacea occurred most frequently with 6,016 individuals followed by Annelida (mainly Polychaeta) with 2,968 individuals. In very general terms, abundance of macrobenthic invertebrates was higher in the eastern abyssal plain than in the western abyssal plain of the Mid Atlantic ridge, potentially due to sampling bias.

Table 7-2: Macrobenthic taxa sampled by means of the C-EBS.

Station-haul	**2-6**	**2-7**	**4-8**	**4-9**	**6-7**	**6-8**	**8-4**	**9-2**	**9-8**	**11-1**	**11-4**	**total**
Annelida	219	471	594	503	298	305	304	18	168	48	40	2968
Brachiopoda	0	0	0	0	0	0	0	1	1	0	0	2
Bryozoa	0	0	0	0	6	0	0	0	6	5	0	17
Chaetognatha	4	22	29	15	8	10	12	2	4	7	0	113
Chelicerata	0	0	0	0	0	0	0	0	1	0	0	1
Chordata	0	0	0	0	0	0	0	0	0	1	0	1
Cnidaria	0	1	4	0	2	14	2	0	3	1	1	28
Crustacea	441	767	1383	1013	668	591	558	60	409	79	47	6016
Echinodermata	9	34	185	110	5	6	5	0	12	0	2	368
Hemichordata	0	3	0	0	0	0	0	0	0	0	0	3
Mollusca	13	41	246	59	68	48	46	8	27	14	9	579
Nematoda	17	41	26	29	19	21	10	3	12	5	0	183
Nemertea	1	2	0	0	8	0	0	1	3	0	0	15
Phoronida	0	2	0	0	0	0	0	0	0	0	0	2
Plathelminthes	2	0	0	0	0	0	0	0	0	0	0	2
Priapulida	0	0	0	0	0	0	0	1	1	0	0	2
Sipunculida	1	4	0	6	17	10	5	0	16	0	5	64
Total	**707**	**1388**	**2467**	**1735**	**1099**	**1005**	**942**	**94**	**663**	**160**	**104**	**10364**

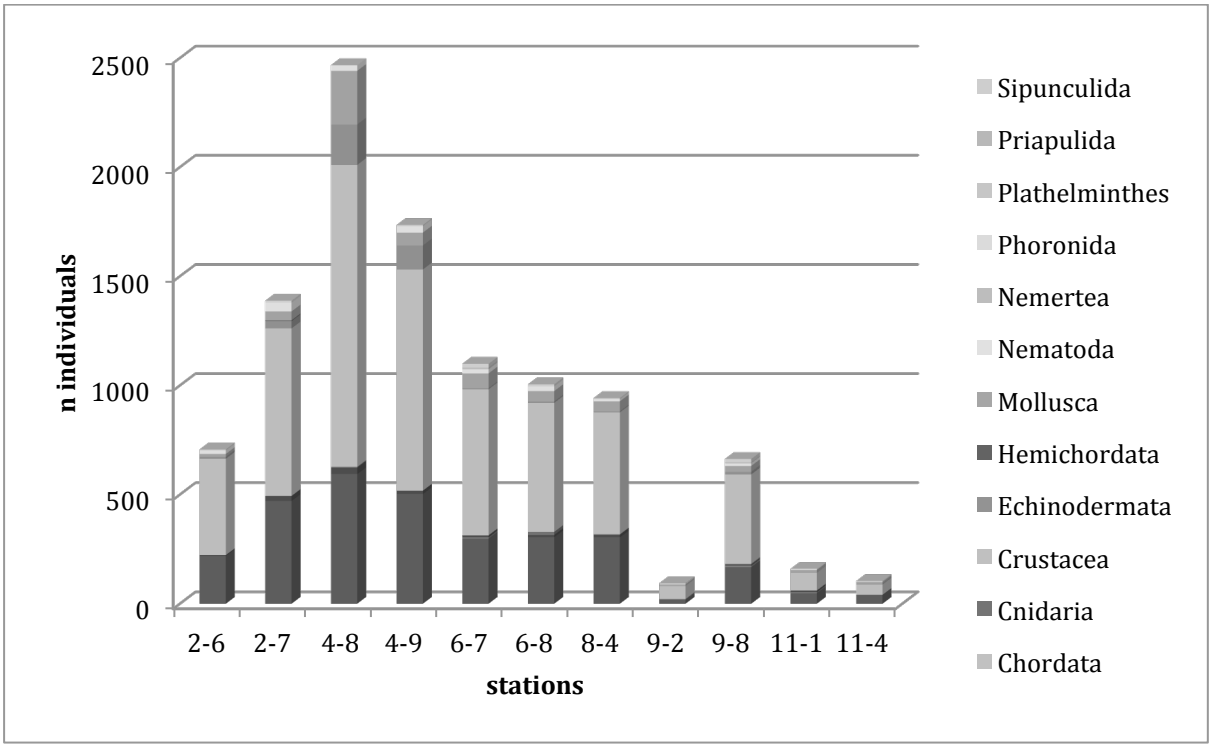

Figure 7-3: Presence/absence data of taxa pooled for all stations of the Vema Fracture zone.

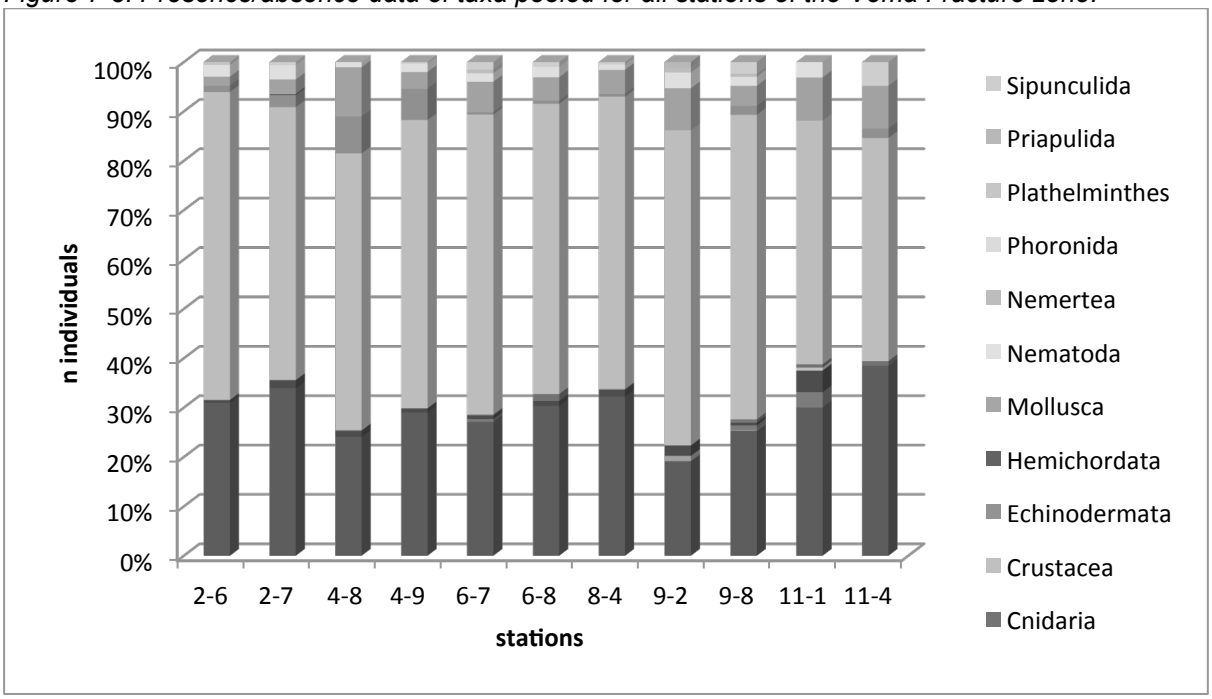

Figure 7-4: Relative percentage of occurrence of taxa per samples pooled for all stations..

Within the macrofaunal Crustacea, Peracarida dominated with 3219 individuals over Copepoda with 2733 individuals (Table 7-3). Ostracoda only occurred with 48 individuals and Euphausiacea and Decapoda were rare.

Table 7-3: Macrobenthic Crustacea sampled by means of the C-EBS.

Station/Haul	2-6	2-7	4-8	4-9	6-7	6-8	8-4	9-2	9-8	11-1	11-4	total
Decapoda	0	2	1	1	2	2	0	0	0	0	0	8
Copepoda	297	484	716	509	178	265	165	17	81	14	7	2733
Euphausiacea	0	0	1	0	0	0	2	0	0	0	0	3
Peracarida	141	269	654	498	484	317	385	43	325	63	40	3219
Ostracoda	3	9	11	4	4	7	6	0	3	1	0	48
total	441	764	1383	1012	668	591	558	60	409	78	47	6011

Peracarid crustaceans (Table 7-4) occurred with five classes of which Isopoda were most dominant and occurred with 2392 individuals, 74 % of all peracarids, followed by Amphipoda (333, 10%), Cumacea, (250, 8%) and Tanaidacea (217, 7%). Mysidacea only occurred with 27 (1%) (and mostly rather damaged) individuals in the samples (Figure 7-5 and Figure 7-6).

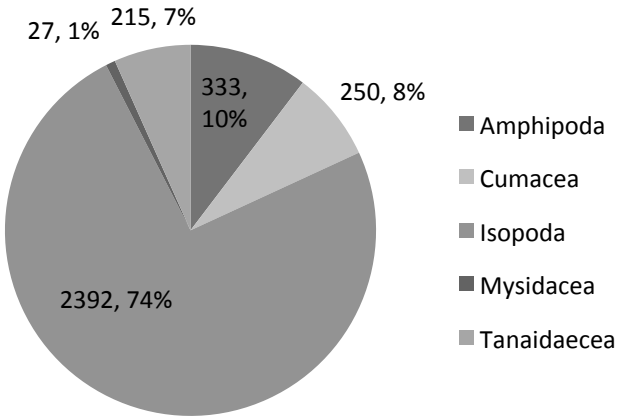

Figure 7-5: Percantage of all peracarid taxa sampled along the Vema Fracture Zone.

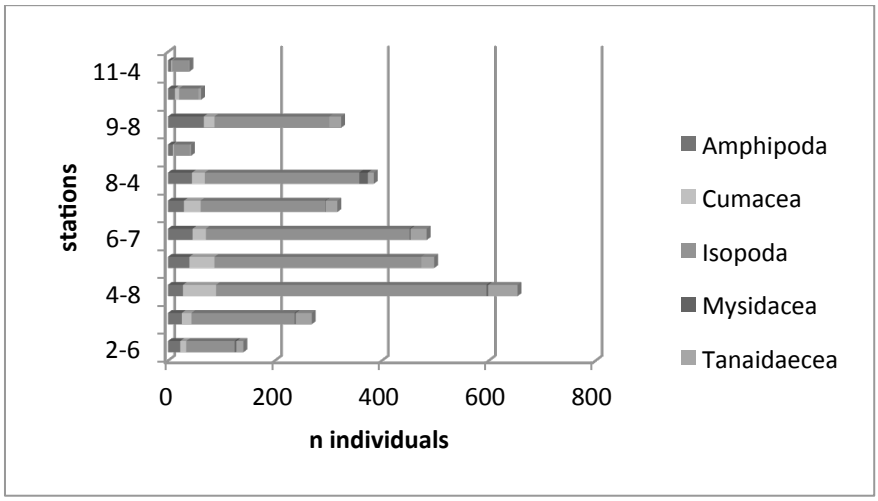

Figure 7-6: Numbers of individuals of peracarid taxa along the Vema Fracture Zone.

Table 7-4: Crustacea Peracarida sampled my means of the C-EBS.

Station-Haul	2-6	2-7	4-8	4-9	6-7	6-8	8-4	9-2	9-8	11-1	11-4	total
Amphipoda	23	26	28	40	46	30	45	9	67	13	6	333
Cumacea	11	18	62	47	25	31	24	2	20	8	2	250
Isopoda	91	193	506	387	381	233	289	30	215	36	31	2392
Mysidacea	3	2	3	0	2	1	16	0	0	0	0	27
Tanaidaecea	13	30	55	24	30	22	11	2	22	5	1	215
total	141	269	654	498	484	317	385	43	324	62	40	3217

Echinodermata occurred with 368 specimens in the C-EBS samples and Ophiuroidea dominated with 165 specimens over Asteroidea (144) and Holothuroidea (54). Crinoidea (4 individuals) and Echinoidea (1 individual) were rare Table 7-5 and Figure 7-7.

Table 7-5: Echinodermata sampled my means of the C-EBS.

Echinodermata	2-6	2-7	4-8	4-9	6-7	6-8	8-4	9-2	9-8	11-1	11-4	total
Asteroidea	0	0	99	43	2	0	0	0	0	0	0	144
Crinoidea	2	0	1	0	0	0	1	0	0	0	0	4
Echinoidea	1	0	0	0	0	0	0	0	0	0	0	1
Holothuroidea	3	21	4	8	1	3	2	0	11	0	1	54
Ophiuroidea	3	13	81	59	2	3	2	0	1	0	1	165
total	9	34	185	110	5	6	5	0	12	0	2	368

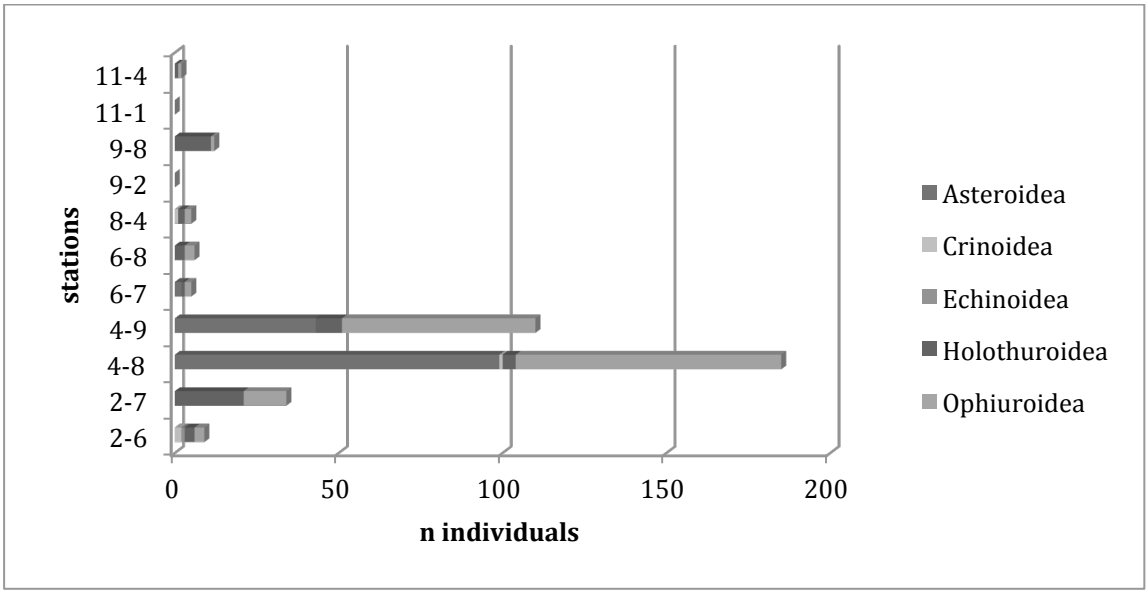

Figure 7-7: Numbers of echinoderm taxa along the Vema Fracture Zone.

Composition of Polychaeta and Mollusca of C-EBS catches are described in more detail in Sections 7.2.3 and 7.2.4 of the cruise report. An example of macrofaunal taxa sampled is presented in Figure 7-8.

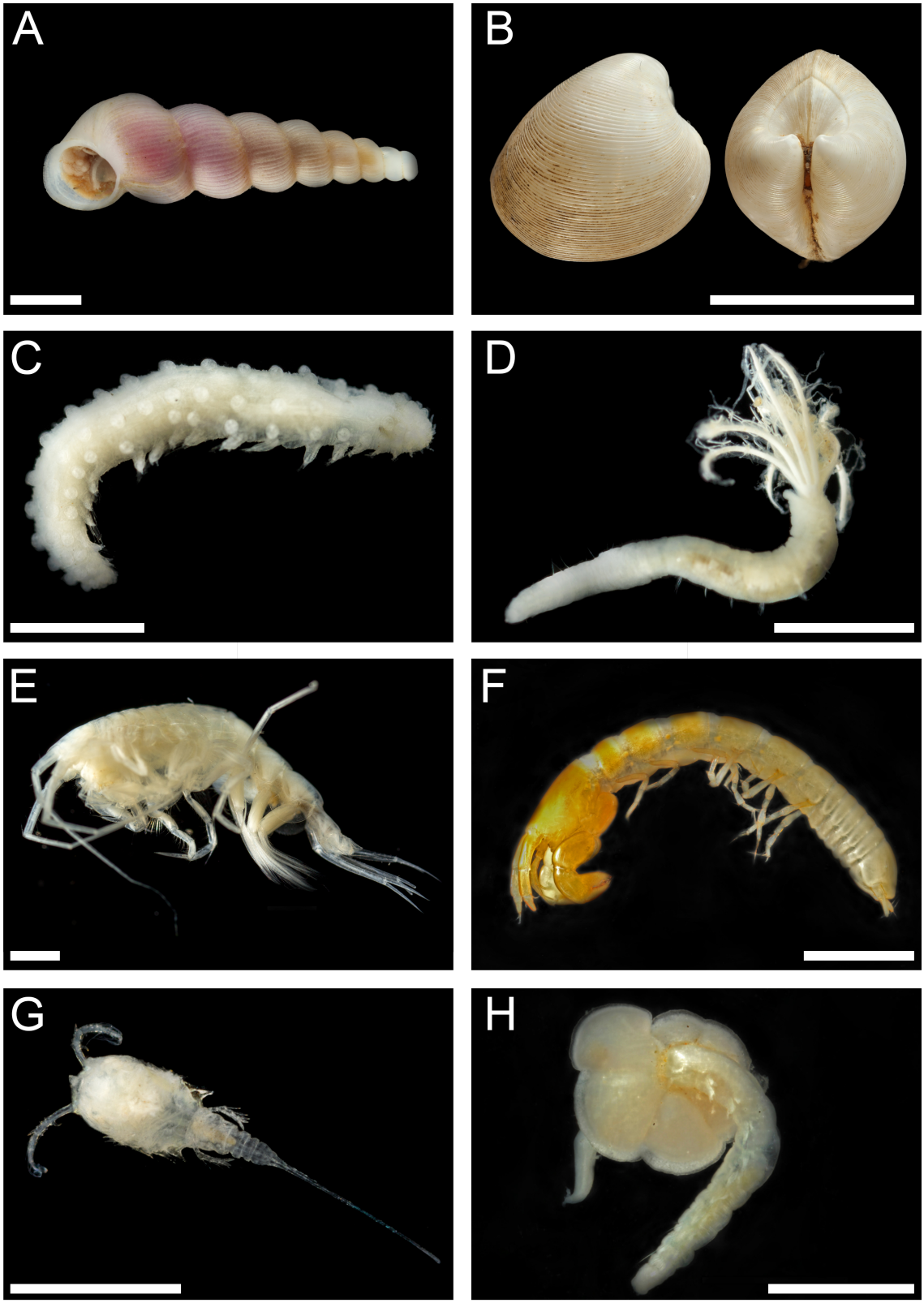

Figure 7-8: Macrofaunal taxa sampled with the EBS: A, Gastropoda, B, Bivalvia, C, Polychaeta, D, Polychaeta (Sabellidae), E, Crustacea (Amphipoda), F, Crustacea (Tanaidacea), G, Crustacea (Harpacticoida), H, Polychaeta in Foraminifera.

7.2.2 The Epibenthic sledge: technical descriptions, sensor data and photo and video documentation of the seabed

(Brenke, N., Elsner, N., Brandt, A.)

The epibenthic sledge (C-EBS) used in the Vema-Transect expedition is equipped with a supra- and epibenthic samplers possessing plankton nets with a cod end as described by Brandt et al. (2013, 2015).

For the C-EBS deployment the ship starts at a position app. 1.5 nm (depending on water depth) prior to the MUC position. The ratio cable length to water depth is usually 1.5 times. While the C-EBS was lowered with 0.7 m/sec. the vessel speed was 1.2 kn to compensate the speed of the wire.

About 100 m above the ground the C-EBS was lowered with 0.5 m (ship speed reduced to 1 kn) until the tension meter indicated that the C-EBS was on the ground. For the rest lowering the wire was done again with 0.7 m/sec. When the maximum cable length is reached, the ship was driven for 10 minutes with 1 kn to tighten the wire. After that the vessel kept the position and the winch started to heave the C-EBS with 0.5 m/sec. When the gear left the ground, the winch speed was increased to 1 m/sec.

The haul distances were calculated by the information from the tension meter and the difference of the wire length at EBS start haul and EBS off ground (see Table 7-6), if possible. If this data is not available, we use the data from the flowmeter. The position in Table 7-6 is only ship position and is not corrected by pinger data. For the calculation of the correct ground position of the sledge, precise calculations will be made after thorough analysis of the data incorporating also the Posidonia data (see, for example, Section 7.4.7). As the haul lengths varied, the data will be standardised to 1000 m hauls for the comparative analysis which is equivalent to a bottom area of 1000 m^2 sampled by the sledge.

Table 7-6: List of all EBS hauls during the Vema-Transect expedition including the preliminary trawling distances for each haul. Hadal stations are marked in blue.

VEMA Transect SO237	Sation	in charge	Date	off Deck	Start Ship Position	Start Ship Position	End Ship Position	End Ship Position	depth	towing distance	
			UTC	UTC	Lon [°W]	Lat [°N]	Lon [°W]	Lat [°N]	[m]	$D_{(TW)}$	
EBS 1	# 2-6	AB	20.12.2014	07:52	25°03.72'	10°43.78'	25°03.73'	10°43.79'	5520	1846	
EBS 2	# 2-7	NB	20.12.2014	16:30	25°03.21'	10°42.891'	25°03.167'	10°42.92'	5507	2020	
EBS 3	# 4-8	AB	26.12.2014	21:59	31°04.40'	10°25.62'	31°04.37'	10°25.62'	5725	1750	
EBS 4	# 4-9	NB	27.12.2014	06:55	31°02.98'	10°25.65'	31°02.98'	10°25.66'	5733	1900	
EBS 5	# 6-7	AB	02.01.2015	14:38	36°55.06'	10°21.82'	36°55.06'	10°21.83'	5079	1980	
EBS 6	# 6-8	NB	02.01.2015	23:12	36°55.35'	10°22.65'	36°55.35'	10°22.66'	5127	1400	
EBS 7	#8-4	AB	06.01.2015	15:45	42°39.73'	10°43.00'	42°39.73'	10°43.00'	5178	1750	
EBS 8	#9-2	AB	11.01.2015	07:41	47°58.03'	11°40.73'	47°59.00'	11°40.45	4986	674	$D_{(F)}$
EBS 9	#9-8	NB	12.01.2015	15:12	47°53.99'	11°39.36'	47°53.97'	11°39.36'	5001	1613	
EBS 10	#11-1	AB	14.01.2015	06:16	50°27.97'	12°05.84'	50°27.96'	12°05.81'	5088	1320	
EBS 11	#11-4	NB	14.01.2015	15:08	50°28.14'	12°04.83'	50°28.14'	12°04.82'	5108	1416	
EBS 12	#12-5	AB	20.01.2015	19:56	66°50.02'	19°46.85'	66°49.99'	19°46.85'	8338	1611	
EBS 13	#12-6	NB	21.01.2015	03:26	66°45.130'	19°48.601'	66°45.120'	19°48.605'	8336	813	
EBS 14	#13-4	AB	23.01.2015	03:00	67°05.79'	19°42.12'	67°05.79'	19°47.13'	8317	1070	
EBS 15	#13-5	NB	23.01.2015	12:05	67°02.617'	19°50.118'	67°02.60'	19°50.14'	8042	840	
EBS 16	#14-1	NB	24.01.2015	16:35	67°09.247'	19°02.097'	67°09.43'	19°02.11'	4552	n/a	
EBS 17	#14-2	AB	24.01.2015	22:23	67°07.77'	19°04.67'	67°07.75	19°04.67'	4925	n/a	

The C-EBS is also a carrier for two camera systems and furthermore a carrier for different measuring instruments: an Aanderaa Seaguard RCM equipped with sensors for temperature, salinity, O_2 concentration and pressure as well as a Posidonia positioning system and a mechanical TSK-flowmeter. Because the pressure cases of the cameras and sensors are limited to 6000 m, (respectively 600 bar), for deeper stations only the mechanical TSK-flowmeter is available. A preliminary overview of the abiotic data is given in Table 7-7.

Table 7-7: Preliminary abiotic data for each haul of different sensors mounted on the C-EBS. Values are bottom values taken when the sledge was on the seafloor. Hadal stations are marked in blue.

VEMA Transect SO237	Sation	Date	depth	O² Bottom	Temp Bottom	mean Bottom Current
		UTC	[m]	[µM]	[°C]	[cm/s]
EBS 1	# 2-6	20.12.2014	5520	236.00	2.30	1.70
EBS 2	# 2-7	20.12.2014	5507	238.00	2.45	1.10
EBS 3	# 4-8	26.12.2014	5725	237.70	2.32	6.50
EBS 4	# 4-9	27.12.2014	5733	237.60	2.31	2.00
EBS 5	# 6-7	02.01.2015	5079	245.49	2.21	2.10
EBS 6	# 6-8	02.01.2015	5127	244.91	2.20	2.10
EBS 7	#8-4	06.01.2015	5178	239.12	1.81	2.60
EBS 8	#9-2	11.01.2015	4986	240.70	1.79	6.10
EBS 9	#9-8	12.01.2015	5001	241.20	1.80	2.17
EBS 10	#11-1	14.01.2015	5088	238.98	1.76	4.90
EBS 11	#11-4	14.01.2015	5108	238.83	1.76	2.20
EBS 12	#12-5	20.01.2015	8338	n/a	n/a	n/a
EBS 13	#12-6	21.01.2015	8336	n/a	n/a	n/a
EBS 14	#13-4	23.01.2015	8317	n/a	n/a	n/a
EBS 15	#13-5	23.01.2015	8042	n/a	n/a	n/a
EBS 16	#14-1	24.01.2015	4552	n/a	n/a	n/a
EBS 17	#14-2	24.01.2015	4925	n/a	n/a	n/a

Deployment of the C-EBS yielded a total of almost 8000 pictures and about 44 hours of video footage from all deployments (Table 7-8). Because the pressure cases of the lights, camera and camcorder are limited to a maximum depth of 6000 m, four deployments in the Puerto-Rico Trench below this depth were conducted without cameras. EBS #17 was deployed, for logistic reasons, without the camera and camcorder. Two examples of the deep sea pictures are given in Figure 7-9 and Figure 7-10.

Table 7-8: Number of pictures and length of videos successfully taken during each haul of the C-EBS. The stations below 6000 m are marked in blue.

VEMA Transect SO237	Sation	Date	Pic. Still	Pic. CC	Video-CC
		UTC	[n]	[n]	[min]
EBS 1	# 2-6	20.12.2014	0	0	0
EBS 2	# 2-7	20.12.2014	0	0	0
EBS 3	# 4-8	26.12.2014	3	502	271
EBS 4	# 4-9	27.12.2014	711	555	304
EBS 5	# 6-7	02.01.2015	16	542	296
EBS 6	# 6-8	02.01.2015	662	516	284
EBS 7	#8-4	06.01.2015	711	554	304
EBS 8	#9-2	11.01.2015	895	697	375
EBS 9	#9-8	12.01.2015	0	556	304
EBS 10	#11-1	14.01.2015	44	479	264
EBS 11	#11-4	14.01.2015	76	455	251
EBS 12	#12-5	20.01.2015	0	0	0
EBS 13	#12-6	21.01.2015	0	0	0
EBS 14	#13-4	23.01.2015	0	0	0
EBS 15	#13-5	23.01.2015	0	0	0
EBS 16	#14-1	24.01.2015	n/a	n/a	n/a
EBS 17	#14-2	24.01.2015	0	0	0
total			3118	4856	2653
sum pic				**7974**	**44h**

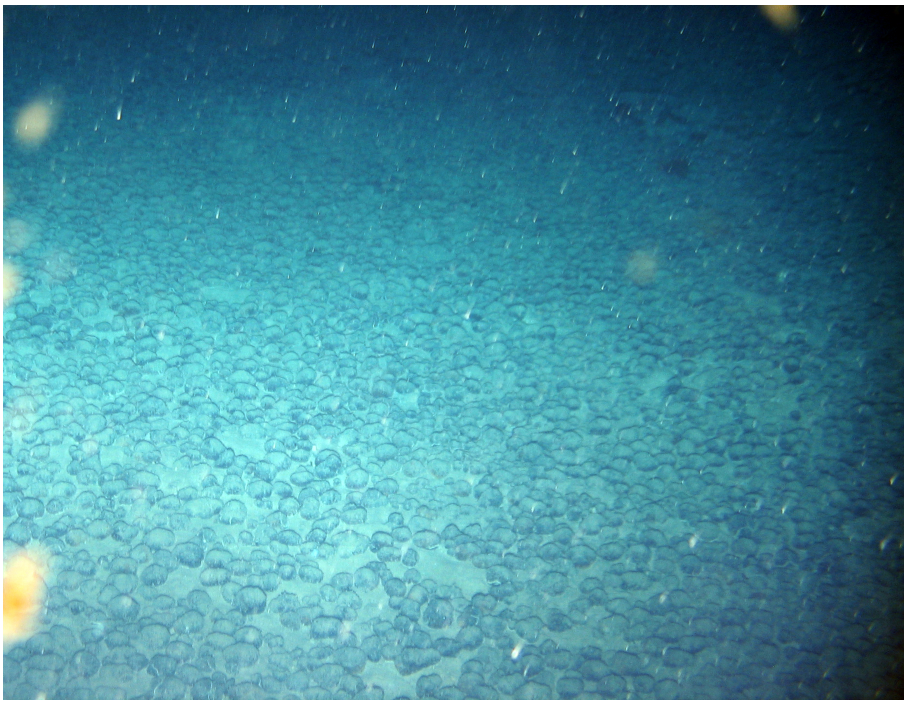

Figure 7-9: The seafloor in 4986 meters depth on station #9-2 shows many manganese nodules.

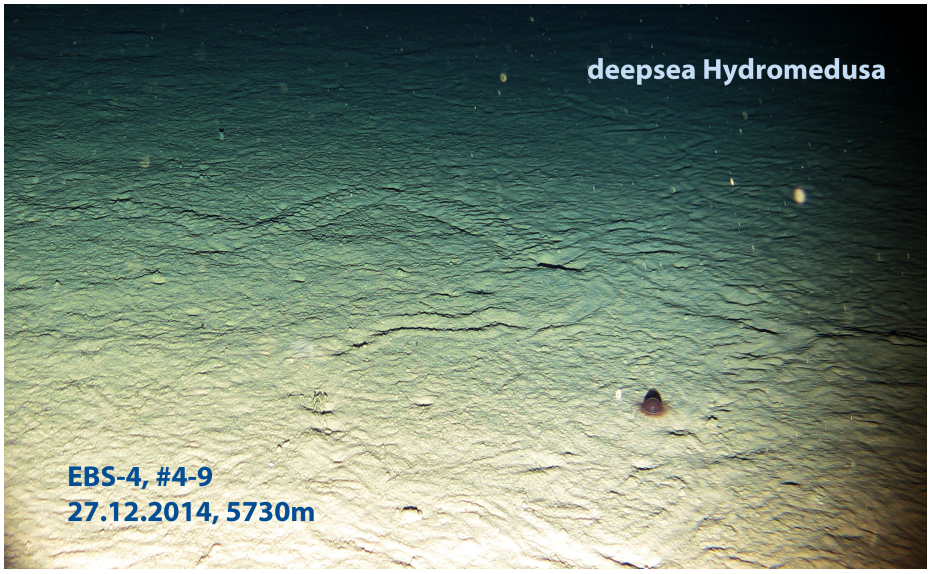

Figure 7-10: The seafloor in 5730 meters depth on station #4-9 shows many life traces and one hydromedusa.

7.2.3 The diversity of macrofaunal Mollusca of the abyssal Vema Transform and hadal Puerto Rico Trench

(K. Linse, E. Schwabe)

Knowledge of abyssal and hadal molluscan fauna of the deep Atlantic Ocean is patchy, depended on the molluscan class and especially scarce for the equatorial zone. The bivalvia of the deep Atlantic were reviewed by Allen (2008) and his account of 468 species and 87 families in the Atlantic lists only 14 families of bivalves to be present in depth below 5000 m. Scarabino & Scarabino (2011) assessed the scaphopod fauna of the Atlantic Ocean with 132 species of which the majority (90) are reported from the Western Atlantic and only 9 species are reported as amphi-Atlantic. To date no summarizing reviews for the Atlantic gastropods, caudofoveats and solenogastres are available, only regional literature, e.g. Dall 1889, Leal 1991, Bouchet & Waren 1993.

The expected results from this expedition to the abyssal (>5000 m depth) Vema Transform valley and to the hadal and abyssal Puerto Rico Trench will increase the faunistic knowledge on deep-sea Atlantic species and might increase the number of amphi-Atlantic species. If numbers of collected specimens per species and across stations permit, phylogeographic studies on the dominant species will be carried out. The other collected species will contribute to ongoing phylogenetic studies on the origin of the deep-sea taxa. The data will also be directly comparable with the EBS results of the ANDEEP, BIOPEARL and DIVA expeditions to the Southern Atlantic as the same type of EBS was deployed in the same way.

At sea, live molluscs as well as empty shells were sorted from the epibenthic sledge samples of the Vema Transform, identified to morphospecies and their abundances counted. Here we present results from the live morphospecies only. Two sets of data are presented 1) the data of the already sorted samples with Epi- and supranet codends and net overflow samples pooled, and 2) the data for the codends only. The EBS samples taken in the hadal of the Puerto Rico Trench will be sorted back on land.

The 11 EBS deployments yielded to date a total of 572 specimens and 36 morphospecies of the Caudofoveata (39/3), Solenogastres (40/4), Gastropoda (12/8), Bivalvia (247/17) and Scaphopoda (237/4) (Appendix Table Mollusca 1). Bivalvia were most rich and abundant closely followed by scaphopods in abundance, but with far lower number of species (Appendix Table F, Figure 7-11). The presence of benthic gastropods was extremely rare and most species were represented by one individual only while monoplacophorans, polyplacophorans and cephalopods were not collected at all.

Morphospecies richness between stations varied from 4 to 20 species (all data; 3 to 18 codends only) and most species were found at station 06_07 with 20 (18) species (Figure 7-11 A, B). Bivalves were present at all 11 stations and dominant in species richness. The bivalves *Dacrydium* sp. and *Malletia* sp. occurred on nine of the 11 stations.

Abundance between stations varied from 8 to 244 (all data; 6 to 64 codends only) and most species were found at station 04_08 with 244 specimens (64 specimens at 06_07 codends only) (Figure 7-11 C, D). Analysing all data, the scaphopod species of

the family Pulsellidae was the most abundant species with a total of 124 specimens followed by the scaphopod of the family Dentallidae with 73 specimens and the bivalve of the genus *Malletia* with 71 specimens.

Concluding these preliminary data, we note high numbers of foraminiferan-eating species and specimens on the stations characterised by foraminiferan rich sediments. Overall the species richness is low compared to Southern Ocean stations of similar depth. The species composition in bivalves is comparable to that reported from the Biovema expedition (Allen, 2008). The current data show that Caudofoveata are only present in eastern part of the Vema Transform and living gastropods were less rare in the western part. At present 14 of the 36 morphospecies are found in the eastern and western part of the Vema Transfrom, crossing the MAR. Further morphological and molecular analyses in the labs on land will confirm or request the overall science hypotheses of Vema-TRANSIT.

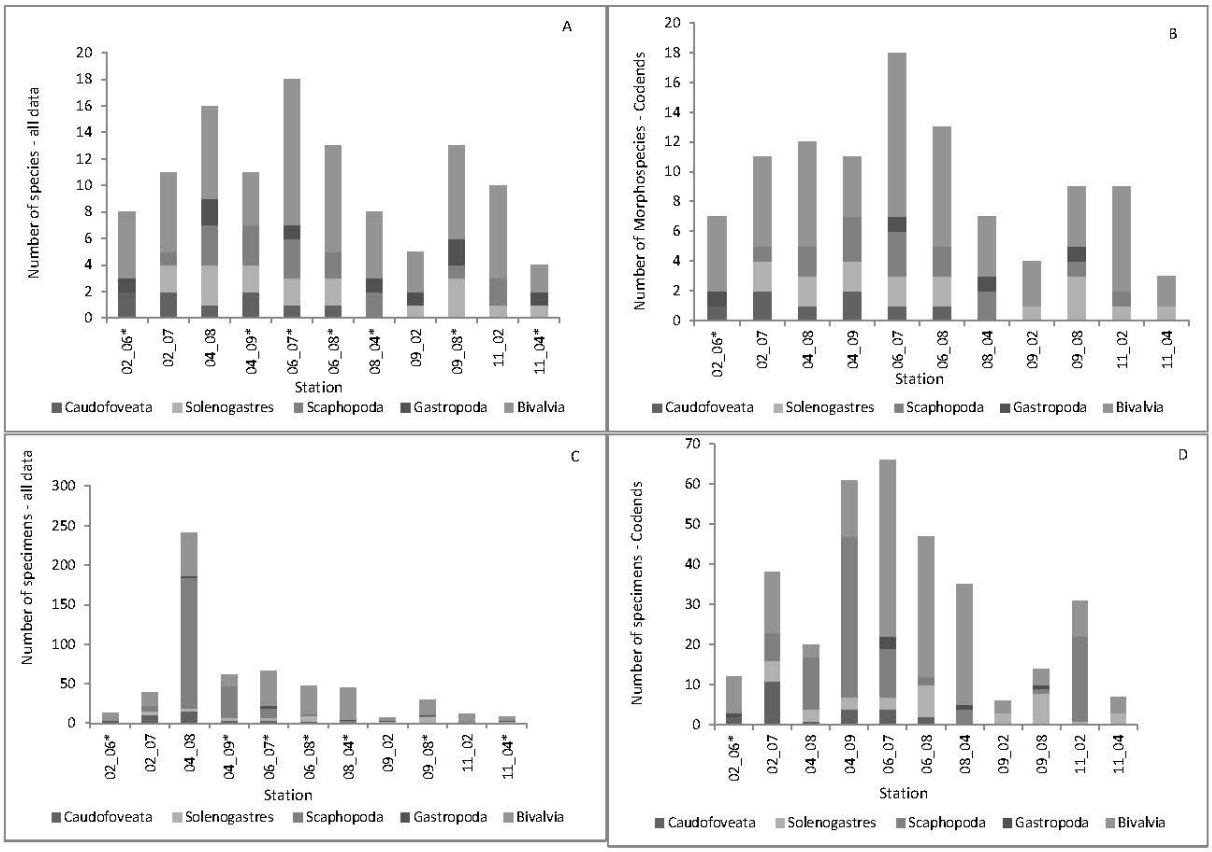

*Figure 7-11: Morphospecies richness and abundance per taxon at the abyssal Vema Transform stations. A, C) Epi- and supranet codends and net overflow samples pooled, B,D) Codends only. Stations marked with * are incomplete.*

7.2.4 The diversity of macrofaunal Polychaeta of the abyssal Vema Transform

(Guggolz, T., Brandt, A.)

7.2.4.1 Preliminary results

A total of 2907 polychaetes (excluding fragments, only heads counted) were found in the sorted samples during the VEMA-Transit expedition (SO 237) (Table 7-9). The number will most likely increase because of further sorting of the formaldehyde fixed overflow samples from the epi- and supra nets back on land. To date 497 polychaetes were identified to family level from two EBS deployments at the first station (station 2-6 and 2-7). 29 different families were determined until now (Figure 7-12). Thorough morphologic and taxonomic examinations will take place at the University of Hamburg. The family composition in the two deployments seems to be very similar to results that have been reported previously from the deep sea (Paterson et al. 2009). First examinations at species level show similarities with species that have been found and described for three abyssal zones of the northeast Atlantic (Böggemann 2009). Particularly, the identification to species level, requires the use of high magnification microscopes, will be done in the home laboratory of the University of Hamburg.

Table 7-9: Polychaete specimens and numbers of families found at different stations.

Station	Gear	polychaetes [n]	families [n]
2-6	EBS	167	28
2-7	EBS	328	29
4-8	EBS	594	
4-9	EBS	503	
6-7	EBS	432	
6-8	EBS	305	
8-4	EBS	304	
9-2	EBS	19	
9-8	EBS	167	
11-1	EBS	48	
11-4	EBS	40	

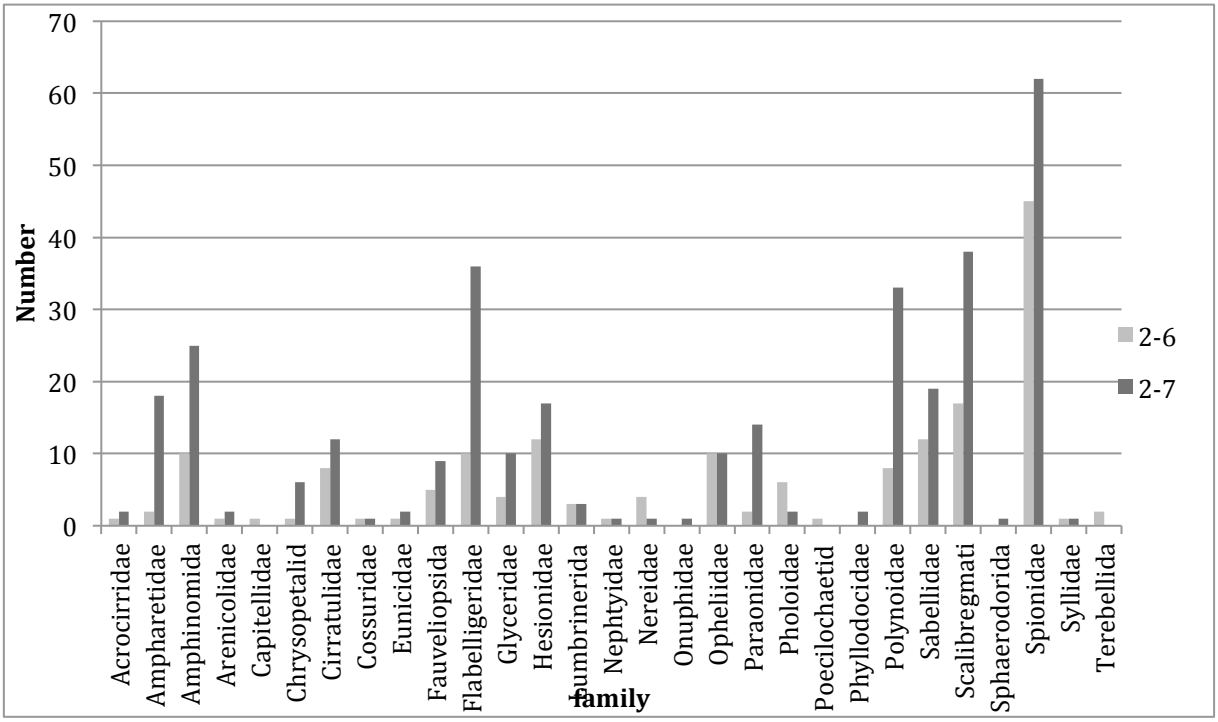

Figure 7-12: Family composition of the first two EBS deployments at station 2-6 and 2-7.

7.2.5 The diversity of macrofaunal Isopoda of the abyssal Vema Transform

(Brandt, A., Bober, S., Brix, Frutos, I., S. Guggolz, T., Heitland, N., Linse, K., Malyutina, M., Riehl, T., Schwabe, E.)

7.2.5.1 Objectives:

Epibenthic sledges (EBS) proved to be the most efficient and a reliable device for macrofauna due to the comparatively small mesh sizes of 300 or 500 µm (e.g. Brenke, 2005; Brandt et al., 2013, 2015). Knowledge of abyssal and hadal isopod fauna of the deep Atlantic Ocean is patchy. Some investigations were performed in the Atlantic Ocean from polar seas towards tropical areas from board of different research vessels. For example, in the North Atlantic the composition, abundance and diversity of isopods has been examined north of Iceland at the Kolbeinsey Ridge (RV *Meteor*) as well as off East Greenland (RV *Polarstern*) (e.g. Brandt 1993, 1995, 1997; Brandt et al., 1996). In the 1960´s the first epibenthic sledge deployments sampled the deep slopes and basins of the East American coast (Sanders et al. 1965, Hessler & Sanders 1967, Sanders & Hessler 1969). In the southern Atlantic Ocean, diversity and abundance of abyssal isopod crustaceans was investigated in the Angola basin off Namibia on board of RV *Meteor* between 5125–5415 m depth (Brandt et al., 2005) during DIVA-1 (*Latitudinal Gradients of deep-sea Biodiversity in the Atlantic Ocean*). The DIVA expeditions connect the VEMA project with the samples from the North Atlantic Ocean. About 2500 isopod specimens were counted from DIVA-2 samples with several publications for single families (unpublished data DZMB database, see Brandt 2004 for Macrostylidae, Brökeland 2010 and Brix et al. 2011 for Haploniscidae, Brix 2007 and Brix et al. 2014 for Desmosomatidae). In the Angola Basin, the diversity of Desmosomatidae (10 genera, approximately 27 species) is comparable with that of Munnopsidae Lilljeborg, 1864 (eight genera, 27 species, see Brandt et al. 2005). During DIVA-3 the Argentine Basin and the Brazilian Basin were sampled recording over 6200 isopod specimens (unpublished data DZMB database) also including rare deep-sea families like the Serolidae (Brandt et al. 2014). In the Beagle Channel, Patagonia, Isopoda were investigated until to 663 m depth and in the Southern Ocean, the abyssal Weddell Sea sector was analyzed (Brandt et al., 2007) and off Southern Thule (South Sandwich Islands; Kaiser et al. 2008). While abundance of Isopoda was highest in the North Atlantic, Biodiversity was highest in the Southern Ocean (Brandt et al., 2014). The present investigation follows the general objectives of the Vema-TRANSIT expedition and aims to investigate the isopod species turnover along the east to west transect, especially with regard to the mobility of the families according to different locomodation types (i.e. swimming Munnopsidae or inbenthic Macrostylidae). Moreover, the investigation of the isopod abundance and diversity will help to understand deep-sea latitudinal gradients in the Atlantic in connection with the DIVA samples (M48-1 in 2001, M63-2 in 2005 and M79-1 in 2009). Hadal investigations in the Puerto Rico Trench have never been performed until now. We are therefore interested to investigate the faunal composition of the trench was well as the question, whether the hadal stations are isolated and inhabited by different species than the abyssal western Atlantic.

7.2.5.2 Work at sea:

We have used an epibenthic sledge to obtain the isopod crustaceans, as described by Brandt et al. and Brenke et al. in this cruise report. The sorting was conducted after 48 hours of samples fixation with a complete cooling chain as described in Riehl et al. (2014).

7.2.5.3 Preliminary results:

Almost all sampled isopods belonged to the suborder Asellota representing 11 primarily deep-sea families (see Table xx). 2392 specimens of Isopoda were sorted so far from the samples along the Vema Transform. The most abundant family was Munnopsidae (975 specimens), followed by Haploniscidae (444 individuals), Desmosomatidae (370 individuals), Macrostylidae (208 individuals), Ischnomesidae (171 individuals) and Nannoniscidae (66 individuals) (Figure 7-13). The other families, Bopyridae, Haplomunnidae, Janirellidae and Thambematidae did not occur frequently in the samples. In general, isopod abundance was higher in the eastern than in the western abyssal basin and total number of specimens was highest at station 4-8 with 506 isopods, the lowest number of isopods was found at station 11-4 with 31 individuals (Table 7-10; Figure 7-14 and Figure 7-15).

Table 7-10: Isopod specimens of all C-EBS samples across the Vema Transform.

Station-Haul	**2-6**	**2-7**	**4-8**	**4-9**	**6-7**	**6-8**	**8-4**	**9-2**	**9-8**	**11-1**	**11-4**	**total**
Bopyridae	2	3	5	16	2	4	2	1	0	0	0	35
Dendrotionidae	5	22	0	0	22	17	1	4	36	4	0	111
Desmosomatidae	18	41	74	41	80	44	42	3	19	3	5	370
Haplomunnidae	1	3	0	0	0	0	0	0	0	0	0	4
Haploniscidae	3	30	145	116	63	54	8	5	16	4	0	444
Ischnomesidae	6	13	38	29	23	12	9	3	26	6	6	171
Janirellidae	0	0	0	0	0	0	0	0	2	0	1	3
Macrostylidae	14	34	48	38	29	10	14	0	9	6	6	208
Munnopsidae	40	44	180	137	151	80	204	13	103	11	12	975
Nannoniscidae	2	1	16	10	10	12	7	1	4	2	1	66
Thambematidae	0	1	0	0	1	0	2	0	0	0	0	4
Indet.	0	1	0	0	0	0	0	0	0	0	0	1
Total	**91**	**193**	**506**	**387**	**381**	**233**	**289**	**30**	**215**	**36**	**31**	**2392**

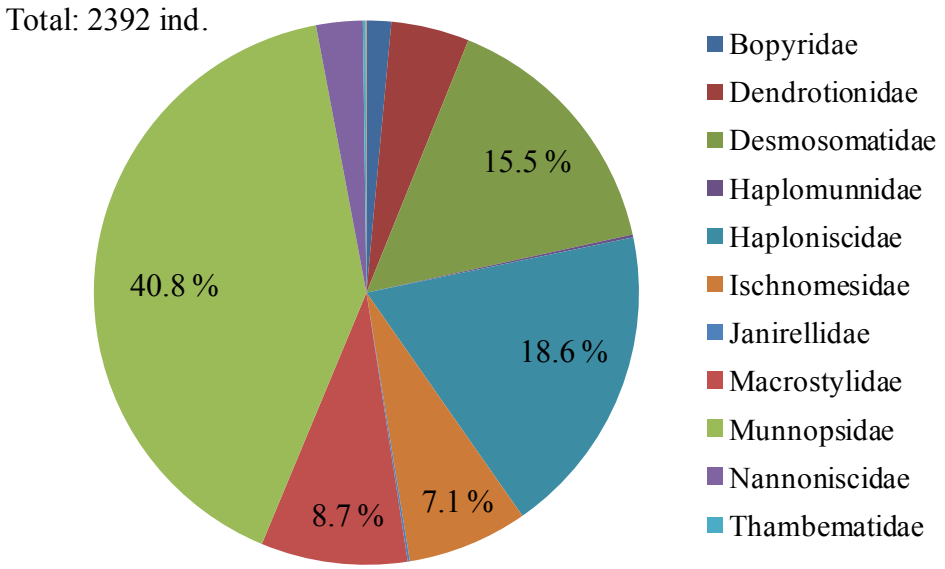

Figure 7-13: Global composition of isopod families at stations of the Vema Transform

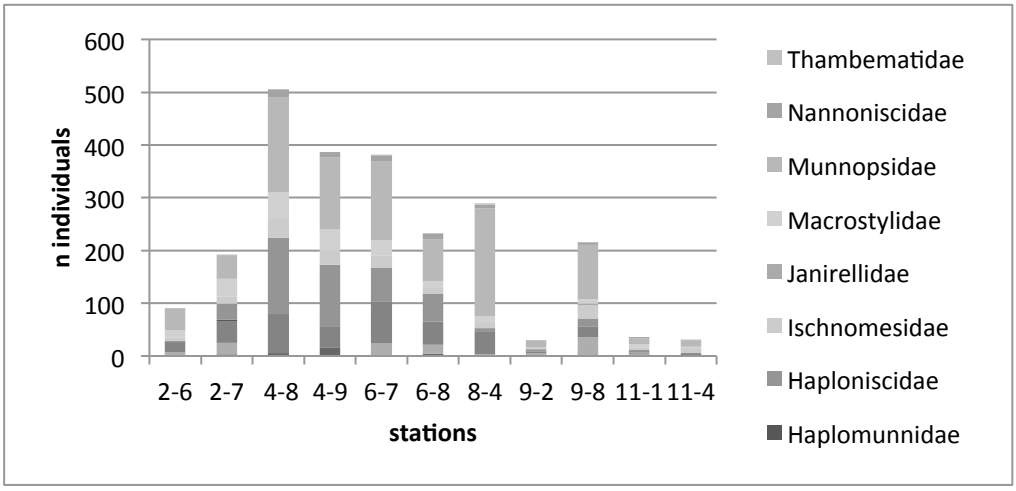

Figure 7-14: Numbers of isopod families at stations at the Vema Transform.

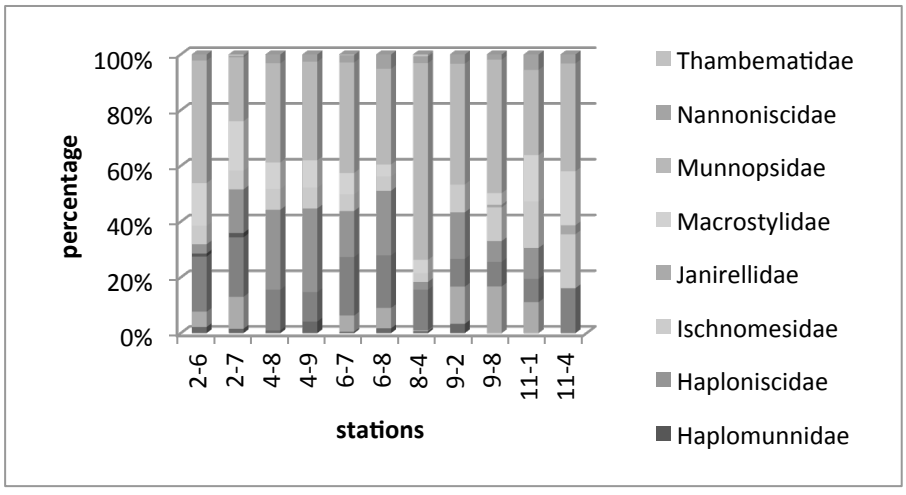

Figure 7-15: Relative occurrence of isopod families at stations of the Vema Transform.

As Munnopsidae are the richest family, their distribution is described in more detail in the following (Figure 7-16 and Figure 7-17). During the expedition isopods of the family Munnopsidae have been collected at each station and almost at each station it was the most abundant and diverse isopods family (975 ind.). The richest station in terms of species richness and abundancy was st. 8-4: d 204 individuals of 16 species, followed by st. 6-7: 147 ind., 14 species. Station with the minimal numbers of the collected species (4) and individuals (9) is st. 9-2. All specimens from sorted samples have been identified to species level. Totally 41 species from 18 genera and 8 subfamilies were identified so far. After the preliminary identification about a half of all species seem to be new to science. The most numerous and frequent was subfamily Eurycopinae (55.7% of individuals) with 15 species of *Eurycope* (44.7% of ind.), 4 species of *Disconectes*, and genera *Dubinectes* and *Belonectes* with one species each. Most of the collected species are rare, but *Betamorpha fusiformis* (153 individuals), *Eurycope* cf. *glabra* (119), *Acanthocope galatheae* (99), *Eurycope* cf. *longiflagrata* (89), and not so numerous but frequent species *Syneurycope parallela* occur the abyssal plain of the both sides of the MAR. Some of these known species (*Betamorpha fusiformis, Syneurycope parallela*) were recorded also through the Atlantic far to the north and to the south of from the studied area and *Acanthocope galatheae* was known from tropical to the southern part of Atlantic and in the tropical Pacific. As we have *Betamorpha fusiformis* and *Acanthocope galatheae* collected during DIVA and ANDEEP expeditions in another parts of Atlantic and in the Pacific and the material was comparable sampled and treated these species will be used for the genetic analysis. Some of the collected species occur only eastern part of the studied area (*Eurycope* sp. 2, 4 ,5 and *Dubinectes* sp.) and another species (*Eurycope* sp. 9, 10, 11, *Storthyngurella triplispinosa*, *Bathybadistes* sp., *Disconectes* sp. 2, 3, 4) were found only at stations in the western side of Atlantic. The number of collected species Munnopsidae and their abundance is less than it was revealed for the Pacific abyssal area near the Kuril-Kamchatka Trench during the KuramBio expedition (80 species) and specially in the ANDEEP area (about 200 species).

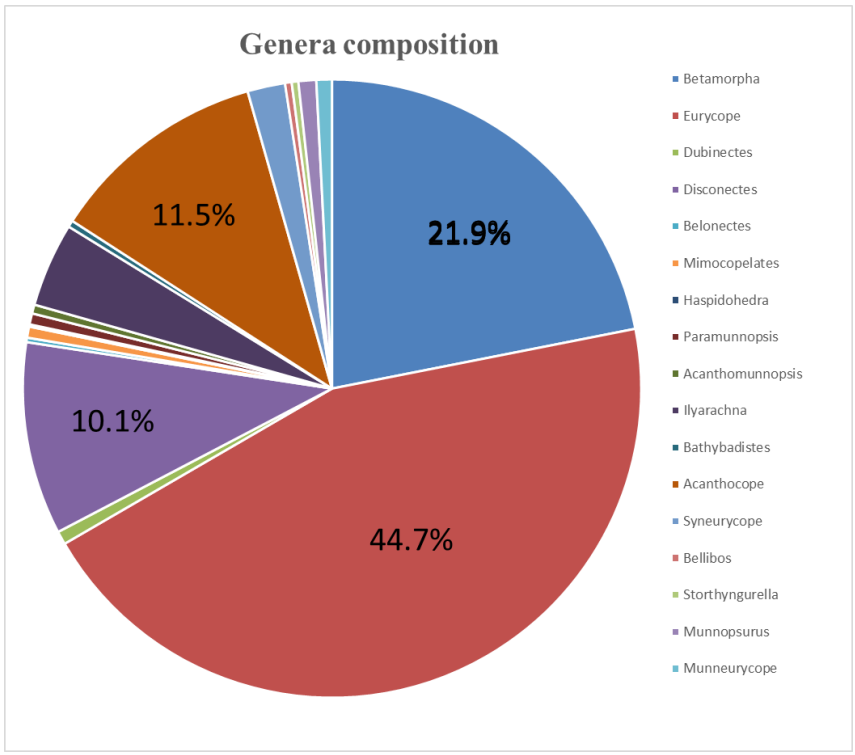

Figure 7-16: Composition of munnopsid genera at the Vema Transform.

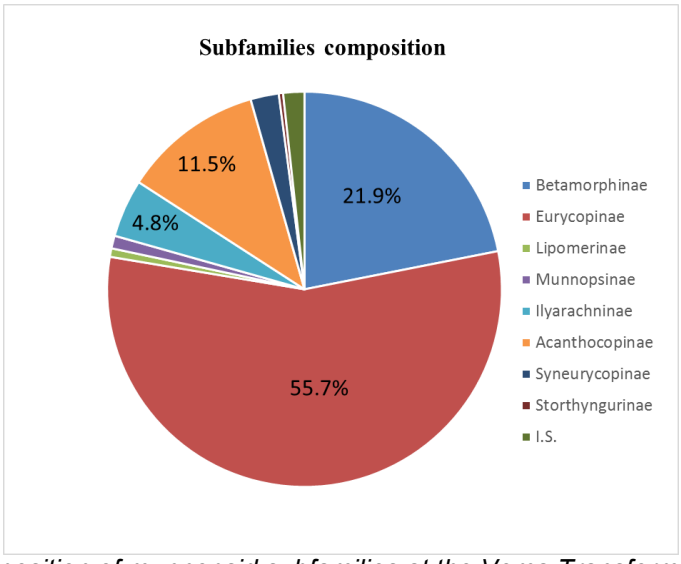

Figure 7-17: Composition of munnopsid subfamilies at the Vema Transform.

Examples of selected Isopoda sampled and photographed during the expedition are presented in Figure 7-18.

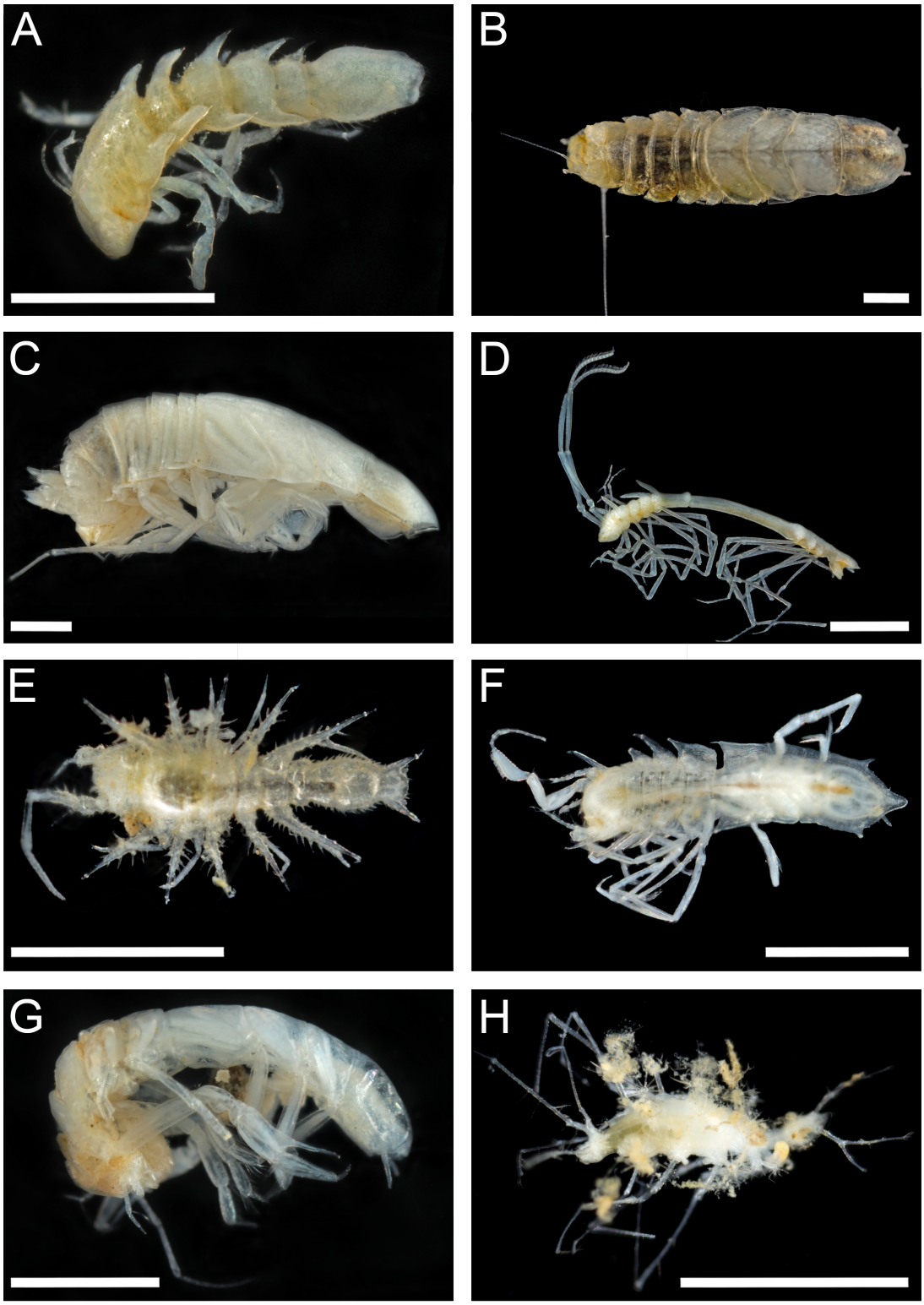

Figure 7-18: Isopoda sampled during the Vema-TRANSIT expedition. Only A, Family Macrostylidae; B, Eurycopinae (Munnopsidae); C, Betamorphinae (Munnopsidae); D, Ischnomesidae; E, Mesosignidae; F, Nannoniscidae; G, Desmosomatidae; H, Dendrotionidae.

7.2.6 Analysis of trans-Mid-Atlantic-Ridge distribution and connectivity of abyssal Isopoda using molecular methods

(T. Riehl, S. Brix, S. Bober, M. Malyutina, N. Heitland, A. Brandt)

7.2.6.1 Background

For a better understanding of deep-sea biodiversity, pinpointing factors that may promote the splitting of lineages (Glazier and Etter, 2014) is of major interest. Geographic isolation may be one of those factors promoting speciation in the deep sea (Faure et al., 2009). And obstacles, such as ridges separating abyssal basins, have been discussed as promoters for allopatry (Wilson and Hessler, 1987). Specialization for certain depth regimes may be responsible for this (France and Kocher, 1996; Havermans et al., 2013). Isopod crustaceans are amongst the better-studied and most diverse as well as abundant groups of deep-sea macrofauna (Brandt et al., 2015, 2013, 2007). They comprise many rare but also some frequently encountered species in the Atlantic and across behavioral categories (e.g. swimmers with supposedly great dispersal abilities versus burrowers with assumed low dispersal). This group hence constitutes a well-suited model for the above-mentioned research.

We aim for a combination of morphological taxonomic and molecular genetic approaches to investigate the diversity, biogeography, and population connectivity of selected common representatives of deep-sea Isopoda. Genetic diversity on the population, species and family level will be analyzed across spatial scales (locally, between sites, trans-MAR, across depth).

7.2.6.2 Methods

During this cruise, specimens were preliminarily identified to species level and separated individually. Isopod crustaceans belonging to the common families Desmosomatidae, Macrostylidae, Munnopsidae, and Nannoniscidae (plus additional selected individuals), as well as the most common species in case of the very abundant Munnopsidae were selected for tissue dissection.

Voucher images were taken from each of these specimens using a macro-photo setup before dissection. A Canon EOS 600D was employed with a Canon MP-E macro lens with 5x magnification. A MT–24EX macro flash and additional SPEEDLITE 430EX slave flashes were used to illuminate the objects from laterally in order to create a black background. The camera was mounted on a stand with manual precision focusing drive. To avoid unnecessary vibration, the Canon software EOS Utility was used to trigger the camera shutter from a laptop and to directly store images on the computer hard drive.

In order to avoid DNA degradation, methods described by Riehl et al. (2014) were followed with modifications. Specimens were identified, separated and dissected on ice. From each individual, one to three posterior pereopods were dissected, preferably from one side only. Legs were transferred from 96% Ethanol to lysis buffer using sterilized probes fitted with tungsten needles or minutia. Sterilization was achieved using a Micro steril © heater with glass beads by exposing the needles to heat for at least 30 seconds. A list of samples taken is given in Table 7-11

Table 7-11: Number of individuals and species used for tissue dissection during the cruise Vema-TRANSIT. This work is to be continued at the home laboratory.

Family	Total number of individuals	Number of species
Desmosomatidae	152	23
Macrostylidae	199	14
Munnopsidae	10	4
Nannoniscidae	49	6

7.2.6.3 Future targets

The tissue will be used for the extraction, amplification and sequencing of the commonly applied genetic markers cytochrome-c-oxidase subunit 1 (COI), the ribosomal rRNA large subunit (16S) (both mitochondrial) and the nuclear small subunit rRNA (18S). Genetic laboratory service will be provided by the company LGC Genomics Germany and performed at the Smithsonian Laboratories of Analytical Biology, Washington D.C., U.S.

Additionally, the phylogenetic relationships of Puerto-Rico-Trench inhabitants will be investigated in context of abyssal, bathyal and shelf species that are potentially related. This will help resolving the question of the origin and isolation of hadal communities.

Taxonomic descriptions of species that are new to science will be performed under consideration of both morphological and DNA data. By generating publicly available DNA Barcodes, we participate in the development of the global database BoLD (Ratnasingham and Hebert, 2007) to support future identifications and biogeographic studies on deep-sea isopods.

7.2.7 Food-web analysis using fatty acids and stable isotope composition of benthic organisms along an east-west transect of the Vema Transform

(Zinkann, A., Minzlaff, U., Peters, J., Kopelmann, R., Brandt, A.)

7.2.7.1 Objectives

Biochemical investigations of the VEMA-Transit project aim at examining the trophic structure and functioning of the abyssal benthic communities of the mid Atlantic Ridge and the Puerto Rico Trench, focusing specifically on the benthic trophic interactions and the influence of abiotic factors in the deep-sea ecosystem along an east-west transect

As one of the main objectives is the comparison between different regions, it was crucial to succeed in sampling the same taxa (preferably genera) at each station. Trophic interactions and food-web interactions will be investigated by comparing the biochemical results with sample parameters. These include fatty-acid composition and stable-isotope ratios of sediment and tissue samples, temperature and velocity data (in cooperation with Dr. Niels Brenke), ADCP data (in cooperation with Dr. Janna Köhler) and specific chlorophyll values of each sampled region (in cooperation with AUV Team).

Various benthic organisms sampled by means of a camera-epibenthic sledge (C-EBS) were collected for biochemical analyses, such as fatty acid and stable isotopes. Analyzing the fatty acid composition provides the opportunity to reconstruct the diet composition and to interpret the importance of specific food sources of each sampled specimen by applying the trophic marker approach (Dalsgaard et al. 2003). Additionally, ratios of the C and N stable isotopes will provide information about the trophic level of the analyzed specimens (Post, 2002). In order to obtain information throughout the whole benthic food web, animals representing different trophic levels were sampled.

7.2.7.2 Work at sea

Specimens for biochemistry were primarily collected with the C-EBS. Voucher pictures were taken of each sampled animal. Identification to the lowest taxonomic level was conducted as far as possible on board and will be finalized in cooperation with taxonomists for each group in the home laboratory. Whole specimens were frozen for biochemical analyses. Sediment samples for comparative fatty acid and stable isotope analyses were collected from the Multiple Corer (MUC). Additionally, samples of surface algae were caught and bottom algae subsampled from the C-EBS.

7.2.7.3 Preliminary results

In total, samples were collected from various gears deployed at nine benthic stations (Table 7-12).

Table 7-12: Details of equipment deployments at different stations for which samples were taken.

station	gear	Longitude	Latitude	depth_start
2 - 3	MUC	025° 03.88' W	10° 43.11' N	5498
2 - 4	MUC	025° 03.88' W	10° 43.10' N	5517
2 - 6	C-EBS	025° 03.83' W	10° 43.68' N	5520
2 - 7	C-EBS	025° 03.38' W	10° 42.75' N	5514
4 - 3	MUC	031° 04.61' W	10° 25.11' N	5771,7
4 - 4	MUC	031° 04.62' W	10° 25.12' N	5759,7
4 - 8	C-EBS	031° 04.52' W	10° 25.52' N	5735
4 - 9	C-EBS	031° 03.10' W	10° 25.54' N	5735
6 - 4	MUC	036° 57.61' W	10° 21.03' N	5134
6 - 7	C-EBS	036° 55.17' W	10° 21.76' N	5085
6 - 8	C-EBS	036° 55.49' W	10° 22.59' N	5119
8 - 1	MUC	042° 41.59' W	10° 43.56' N	5183
8 - 4	C-EBS	042° 39.91' W	10° 43.00' N	5176
8 - 10	MUC	042° 40.99' W	10° 42.58' N	5117
9 - 2	C-EBS	047° 58.19' W	11° 40.70' N	4995
9 - 3	MUC	047° 57.36' W	11° 41.37' N	4996
9 - 4	MUC	047° 57.34' W	11° 41.36' N	4999,6
9 - 8	C-EBS	047° 54.15' W	11° 39.33' N	5004
11 - 1	C-EBS	050° 28.13' W	12° 05.83' N	5089
11 - 4	C-EBS	050° 28.30' W	12° 04.81' N	5112
11 - 5	MUC	050° 26.98' W	12° 05.40' N	5091
11 - 6	MUC	050° 26.98' W	12° 05.42' N	5090
12 - 3	MUC	066° 50.00' W	19° 46.01' N	8336
12 - 5	C-EBS	066° 50.18' W	19° 49.76' N	8336
12 - 6	C-EBS	066° 45.13' W	19° 48.60' N	8339
12 - 7	MUC	066° 49.99' W	19° 46.00' N	8335
13 - 2	MUC	067° 09.28' W	19° 43.81' N	8350
13 - 3	MUC	067° 92.85' W	19° 43.81' N	8350
13 - 4	C-EBS	067° 05.92' W	19° 47.00' N	8324
13 - 5	C-EBS	067° 02.62' W	19° 50.12' N	8056
14 - 1	C-EBS	067° 09.44' W	19° 02.08' N	4552
14 - 2	C-EBS	067° 07.86' W	19° 04.55' N	4934
14 - 3	MUC	067° 07.77' W	19° 04.68' N	4924,9
14 - 4	MUC	067° 07.75' W	19° 04.66' N	4924,8

A total of 514 organisms were sampled for biochemical analyses in course of the expedition. We were successful in obtaining comparable samples at the different sites of the VEMA fracture Zone. This accounts especially for Crustacea and Annelida, of which the same genera (possibly species) were found at different stations (Table 7-13). In case of other taxa (e.g., Echinodermata, Mollusca) we were able to sample representative species of different trophic levels which will also allow comparison between the stations.

Table 7-13: Organisms sampled for biochemical analyses at each station.

Station	2_6	2_7	4_8	4_9	6_7	6_8	8_4	9_2	9_8	11_1	11_4	12_5	12_6	13_4	13_5	14_1	14_2	sum
Annelida	3	6	5	6	5	6	6	1	8	2	7	2	13	5	8	2	1	86
Crustacea	9	7	8	14	19	15	27	5	27	7	4	17	24	17	23	36	30	289
Mollusca					2	1	1	1										5
Sipuncula									2									2
Priapula								1										1
Echinodermata		4	26	17	1	1	2		1		1	6	2	3	2		7	66
Chaetognatha				1	1	1		1										4
Cnidaria							1											1
Porifera										1								1
Tunicata										1								1
Algae		1	3	2	2	1	2	2	2	2	2	2	3	4	2	2	2	28
Total sum																		**484**

7.3 Multicorer Deployments

7.3.1 Description of the multicorer (MUC), deployment and distribution of samples

(C. Schmidt, V. Borges, N. Elsner)

7.3.1.1 Gear description

The Multiple Corer (multicorer, MUC) is a gear designed for sampling meiofauna as well as sediment samples (Barnett et al. 1984). The employed multicorer is equipped with 12 transparent acryl-glass-cylinders (tubes), each 62 cm in length, providing up to 12 parallel, undisturbed sediment samples per deployment. Each tube has an outer diameter of 99 mm, and an inner diameter of 94 mm. Consequently, the surface of sediment sample taken with one tube covers an inner area of 69.4 cm². During this expedition, 33 deployments covering 9 stations took place. Figure 7-19 shows the multicorer after sampling. The locations of all deployments are given in the Station List (Section 6).

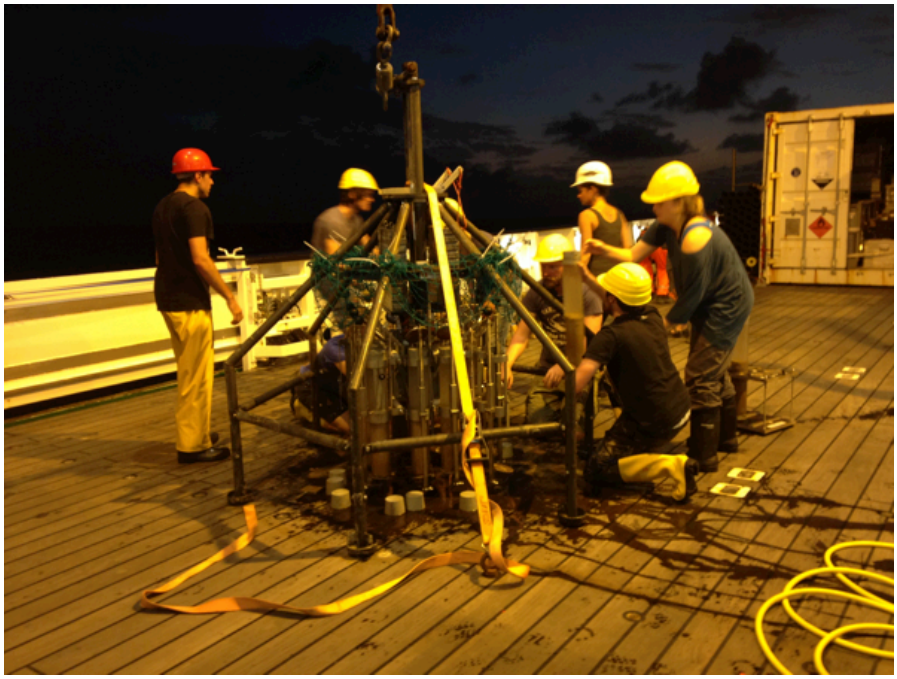

Figure 7-19: The multicorer after sampling. Photo taken by: Marina Malyutina.

7.3.1.2 Deployment procedure

The multicorer was deployed from starboard. The regular deployment starts with lowering at 0.3-0.5 m/sec the first 50 m of cable. At most stations the MAPPR sensor (see Section 7.4.4) was used at 20 m and at 50 m the Posidonia sensor were fixed on the cable. After fixing, lowering was continued with 1.0 m/sec to app. 50 m above the seafloor, where the winch stopped and the MUC remained standing during 1-2 min. Then the MUC was lowered, depending on the bottom and the waves with 0.1 – 0.7 m/sec until the landing on the bottom. When the MUC touched the bottom, 15-20 m of cable were released. The MUC stayed for 1-3 minutes on the bottom. Heaving normally started with 0.5 m/sec, and after the gear was free from the bottom heaving was continued with 1.0 m/sec until the sensors are arrived.

7.3.1.3 Distribution of samples

Multicorer samples were distributed among six research groups. For each deployment, tubes were taken for biodiversity studies, genetics, biochemistry, sediment analyses and taxonomic studies (protists, foraminiferans, nematodes, copepods). The exact distribution and fixation at every deployment can be found in Table 7-14.

Table 7-14: Multicorer deployment, distribution and fixation of tube samples

Core number													
Station	Deployment	1	2	3	4	5	6	7	8	9	10	11	12
A1	2_3	BchemL	Abio	MeioSl	—	MF	—	MDSl	For	MD	MF2	Prot	ProChem
A1	2_4	MD	Abio	MeioSl	MF2	MF	MDSl	BchemU	SedPore	ForSedPore	For	Prot	Prot
A1	2_5	—	—	—	—	—	Abio	MeioSl	MF2	MDSl	MD	ForSedPore	ProChem
A2	4_3	BchemL	Abio	MeioSl	MF2	MF	MDSl	MD	PorMefo	ForSedPore	For	Prot	ProChem
A2	4_4	MD	Abio	MeioSl	MF2	MF	MDSl	MD	—	For	For	Prot	ProChem
A2	4_5	MD	Abio	MeioSl	MF2	MD	MDSl	MD	For	For	MD	Prot	ProtMeio
A3	6_1	—	—	—	—	—	—	—	—	—	—	—	—
A3	6_3	BchemL	Abio	MeioSl	MF2	For	For	MD	MD	MF	MDSl	ProChem	Prot
A3	6_4	MDSl	Abio	For	MeioSl	MF	For	MD	MF2	MD	MD	ProChem	Prot
A3	6_5	MDSl	Abio	MeioSl	MF2	MF	For	MD	MD	For	—	Prot	Prot
A4	8_2	BchemL	Abio	MeioSl	MF2	MF	Protpor	MD	MDSl	For	For	Prot	ProChem
A4	8_5	—	—	—	—	—	—	—	—	—	—	—	—
A4	8_6	—	—	—	—	—	—	—	—	—	—	—	—
A4	8_7	—	—	—	—	—	—	—	—	—	—	—	—
A4	8_10	MDSl	Abio	MeioSl	MF2	MF	MD	MDSl	Prot	For	For	ProChem	Prot
A4	8_11	MDSl	Abio	MeioSl	—	MF	MD	MD	MF2	For	Abio	Prot	Prot
B1	9_3	BchemL	Abio	MeioSl	MF2	MF	MD	—	MD	For	—	BchemU	Prot
B1	9_4	MDSl	Abio	MeioSl	MF2	MF	For	MD	MD	MD	For	Prot	ProChem
B1	9_5	—	—	—	—	—	—	—	—	—	Prot	—	—
B2	11_5	BchemL	Abio	For	MF2	MD	SedPore	MDSl	For	MeioSl	MF	Prot	ProChem
B2	11_6	MD	Abio	MeioSl	MF2	MF	For	MD	MF	SedPore	MD	Prot	ProChem
B2	11_7	MD	Abio	MeioSl	For	MF	MD	MD	MF	For	MF2	Prot	Prot
C1	12_1	MD	—	—	—	—	—	—	—	—	—	MD	—
C1	12_2	—	—	—	—	—	Prot	MD	MD	MD	—	—	—
C1	12_3	Abio	MeioSl	MF	MF	MF	MD	MDSl2	MD	For	For	Prot	ProChem
C1	12_7	Abio	MeioSl	MF	MF	MF	MD	MDSl2	SedPore	For	For	Prot	ProChem
C1	12_8	Abio	MeioSl	MF	MF	MF	MD	MDSl2	—	For	SedPore	Prot	ProChem
C2	13_1	Abio	MeioSl	SedPore	MF	For	MDSl2	MD	MF	MD	MD	Prot	Prot
C2	13_2	Abio	MeioSl	MF	MD	MD	MF	MDSl2	SedPore	For	For	Prot	Prot
C2	13_3	—	MeioSl	MF	MDSl2	MD	MF	MF	Abio	For	For	Prot	Prot
C3	14_3	Abio	MeioSl	MF	MDSl2	MD	MF	MF	For	For	For	Prot	ProChem
C3	14_4	Abio	MeioSl	MF	MDSl2	MD	MF	MF	BiochemU	For	For	Prot	Prot
C3	14_5	Abio	MeioSl	MF	MDSl2	MD	—	MF	MF	For	For	Prot	Prot

Abbreviations:

—	empty or lost core
BchemL	for biochemistery, sliced in 0-1 cm, 1-2 cm, 2-3 cm, 3-4 cm, and 4-5 cm sediment layers (5 samples), reponsible person Lidia Lins
Abio	for abiotic sediment analyses, sliced in 0-1 cm, 1-2 cm, 2-3 cm, 3-4 cm and 4-5 cm sediment layers (5 samples), responsible person Lidia Lins
MeioSl	5 cm sediment layer for meiobenthos, sliced in 0-1 cm, 1-2 cm, 2-3 cm, 3-4 cm and 4-5 cm sediment layers (5 samples); fixed with formol; responsible person Lidia Lins
MF	for meiobenthos 0-5 cm layer (1 sample); fixed with formol; responsible person Christina Schmidt
MDSl	5 cm sediment layer for meiobenthos, sliced in 0-1 cm, 1-2 cm, 2-3 cm, 3-4 cm and 4-5 cm sediment layers (5 samples); fixed with DESS; responsible person Christina Schmidt

For	for study of formaminiferans; picking, RNA preservation solution, and freezing; responsible persons Franck Lejzerowicz and Ivan Voltski
MD	for meiobenthos 0-5 cm layer (1 sample); fixed with DESS; responsible person Christina Schmidt
MF2	for meiobenthos 0-5 cm layer (1 sample); fixed with formol; responsible person Lidia Lins
Prot	for study of protists, responsible person Hartmut Arndt
ProChem	for study of protist, responsible person Hartmut Arndt and for Biochemistery, responsible person Ulrike Minzlaff
BchemU	for biochemistery, responsible person Ulrike Minzlaff
SedPore	Porewater and Sedimentanalyses, responsible person Christopher Schmidt
ForSedPore	for study of formaminiferans; picking, RNA preservation solution and freezing; responsible persons Franck Lejzerowicz and Ivan Voltski and for study of Porewater and Sedimentanalyses, responsible person Christopher Schmidt
PorMefo	Porewater, responsible person Christopher Schmidt and Meiofauna study, responsible person Christina Schmidt
ProtMeio	for study of protists, responsible person Hartmut Arndt and for Meiofauna study responsible person Lidia Lins
Protpor	for study of protists, responsible person Hartmut Arndt and for Porewater Christopher Schmidt
MDSl2	5 cm sediment layer for meiobenthos, sliced in 0-2 cm and 2-5 cm sediment layers (2 samples); fixed with DESS; responsible person Christina Schmidt

7.3.2 Meiobenthic studies with the Multicorer: Does the Mid-Atlantic Ridge serve as a dispersal barrier to meiofaunal organisms? Is the Puerto Rico Trench a biodiversity hotspot?

(C. Schmidt, L. Lins)

7.3.2.1 Objectives

Nematodes and copepods are the most abundant metazoan meiobenthic taxa in many areas of the world's ocean. Also in the deep sea they tend to be dominant and densities can be high, which makes them important players in the benthic food web. However, knowledge on meiobenthic dispersal is still very scarce, especially in the deep sea. In the case of nematodes, the lack of a larval stage enable them only to passively disperse between different environments, although they exhibit active swimming capacities towards a food cue when present in the water column (Lins et al., 2013; Ullberg and Ólafsson, 2003). This study aims to investigate whether the Middle Atlantic Ridge (MAR) offers a physical barrier in dispersal mechanisms from copepods and nematodes by comparing east and west sampled stations. Moreover, data on density and community structure from the MAR and the Puerto Rico Trench are going to be compared in order to elucidate whether trenches can be considered hotspots of biodiversity for these organisms, due to the high organic matter input normally found in these environments. The data of the Puerto Rico Trench will be compared with available material from the Kuril-Kamchatka Trench. Deep-sea regions like trenches, long narrow depressions with a connection to a subduction zone, represent a special ecosystem and are one of the last frontiers in deep-sea research (Jamieson et al., 2010; Ramirez-Llodra et al., 2010). The Kuril-Kamchatka Trench is located in a highly productive boreal region of the northwest Pacific Ocean. Productive surface waters are known to have the potential to lead to higher meiofauna standing stocks in trenches (Danovaro et al., 2002, 2003; Itoh et al., 2011). A literature comparison showed that the lowest values of meiofauna abundances were observed in the Puerto Rico Trench - therefore we expect less abundances than in the Kuril-Kamchatka Trench (Schmidt & Martínez Arbizu, 2015).

7.3.2.2 Work at sea

At all stations, cores were selected for meiofauna community analysis, genetic biodiversity and fatty acid profiles. Meiofauna samples were fixed with Formalin; samples for genetics with DESS. The samples for environmental analyses and fatty acids were stored in -80 °C freezer and will be used to determine pigment concentration, granulometry, total organic carbon, total nitrogen and total organic matter.

7.3.2.3 Preliminary (expected) results

Since extraction of animals and the analysis of environmental variables and fatty acids have to be done in a standardised way in the lab, no preliminary results are available for the meiobenthos. For further treatment, meiobenthic organisms will be

separated from sediments in the laboratory of the German Centre for Study of Marine Biodiversity (DZMB, Wilhelmshaven) and Ghent University (Marine Biology Section, Ghent). Then samples will be centrifuged 3 times at 4000 rpm for 6 min. After centrifugation, the upper fraction containing meiobenthic organisms will be filtered through a sieve of mesh size 32 μm and then washed with fresh water. The concentrate will then be fixed with 4% formalin (if samples were initially fixed with formalin) or with DESS (if samples were initially fixed with DESS). For staining animals, Bengal Rose will be used to allow selecting these animals from other organic remains in the centrifuged sample.

The environmental samples will be used for the analysis of abiotic factors: grain size composition; content of organic carbon, chlorophyll α, phaeopigments, chloroplastic pigment equivalents, total organic carbon, total nitrogen and total organic matter. These data will be used for explanation of possible differences observed in meiobenthic density and community composition in samples taken from different stations.

7.3.3 Diversity and distribution of abyssal and hadal protists along the VEMA-Fracture Zone and Puerto Rico Trench: Environmental massive sequencing, direct counting and cultivation (PROTABYSS)

(H. Arndt, A. Schönle, A. Jeuck, D. Prausse)

7.3.3.1 Objectives

The abyssal sea floor (3,000–6,000 m depth) represents the largest benthic environment on this planet, covering 54 % of the Earth's surface, and emerging evidences point at the dark ocean as a site with a major role in ocean biogeochemistry and an „untapped reservoir" (Arístegui et al. 2009) of high genetic and metabolic microbial diversity. Although, the local diversity of some deep-sea ecosystems has been documented, very little is known about the biodiversity of these systems at greater spatial scales. In fact, a great proportion (> 99 %) of the deep-sea has never been studied, and most of the studies focused on specialized environments, such as vent, ridge or seep habitats. The vast expanses of the deep-sea floor, covered with muddy soft sediments, have received much less attention even though their extent is orders of magnitude greater and are assumed to play a much larger role in marine carbon cycling. Large-scale studies demonstrated a close link between benthic biodiversity and ecosystem functioning (e.g., Danovaro et al. 2008a) and estimated that a biodiversity loss of 20—30 % can result in a 50—80 % reduction of deep-sea ecosystems' key processes and their „consequent collapse" (Danovaro et al. 2008b). In addition, abyssal planes are of increasing interest for mining activities since mining methodology has been significantly improved within the last decade and there is a growing interest for mineral extraction from abyssal regions (van Dover 2011, Collins et al. 2013). Most actual mining activities are those regarding harvesting abyssal nodules or petroleum production from deep-sea regions.

It is therefore very important to study deep-sea ecosystems and especially deep-sea biogeographic domains as well as the mechanisms driving diversity in the deep sea before deep-sea ecosystems are irreversible damaged. Our previous studies of deep-sea nanofauna (Arndt et al. 2003, Hausmann et al. 2006, Scheckenbach et al. 2005, 2006, 2010) have documented that there should exist a specific abyssal nanofauna - including some strange morphologies (e.g. *Meteora sporadica*, Hausmann et al. 2002) - which may contain a large number of endemic taxa (Nitsche & Arndt 2007, Scheckenbach et al. 2010). To study the biodiversity and biogeography of deep-sea microbial communities, environmental sequencing combining next generation sequencing and sequencing of isolated deep-sea organisms is the method of choice at the moment (see Scheckenbach et al. 2010). We found relatively similar communities of kinetoplastids in the range of hundreds and thousands of kilometers for the South-West Atlantic (Argentine and Brazil Basin) and the South-East Atlantic (Angola and Guinea Basin) (Salani et al. 2012). We recorded statistically significant differences among several communities (i.a., the Mediterranean communities) indicating that deep-sea communities of kinetoplastids are shaped at larger spatial scales by differences in environmental conditions.

While these previously mentioned studies originated mainly from clone libraries based on Sanger sequencing, we established a protocol to study deep-sea protists also

by the use of next generation sequencing in combination with direct counts and cultivation techniques. A major problem up to now is the quality check of obtained sequences and the comparison of sequence reads with a thoroughly established sequence library with well-established assignment to modern systematics (e.g. Adl et al. 2012).

Sampling the abyssal protists from various deep-sea basins will allow for a global comparison of deep-sea nanofauna (for a general scheme of the intended investigations see Figure 7-20). Onboard we intended to obtain undisturbed multicorer samples, isolate cultivable protists, use high pressure chambers to study the influence of pressure on selected protists, and fix samples for RNA and DNA analysis (active organisms) in the home laboratory for next generation sequencing. Molecular characterization of isolates in Cologne should allow for a quality check of deep-sea sampling and the identification of indigenous deep-sea protists. We expect a new understanding of the role of nano- and microprotists (heterotrophic flagellates, amoebae and ciliates) which seem to be more species rich than the traditionally considered foraminiferans and should be distinct from other marine habitats. We anticipate that lower diversities of protists compared to prokaryotes (but higher than meio- and macrofauna) will offer a useful indicator for disturbances of processes in the deep sea.

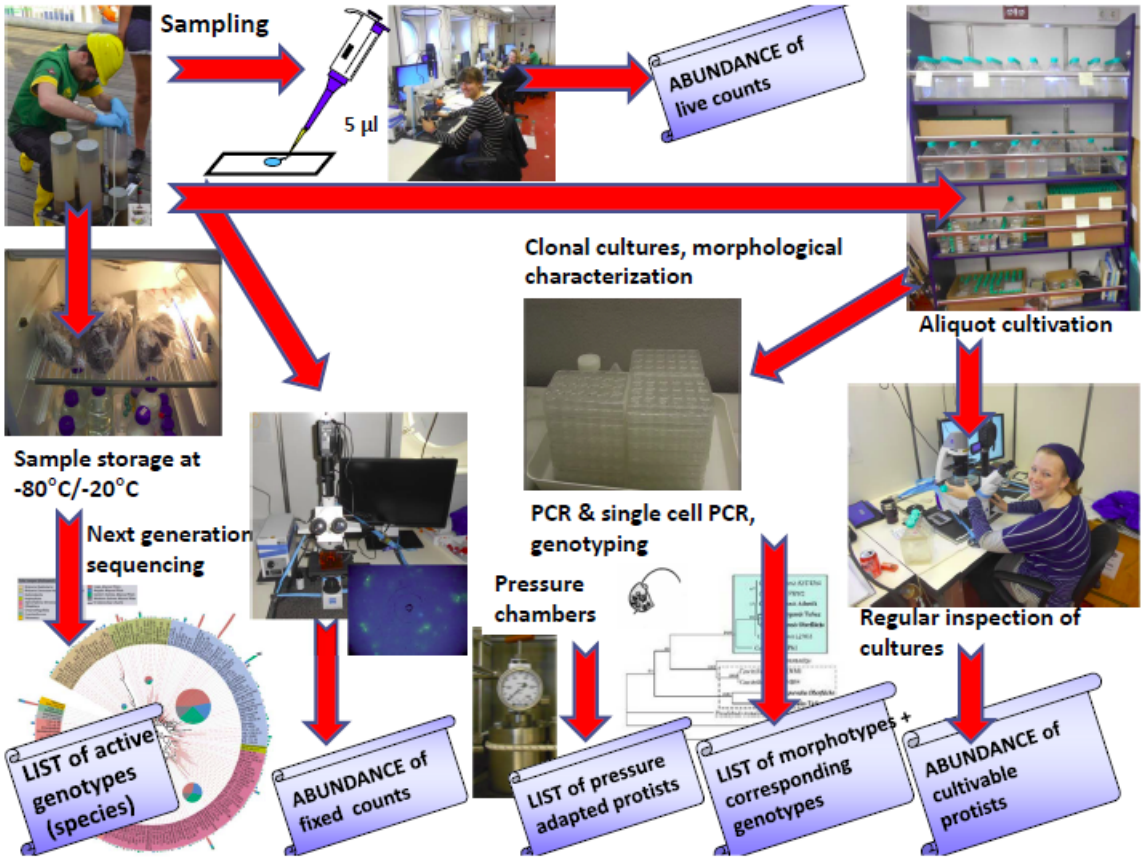

Figure 7-20: Combination of six different techniques to approach the abundance and diversity of microbial eukaryotes during deep-sea investigations of VEMA Transit.

7.3.3.2 Onboard investigations

Sampling: Undisturbed sediment cores obtained by a multi-corer system (diameter of an individual core 93mm) were used for quantitative and qualitative analysis of abyssal and hadal nanobenthos. We were able to take samples at all routine stations incl. two hadal stations in the Puerto Rico Trench. Once on deck, cores were immediately investigated. Samples were taken from the overlaying water as well as from different sediment layers (upper 5mm, 5-15mm, 15-25mm and 25-35mm). Immediately after sampling, sets of sediment subsamples were transferred into RNAlater for later molecular biological studies of active protists by later investigations of rRNA (e.g., Stoeck et al., 2007) and to 70% ethanol (stored at -80°C) for later studies of rDNA of all microbial eukaryotes. The high-dispersal capacities and the possibility to form resting stages of many nanoprotists make it difficult to discriminate surface derived protists using only rDNA.

Another set of sediment subsamples was fixed with formaldehyde, stained with fluorescent dye and filtered on 0.2 µm membrane filters for epifluorescence counts of nanofauna. For additional quantitative estimates, two methods were used: live-counting of untreated samples and cultivation of defined aliquots of the sample. The direct counts served as an estimate of deep-sea protistan abundance and were carried out within a few minutes after sampling in a miniaturized version of a Sedgewick-Rafter chamber filled by a calibrated micropipette. Inspections and counting of 5-10 µL subsamples of the sediment suspension was done using ZEISS upright microscopes.

Cultivation of deep-sea protists: Defined aliquots of the sediment samples were cultivated using the liquid aliquot method (Butler and Rogerson 1995). The liquid aliquot method should serve as an estimate of the abundance of cultivable nanoprotists. Subsamples of a few milliliters of the sediment suspension were added into 50ml tissue culture flasks. In addition, 500ml aliquots of the overlaying water were incubated in tissue-culture flasks (Sarstedt). All cultures were supplied with sterilized quinoa grains. Culture flasks and plates were incubated at 20°C, inspections were carried out using an inverted microscopes (200-400x magnification) every 3-4 days. The number of culture vessels containing a certain species allowed for an estimate of the abundance of cultivable active organisms/cysts.

Without the possibility to sample and cultivate the organisms under deep-sea conditions, culture-dependent studies are generally biased and can only be added to clone library studies in having the possibility to consider also some rare taxa in the study of deep-sea biodiversity and biogeography (Pedros-Alio 2006). In addition, clone library or next generation sequencing (NGS) studies are worthless without a control indicating that the genotypes found stem from organisms really living in the deep sea. The cultivation of microbial eukaryotes originating from the abyss and the hadal region offered the unique possibility to study functional aspects of deep-sea communities in the laboratory at home. There are only a very few cultures of deep-sea organisms available world-wide, most of them are cultivated in our laboratory.

Pressure tolerance of protists and selection of deep-sea isolates: Survival of a *Salpingoeca* strain (Choanoflagellata) isolated from the deep sea was studied in a

newly designed pressure chamber where protists could be observed under an inverted microscope at increasing hydrostatic pressure up to 420bar.

7.3.3.3 Preliminary results

The preliminary results of our study may be summarized as follows: A) For the first time, it was possible to determine **living** nanoprotists from the abyssal sea floor from depths >5,000m. Abundance estimates reached relatively low values, though comparable with earlier studies from other deep-sea basins up to depth of <5,000m. B) Abundance estimates of cultivable species during VEMA Transit were relatively similar to those obtained for the deep-sea basins of the Southern Atlantic (ME 63/2, ME 79/1) and Pacific (SO 223T). C) Even among the cultivable protists new species were recorded indicating that we just begin to understand the nanofauna diversity of the deep sea. D) For the first time nanoprotist samples could be collected from the hadal of depth >8,000m. E) Polar populations of cold adapted acanthoecid choanoflagellates were thought to be separated by the warm surface waters of the tropics. For the first time we could identify a *Stephanoeca*-like acanthoecid from 5,300m depth indicating the potential transport of members of this choanoflagellate group via the deep bottom waters.

Previous studies showed that morphotypes of protist taxa, which we also found during the present cruise, consist of a large number of hidden genotypes. To test this hypothesis, clonal cultures of different nanoprotist species from the mid Atlantic abyss were established onboard and will be transported to Cologne to be characterized by molecular techniques.

As a preliminary result, the following genera of cultivable heterotrophic flagellate taxa have been recorded from VEMA Transit deep-sea basins (>5,000 m depth): *Amastigomonas, Bodo, Caecitellus, Cafeteria, Neobodo, Pseudobodo, Rhynchomonas, Salpingoeca, Stephanoeca, Spumella,* and several undetermined Cercozoans. Some representatives are shown in Figure 7-21. We found several species which have to be further studied in detail including some potentially new species. Preliminary direct counts revealed ~10-100 nanoprotists per cm^3 as a minimum estimate of active nanoprotists. The qualitative and quantitative studies complemented our earlier cultivation based studies of deep-sea sediments from the Southern Atlantic, Mediterranean and Pacific. Abundance estimates were in the same range as those obtained from the Mediterranean abyssal plains and they were significantly higher than estimates from Pacific and Southeast Atlantic deep-sea basins.

In addition to life counts and liquid aliquot cultivation techniques, sediment samples were collected for subsequent mass sequencing of eukaryotic protists in Cologne (fixed with RNAlater and ethanol). Our aim is to establish a clone library of heterotrophic flagellates from the deep-sea sediments to analyze the genotype diversity independent from the cultivation approaches. We expect new genotypes that do not appear in surface waters and will probably never appear in cultures. The cultivated strains should serve as a valuable qualitative test for the established clone library. The combination of different methods offers a unique possibility to receive

detailed information on nanofaunal life in the abyssal plains and a hadal region of the Atlantic.

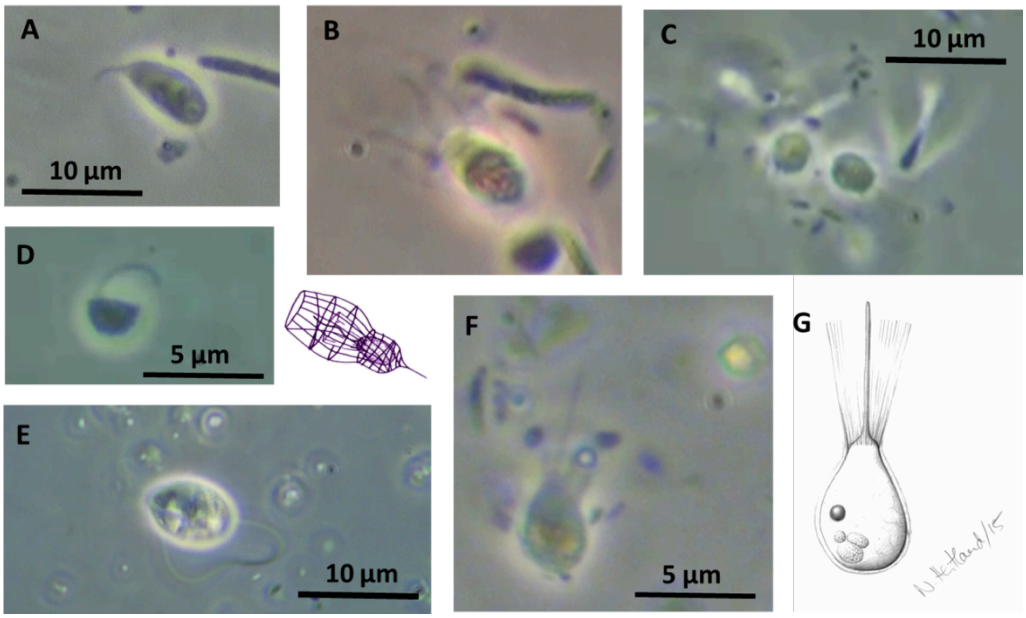

Figure 7-21: Heterotrophic nanoflagellates of different genera isolated from depths of more than 5,500m during SO-237 cruise. A) Amastigomonas sp., B) and C) first records of acanthoecids: Stephanoeca-like choanoflagellate, D) Cafeteria sp., E) undetermined euglenid, F) and G) Salpingoeca-like choanoflagellate. Live observations (A, B, C, D, E, F) and a drawing by Nele Heitland (G).

Additionally, experiments were carried out onboard to investigate survival and reproduction of nanofauna exposed to various hydrostatic pressures. A pressure generating system was established based on a hydraulic pressure intensifier (Figure 7-22, left). Incubations included either a) deep-sea sediment (Station A3, MUC1) exposed for three weeks immediately after sampling to 420bar or b) deep-sea nanofauna cultures (*Salpingoeca*) isolated during the cruise. Isolates were pre-cultivated in 50 ml tissue culture flasks. The latter experiments were run for 10-24 hours. In addition, c) Protistan communities inhabiting surface floating *Sargassum* kelps were exposed to deep-sea pressure conditions. The sediment samples exposed to high pressures did not show significant growth of protists detectable after 3 weeks of exposure. However, the pressure experiments, where protist communities isolated from *Sargassum* kelps were exposed to high pressures showed that several protists survived a hydrostatic pressure of up to 400bar. These are the first indications that *Sargassum* protistan communities might be transported to the deep sea alive or in cysts and might potentially contribute to deep-sea communities. This phenomenon will be studied in more detail in near future. Preliminary studies of the pressure tolerance of the isolated deep-sea clone showed a survival up to 420bar.

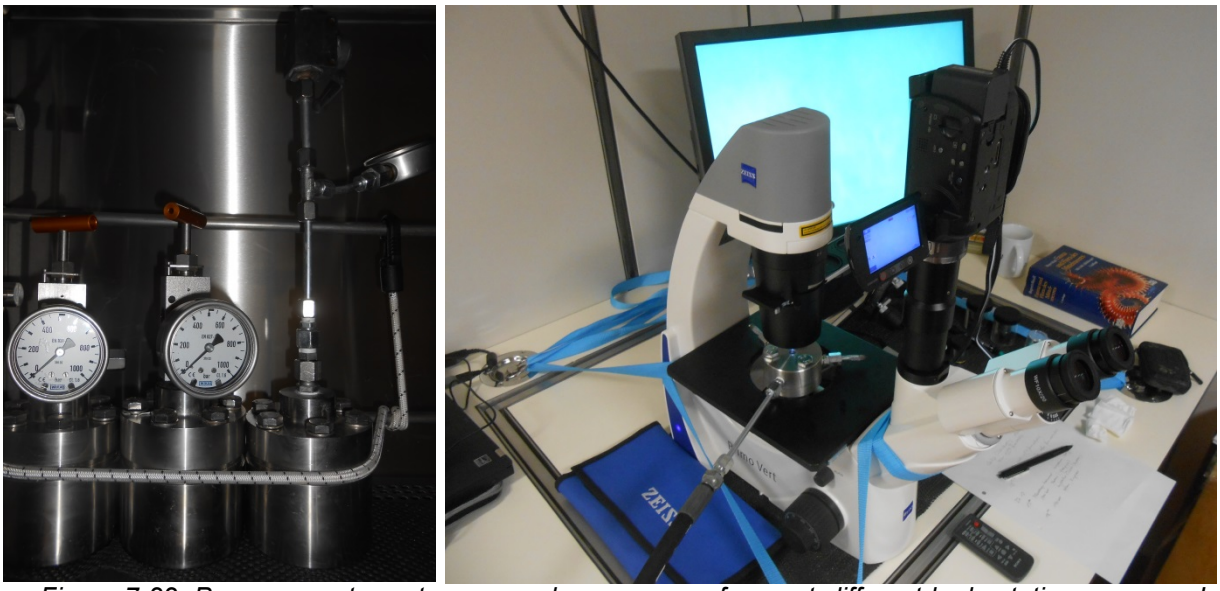

Figure 7-22: Pressure systems to expose deep-sea nanofauna at different hydrostatic pressures. Left: Pressure chambers used to expose sediment samples up to 420bar. Right: Pressure chamber for light microscopic studies on board to investigate the resistance of Sargassum protist communities to deep-sea pressure.

In cooperation with the group of Angelika Brandt, epizooic ciliates were investigated on deep-sea isopods. It seems that there is a very selective population of crustacean species with specific ciliate species (Figure 7-23). This phenomenon will be in our focus for further collaborative investigations in our laboratories in Hamburg and Cologne.

Figure 7-23: Isopod Eurycope *from Station A2 with attached epizoan peritrichs (isopod fotographs by Torben Riehl and Saskia Brix-Elsig)*

7.3.4 Molecular diversity of the deep-sea Foraminifera and related protists across the Atlantic: phylogenetics and environmental sequencing

(Lejzerowicz, F., Voltski, I.)

Foraminifera is a highly diversified group of single-celled eukaryotes that are among the most abundant organisms thriving in deep-sea sediments, where they contribute enormously to ecosystem functioning and biogeochemical cycles (Gooday 1993). Their extant diversity, biology and biogeography remain poorly understood and the deep-sea environment conceals the existence of completely new, highly divergent lineages of the Foraminifera. Molecular studies of Foraminifera yielded are able to provide invaluable insights into these unknowns, especially since the advent of high-throughput sequencing (HTS) technologies. We base our research on sequence data generated either after the sorting of Foraminifera specimens from freshly sieved sediment followed by single-cell DNA extractions (Pawlowski et al. 2005, Habura et al., 2008), or after the extraction of the total environmental DNA (eDNA) and RNA (eRNA) content of frozen raw sediment samples (e.g. Pawlowski et al. 2011).

7.3.4.1 Molecular and morphological diversity of deep-sea Foraminifera

Rationale: The transects of stations along the Vema Fracture Zone and in the Puerto Rico trench planned for the cruise SO-237 provide a remarkable opportunity to sample and collect foraminifera inhabiting several different deep-sea biomes. In particular, we focuse our effort on single-chambered foraminifera, or monothalamids: a diverse group radiating early in the evolution of the Foraminifera (Pawlowski 2003) and accounting for the largest part of their unknown diversity in the Deep Sea (Lecroq et al. 2011). For this reason, and for strengthening the link between the sequence data and taxonomic databases the search for morphological information and accelerated description of new species is necessary.

A major challenge for robust molecular phylogenetic analyses is to ascertain that the sequenced DNA molecules originate from the identified specimen. Indeed, in a recent study conducted in the Mid-Atlantic Ridge area have been reported unknown foraminiferal species squatting the test of well-described, dead species (Gooday et al. 2013). This is particularly challenging for the large Foraminifera under focus during SO-237: large suspension-feeding monothalamids and xenophyophores. Indeed, these organisms agglutinate large amounts of sediment particles for their test construction, on which extraneous DNA material might be adsorbed. On the other hand, the inherent variability of rDNA and ITS regions might provide new insights into the intra-individual and population genetic divergence of the deep-sea monothalamids, as was previously shown for a few deep-sea rotaliids (Pawlowski et al. 2007).

Aims: We collected single-cell Foraminifera to (1) provide morphological and molecular characterisation and incorporate new species into the World Register of Marine Species and the Foraminifera Barcoding Database (http://forambarcoding.unige.ch) (2) expand our rDNA reference database for improved assignment of environmental DNA sequences and (3) perform single-cell DNA analyses assorted with detailed morphological/histological examinations in order to characterize

the unexpected diversity that could be sequenced as “natural contaminants” of the DNA of large agglutinated species. (4) Unambiguously demonstrate the phylogenetic placement of enigmatic foraminifera-like organisms (the Komokiacea and komoki-like species).

Work at sea: We collected surface sediment samples from abyssal and hadal depths using the multiple corer. The top 1-2 centimeters of one to three cores per station were sieved at 4°C upon recovery and living foraminifera were picked under stereomicroscopes. Living specimens were photographed and either (i) dried (for hard-shelled calcareous species), or immersed in (ii) RNAlater® to preserve morphological characters as well as DNA and RNA molecules or (iii) stained with the CellTracker™ Green fluorescent dye at 4 ºC and fixed with 4% formaldehyde for morphological examination. Significant part of material was also obtained from the thermally insulated cod ends of the epibenthic sledge (C-EBS), accounting for the majority of komokiaceans and some large monothalamids.

Preliminary results: In total, we isolated 726 specimens in RNAlater, mostly monothalamous foraminifera and komokiaceans (Figure 7-24). Additionally, ~300 specimens were stored collectively in RNAlater, to be sorted in the lab. Some representative specimens are shown in the Figure 7-25.

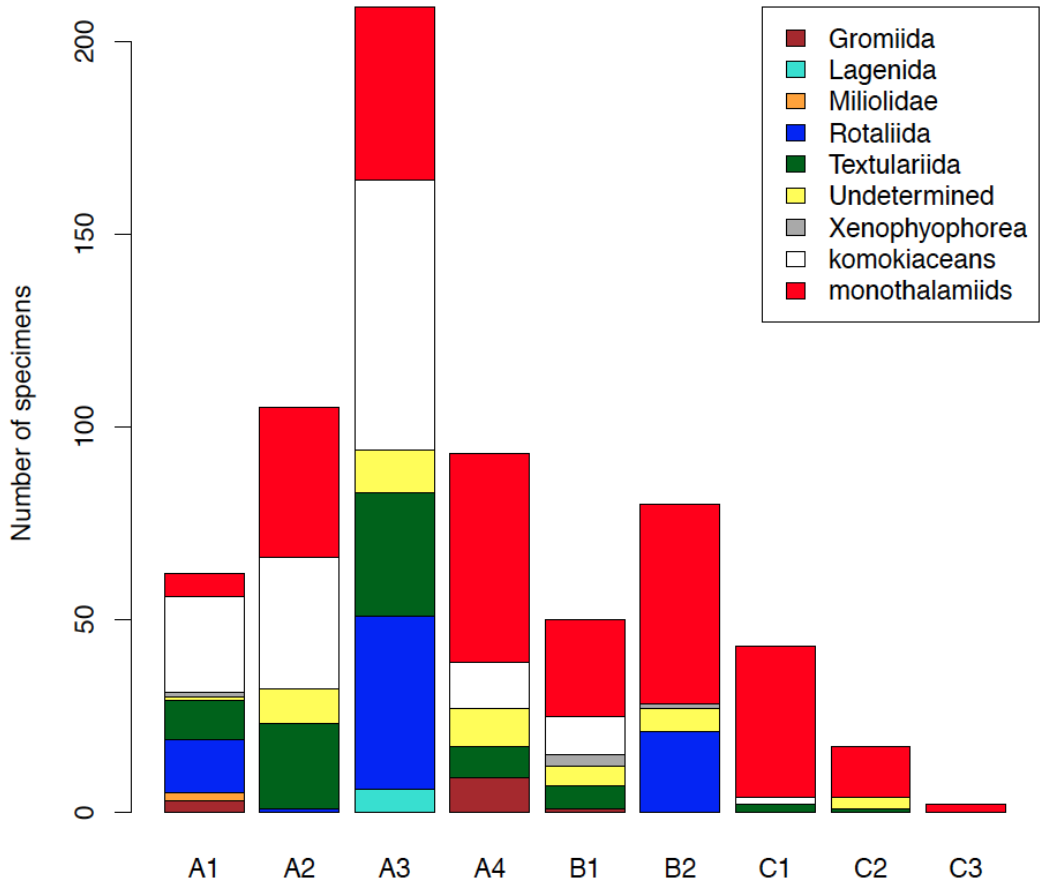

Figure 7-24: Taxonomic composition of the specimens collected for DNA analyses during SO237. Only higher-level Foraminifera taxonomy is shown.

Large suspension-feeding monothalamids were common in multiple corer samples at stations A3, B1 and B2. All of these species did not belong to any known species, and we used temporary names to designate them. The bizarre-looking species ‘Umbrella_SO-237’ (Figure 7-25A) was found at station A3; the peculiar feature of it being the large disk-shaped superstructure raised on a stalk and bearing greenish phytodetritus patches on its upper surface. Two other prominent species, ‘Conifer-B2’ and ‘Hard-B2’ were standing on the sediment surface and ferro-manganese crust pieces in man cores from the station B1. The latter one strikingly resembled a shallow-water Antarctic species *Notodendrodes antarctikos*.

Figure 7-25: (A) Undescribed suspension-feeding foraminifer 'Umbrella_SO-237', (B) Nemogullmia sp. *(organic-walled monothalamous foraminifer); (C)* Hormosinella distans *(a textulariid), (D)* Eratidus sp. *(a textulariid), (E)* Rhizammina*-like foraminifer, (F)* Baculella *sp. (a komokiacean); (G)* Bathysiphon sp. *(monothlamous foraminifer), (H)* Gromia sp. *(a gromiid), (I)* Normanina sp. *(a komokiacean)*

Representatives of the enigmatic deep-sea genera *Nodellum* and *Chitinosiphon* were common in many multicorer samples, with significant numbers found in the top fluffy layer of some sediment cores. This material will help to resolve the challenge of obtaining the genetic data for these foraminifera.

7.3.4.2 Diversity and biogeography: high-throughput sequencing of eDNA and eRNA

Rationale: There is molecular evidence that benthic species might be able to disperse across the Atlantic Ocean latitudes (Pawlowski et al. 2007), but no eDNA data exists to document longitudinal dispersal patterns across the Mid-Atlantic Ridge. Additional geographic information on species biogeography could help testing the hypothesis that the deep sea represents a continuous, homogeneous ecosystem.

Moreover, the suggestion that geological features observed in the Mid-Atlantic area may support significantly higher levels of diversity than adjacent abyssal plains (Priede et al., 2013) could readily be tested for the micro-eukaryotes using the eDNA sequencing of numerous samples. High-throughput sequencing (HTS) of eDNA proved efficient for the characterization of micro-eukaryotes in the deep sea, as inconspicuous species could be included (Lecroq et al. 2011) and numerous samples could be processed simultaneously (Lejzerowicz et al., 2014). Moreover, it is possible to restrict diversity estimates to active species by analyzing eRNA molecules (Lejzerowicz et al., 2013), and thus to avoid artifacts due to the extreme abundance of extracellular DNA (Dell'Anno and Danovaro 2005) from dead cells and deposited phytodetritus. The response to phytodetritus pulses differs among species of benthic foraminifera (Enge et al. 2011). Sampling the trench area offers the opportunity to characterize this response at different oceanic depths.

Aims: Our main objectives are (1) to provide faithful estimates of the micro-eukaryotic richness and diversity occurring at abyssal to hadal depths based on highly replicated, robust HTS data, (2) to describe biogeographic and cosmopolitanism patterns related to the dispersal of Foraminifera across the Mid-Atlantic Ridge in order to document species dispersal propensities and distances and (3) to describe the vertical distribution of inconspicuous Foraminifera in deep-sea sediments of different depths and thus exposed to different pelago-benthic coupling regimes in order to further understand the response of benthic species to organic enrichment.

Work at sea: At each station three sediment cores were sub-sampled (three multicorer deployments, one core per deployment) to account for small-scale heterogeneity patterns during the investigating of large-scale cosmopolitanism. From each core surface (0-1 cm), three sub-samples were taken for DNA and RNA-based diversity analyses. At trench stations, two undisturbed sediment cores (from two separate deployments) were sub-sampled downcore at a rate of 3 replicates at each of the first five 1-centimeter layers. We always used disposable spatulas and gloves (and ethanol-rinsed slicer for downcore sub-sampling). The sediments were immediately frozen at -80 °C to ensure RNA preservation.

7.4 Geology and Bathymetry

7.4.1 Rock sampling

(K. Zoeller, D. Palgan)

A total of 7 dredges were conducted on SO237, all but one were successful in retrieving samples of various seafloor lithologies. Additionally, samples were collected in the gravity corer and EBS. Lithologies collected include basalt, gabbro, serpentinite, carbonates, sedimentary rocks (e.g. mudstone), and Mn-nodules/crusts. Refer to Apendices C and D for detailed sample descriptions and photos.

Station Nr.	Equipment	Latitude/ Longitude Date	Water Depth (m)	Dredge location description	Sample description
3-1	Dredge	Start: 10°39.10'N 25°6.20'W End: 10°39.60'N 25°05.30' W 21/12/14	Start: 5143 End: 4879	N-S trending ridge: Elevation difference of ~250 m with a slope of ~27º	Mn-nodules and crusts: predominantly balls of carbonate with a crust of Mn (thickness varies from <1 cm to 3 cm). Mn-crusts of varying thickness (3-7 cm) are sampled. No oceanic crustal rocks were sampled.
5-1	Dredge	Start: 10°22.49'N 32°13.01' W End: 10°22.87'N 32°12.75' W 29/12/14	Start: 5537 End: 5005	Scarp-like feature, a W-E trending uplifted section of ocean crust. Total elevation difference of 1284m (however it was not all dredged), with a slope of ~31º.	Dredge was half full of samples of varying lithologies. Basalts: lavas and dikes, gabbros, breccias, mudstone, sandstone, Mn-nodules, and carbonates were all present. Most dominant rock type was basalt (altered). A large piece of highly altered gabbro clogged the dredge; therefore additional rocks could not be sampled.
7-1	Dredge	Start: 10°13.62'N 36°31.99'	Start: 5063 End:	Scarp-like feature, a W-E trending	5 samples collected in total. All samples are basalt, however with

		W End: 10°13.76'N 36º31.85' W 03/01/15	4760	uplifted section of ocean crust. Total elevation difference of ~500m (however it was not all dredged), with a slope of ~50º.	varying degrees of alteration. Some fresh glass may be present, along with some fresh phenocrysts.
8-9	Gravity Corer	10º42.79'N 42º41.76' W	5176	Base of cliff, located near the Biology Dredge track	Small, pebble sized, fragments of serpentinite
8-13	Biology Dredge	Start: 10º42.65' N 42º41.89' W End: 10º42.82' N 42º49.22' W 08/01/15	Start: 5173 End: 5154	Dredge dragged along seafloor (base of Vema Ridge) in attempt to sample clams in hydrothermally active area	Empty
9-2	EBS	Start: 11º40.19'N 48º00.80' W End: 11º40.33'N 47º59.91' W 11/01/15	Start: 5050 End: 4925	Sampling occurred in transform valley, EBS became stuck on the W side of a N-S trending ridge crossing the transform valley.	Mn-nodules were collected. Varying in size, 3-15 cm in diameter. All samples that were cut were "real" Mn-nodules, almost all Mn with layering textures. The nucleus varied, some were rock fragments, some were mud particles or carbonate, and some are unknown.
10-1	Dredge	Start: 11º39.96'N 48º20.91' W End: 11º40.44'N	Start: 4247 End: 3625	Scarp-like feature, a W-E trending uplifted section of ocean crust. Total elevation	Dredge returned to ship damaged- no samples collected

		48º19.56’ W 14/01/15		difference of ~600m (however it was not all dredged), with a slope of ~17º.	

7.4.2 Gravity Corer

(Chr. Schmidt)

7.4.2.1 Gravity Corer and Pore water chemistry

During cruise SO237 sediment and pore water samples were taken at 10 stations with a 5 meter Gravity Corer (GC) at an interval of 20 cm, and 6 stations with a Multicorer (MUC) at an interval of 2 cm. 6 of the GC stations were located east and 1 west of the Vema Transform;- 3 GCs were deployed in the Puerto Rico Trench. Sampling sites were selected based on the bathymetry data collected during the cruise. The GC positions were located near to the edge of the sediment basin as this was considered a more likely site for fluid flow. The MUC positions were located in the central part of the sediment basin. The weight for the Gravity Corer was reduced from 1.3 tons to 1 ton at 3 stations due to very soft sediment being sampled to avoid losing the top of the sedimentary section. The deployments and recoveries are summarized in Table 7-15.

Table 7-15: Overview about deployments for pore water chemistry during SO2237

Station	Latitude	Longitude	Depth [m]	Recovery [m]	Samples
2-2 GC1	10°43,11N	25°03,88 W	5515	4,41	22
4-6 GC2	10°24,84N	31°04,54W	5805	5,00	19
4-10 GC3	10°27,48N	31°05,31W	5818	5,00	19
6-6GC4	10°21,02N	36°57,60W	5135	5,00	25
8-9GC5	10°42,67N	42°41,75W	5154	empty	0
8-12GC6	10°42,79N	42°41,76W	5176	3,35	15
9-7GC7	11°32,00N	47°51,64W	4941	empty	0
12-4GC8	19°50,20N	66°50,30W	8323	1,44	6
12-10GC9	19°48,81N	66°58,39W	8316	empty	0
13-6GC10	19°48,63N	66°58,43W	8321	empty	0
2-4MUC2	10°43.11N	25°03.89 W	5517	0,36	17
4-3MUC4	10°25,11N	31°04,61W	5771	0,38	19
8-2MUC11	10°42,59´N	42°40,99´W	5121	0,36	19
11-6MUC	12°05,42´N	50°26,98´W	5091	0,28	13
12-7MUC	19°46,00´N	66°49,99´W	8338	0,42	21
13-1MUC	19°43,82´N	67°09,30´W	8349	0,4	20

7.4.2.2 Geochemical analyses.

To extract the pore water from the sediment, rhizons were used to minimize contamination with atmospheric oxygen. Subsamples for subsequent analyses of major anions, cations and specific isotopes were taken and stored in a 4°C cold room.

From each core sediment samples were taken for methane and physical property analysis.

Analyses for Total alkalinity (TA) were carried out on board using a METROHM Titrationunit SIS665. The TA was determined by titration with 0.02 NHCL using a methyl red indicator. The titration vessel was bubbled with argon to strip any CO_2 or H_2S during the titration. The IAPSO seawater standard was used to check the reproducibility and accuracy of the analyses. The chemical analyses followed standard procedures as describe on the GEOMAR webpage (http://www.geomar.de/forschen/fb2/fb2-mg/benthische-biogeochemie/mg-analytik).

7.4.2.3 Preliminary Results

Figure 7-26 shows various TA depth profiles. At most of the stations along the Vema Transform fault TA values show only a slight increase of sediment depth. This is characteristic for deep-sea sediments, which receive low amounts of degradable organic carbon, resulting in low mineralization intensities. GC6 at station 8-12 shows a distinctively different profile. TA increases up to 12 meq/L, indicating enhanced mineralization processes at this site. Since increased organic matter input can be ruled out as potential source seepage of upward flowing fluids –carrying a geochemical signature of geochemical processes occurring at greater sediment and/or higher temperatures - offer a likely explanation for this observation. In the MUC profiles no higher TA was observed.

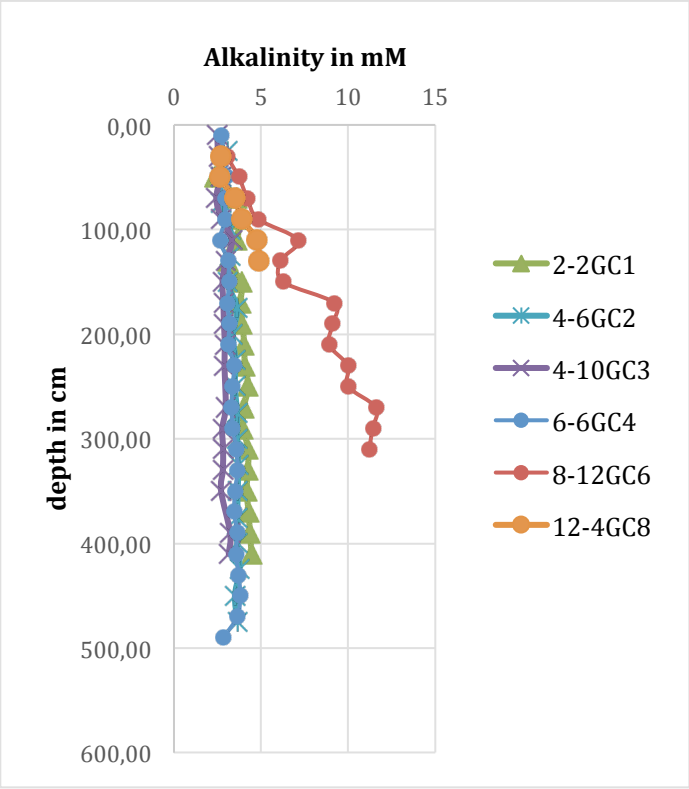

Figure 7-26: Total Alkalinity depth profiles for GC deployments

7.4.3 CTD measurements and water samples from carousel water sampler

(J. Köhler)

During this cruise one full-depth regular conductivity-temperature-depth (CTD) cast, one test cast to 300m depth and one 2.3nm long tow-yo station were carried out using the ships Sea-Bird Electronics, Inc. SBE9plus system with two temperature sensors, two conductivity sensors, a WET Labs ECO fluorescence and turbidity sensor (FLNTURTD), an SBE 43 oxygen sensor and a surface PAR sensor (Biospherical QSR2200). The underwater unit was attached to a carousel water sampler with 24 Niskin bottles.

The tow-yo station (station 8-8, Figure 7-27) was carried out within the transform fault where pictures taken during the Vemanaut cruise in 1987 showed Caliptogena mussels (Cannat et al., 1991), indicating discharge of hydrothermal fluids. During the tow-yo the CTD was repeatedly lowered and heaved between 10m above the seafloor and approximately 300m above the seafloor. Even though no indications for hydrothermalism were found in the CTD data, a MAPR attached to the water sampler showed an anomaly in redox potential (see Section 7.4.4) close to the end of the track.

A list of the number of water bottles closed at each station along with the corresponding depths can be found in Appendix E.

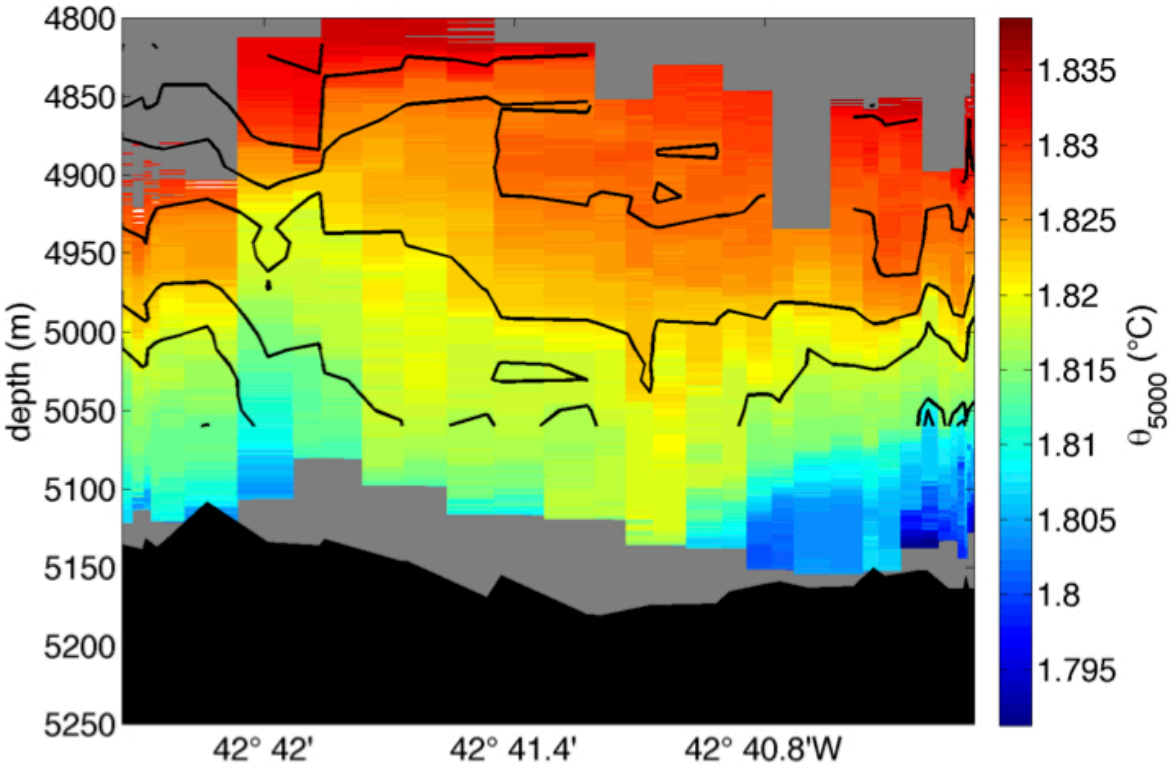

Figure 7-27: Potential temperature measured during the tow-yo shows a hydraulically controlled flow situation along the track.

7.4.4 MAPR deployments

(D. Palgan)

7.4.4.1 Introduction to MAPR studies

During the SO237 cruise we used MAPRs (Miniature Autonomous Plume Recorders) to explore hydrothermal activity and plume existence along the Vema Transform Fault between 25°W and 50°W. MAPRs were used to collect basic physical and chemical parameters of the water column which can indicate presence of hydrothermal plumes: temperature, pressure, optical backscatter (LBSS or nephelometer with Nephelometric Turbidity Units - NTU) and oxidation-reduction potential (Eh). For this purpose we have rented 3 MAPRs from the National Oceanographic and Atmospheric Association (NOAA) - Pacific Marine Environmental Laboratories (PMEL). Their serial numbers were: 53, 54 and 56. We observed the biggest Eh anomalies during one Tow-Yo deployment performed along southern wall of seismically active Vema Transform Fault. During one station, the MAPR No 56 was damaged. The reason is not clear; however, after recovery we observed that two pins in the COM port are missing, indicating that "dummy plug" leaked or sea water was in the port at the time of deployment. During the rest of the cruise the remaining MAPRs worked without problems.

7.4.4.2 Method

For the deployments, MAPRs were lower from the ship either attached to CTD rosette or to the wire above other two instruments used during this cruise: Multi Corer (MUC) and Gravity Corer (GC). During MUCs and GCs deployments, one MAPR was attached 20m above the instrument. During one GC deployment (station 4-4) two MAPRs were attached to the wire (20m and 50m above the instrument) to confirm Eh anomaly recorded by AUV Eh sensor. During the cruise we performed one Tow-Yo CTD deployment, where one MAPR was located at the CTD rosette while second was attached to the wire 30m above it. During MUC and GC stations, MAPR reached various depths (Table 7-16). In order to receive the best quality of measurements, recording interval of 5 seconds was chosen and after each station graphs of turbidity (volts), temperature (^{o}C) and Eh (mV) versus depth (m) were plotted using provided by NOAA Excel *MAPRWorkbook* in order to identify the presence of any anomalies in any of the measured parameters as quickly as possible.

Conversion from voltage values to Nephelometric Turbidity Units (NTUs) can be done with equation:

$$\Delta NTU = (Vr - Vb)/a_n$$

where V_r is the raw voltage, V_b is the background voltage of ambient seawater, not affected by hydrothermal plumes and a_n is a factor unique for each backscatter sensor, which has been determined by the NOAA labs, servicing the MAPR units. In this report we only plotted raw data (roughly 0,02V ≈ light attenuation of 0,01 m^{-1}).

Depth values recorded by individual MAPR are not readjusted to the pressure. Therefore, according to Fofonoff and Millard (1983) they have been recalculated as a function of pressure (db) and latitude (°). In our plots we used corrected depth values. In

total, MAPR were deployed 21 times. No MAPRs were used in the Puerto Rico Trench as their max. depth rating is 5500m.

Table 7-16: Summary of MAPR deployments attached to CTD, MUC and GC. Start logging in 5 sec intervals begins around 5 min before MAPRs gets in the water and ends around 5 min after the recovery

Station ID	MAPR No.	Date/Time (UTC)	GPS Coordinates	Deployed Equipment	Water Depth (m)	Comments
1-1	53	18.12.2015 19:56-23:45	10°38.092'N 25°3.827'W	CTD	~4785	No turbidity or Eh anomialies
2-2	54	19.12.2014 09:19-13:05	10°43.108'N 25°3.883'W	GC	5515	No Eh anomalie. Many single Neph spikes in upper cast
2-3	56	19.12.2014 12:21-15:56	10°43.120'N 25°3.891'W	MUC	5498	Big Eh and Neph spikes at ~600m depth
4-3	56	26.12.2014 00:58-05:07	10°25.122'N 31°4.621'W	MUC	5772	MAPR demaged. No data
4-3	54	26.12.2014 00:58-05:07	10°25.122'N 31°4.621'W	MUC	5772	Single Neph spikes ~5500m depth
4-4	53	26.12.2014 15:44-19:23	10°24.462'N 31°5.338'W	GC	5805	No turbidity or Eh anomialies
4-4	54	26.12.2014 15:44-19:23	10°24.462'N 31°5.338'W	GC	5805	No turbidity or Eh anomialies
6-1	53	01.01.2015 17:38-21:21	10°20.979'N 36°57.662'W	MUC	5148	No Eh anomalie. Many single Neph spikes in down cast
6-3	53	01-02.01.2015 21:52-01:36	10°21.012'N 36°57.581'W	MUC	5137	No turbidity or Eh anomialies
6-4	53	02.01.2015 01:51-05:14	10°21.022'N 36°57.603'W	MUC	5134	No turbidity or Eh anomialies
6-5	53	02.01.2015 05:30-08:53	10°21.020'N 36°57.607'W	MUC	5136	No Eh anomalie. Single Neph spike at 4900m depth (down cast)
6-5	53	02.01.2015 09:10-12:45	10°21.017'N 36°57.598'W	GC	5135	No Eh anomalie. Single Neph spike at ~5100m depth (up cast)
8-1	53	06.01.2015 06:20-09:54	10°43.563'N 42°41.592'W	MUC	5184	No turbidity or Eh anomialies
8-8	53	-	see Tab. 2	CTD	5178	MAPR on CTD, Eh anomalie during Tow-Yo deployment
8-8	54	-	see Tab. 2	CTD	5178	MAPR 30m above CTD, small Eh anomalie during Tow-Yo deployment
8-9	54	06-07.01.2015 22:54-02:36	10°42.678'N 42°41.752'W	GC	5134	No turbidity or Eh anomialies
8-10	54	08.01.2015 13:24-16:57	10°42.802'N 42°41.762'W	GC	5179	No Eh anomalie. Single Neph spikes in down and up cast
9-3	54	11.01.2015 17:57-19:28	11°41.364'N 47°57.370'W	MUC	4996	No Eh anomalie. Many Neph spikes in down/up cast
9-4	54	11-12.01.2015 22:51-02:39	11°41.370'N 47°57.339'W	MUC	5000	No Eh anomalie. Neph spikes in down/up cast
9-7	54	12.01.2015 09:45-13:05	11°32.006'N 47°51.634'W	GC	4941	No Eh anomalie. Many Neph spikes in down and up cast
11-5	53	14.01.2015 21:38-01:04	12°5.400'N 50°26.980'W	MUC	5091	No significant anomalies

7.4.4.3 Results

During regular casts (with MUC and GC) along older and seismically non-active flanks of the Vema Transform Fault data collected by MAPRs showed no anomalies in temperature, turbidity or oxidation-reduction potential (e.g. Figure 7-28) than could be associated witch hydrothermal plumes.

Slight increase in turbidity at the bottom was observed during deployments in the western bank of the Atlantic, along western extension of the Vema. However, the deviations were too small to be interpreted as hydrothermal plumes. Increase of order of 0,02-0,03 volts could be associated with local ocean bottom currents and/or sediments transport (Figure 7-29).

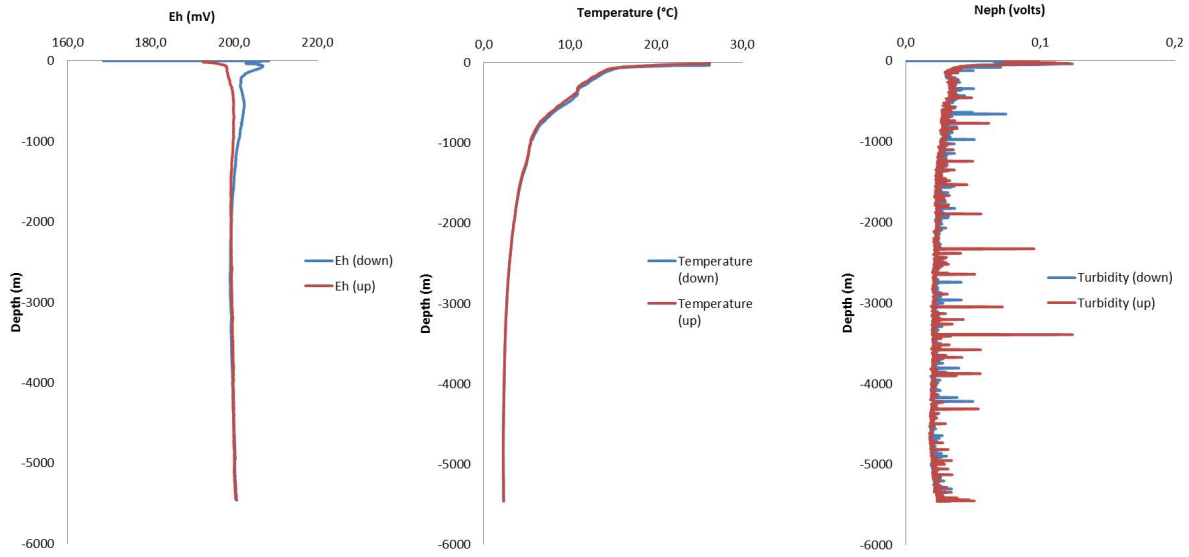

Figure 7-28: Data recorded by MAPR attached to GC at Station 2. Plotted are Eh, temperature and turbidity values against the corrected depth. Blue represents down casts while red up casts. Single spikes in turbidity do not represent presence of a plume

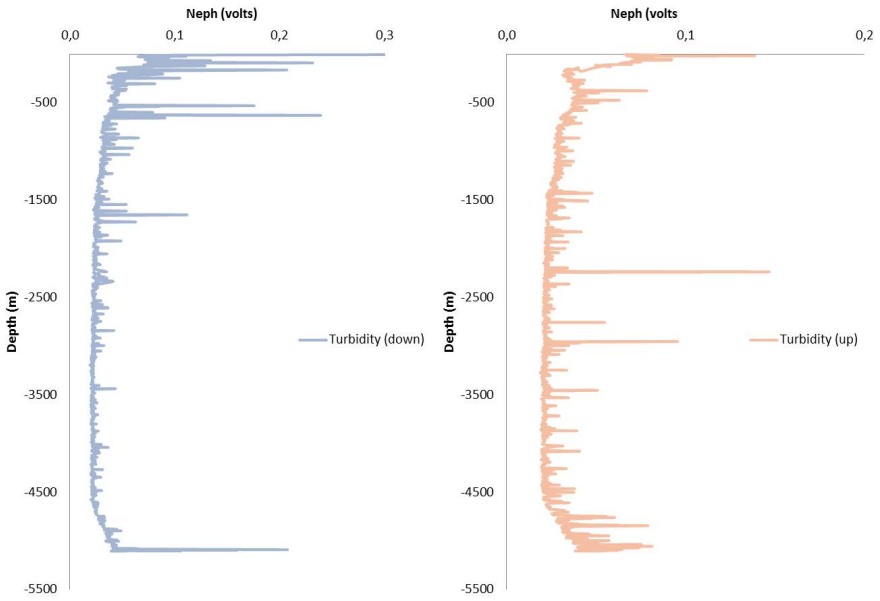

Figure 7-29: Turbidity values (Neph) plotted against corrected depth (m) from Station 12 (MUC). Increase in turbidity at the sea bottom is not typical for hydrothermal plumes. Blue is the down cast while orange is up cast

We performed one Tow-Yo CTD during the cruise at station 8-8. Deployment was located along the northern scarp of the southern part of the Vema Transform Fault (see Figure 3-1, Area A4). It has been suggested that this area can be hydrothermally active based on presence of clam colonies observed during one of the Nautile dives in the area (Cannat et al., 1991). It suggests that warm fluids (no evidence of high-temperature flow) leak along fractures in outcrops of serpentinized ultramafics and that serpentenization can drive local off-axis activity. The summary of this event is presented in Table 7-17.

Table 7-17: Summary of the CTD Tow-Yo deployment. Start logging in 5 sec intervals begins around 5 min before MAPRs gets in the water and ends around 5 min after the recovery

Station ID	MAPR No.	Date/Time (UTC)	GPS Coordinates START	GPS Coordinates STOP	Deployed Equipment	Water Depth (m)	Comments
8-8	53,54	07.01.2015 12:14-22:00	10°42.263'N 42°42.343'W	10°42.792'N 42°40.264'W	CTD (Tow-Yo)	~5200	Eh anomalies in both MAPRs

For this deployment two MAPRs were attached to the equipment. First MAPR (No 53) was located directly on the CTD rosette while second (No 54) was attached to the wire 30m above it. CTD was lowered from the ship until ~10m above the seafloor and then Tow-Yo'ed along ~2.2nm with ships speed 1.0kn. In total, CTD performed 18 down/up casts. Towards the end of the deployment, both MAPRs recorded an Eh anomaly at ~5125m depth. This anomaly is clearly visible in the data from MAPR 53 which was located on the CTD rosette. However, we also observed the presence of anomaly in the data from MAPR 54 (30m above CTD) suggesting that the plum is at least 30m thick (Figure 7-30).

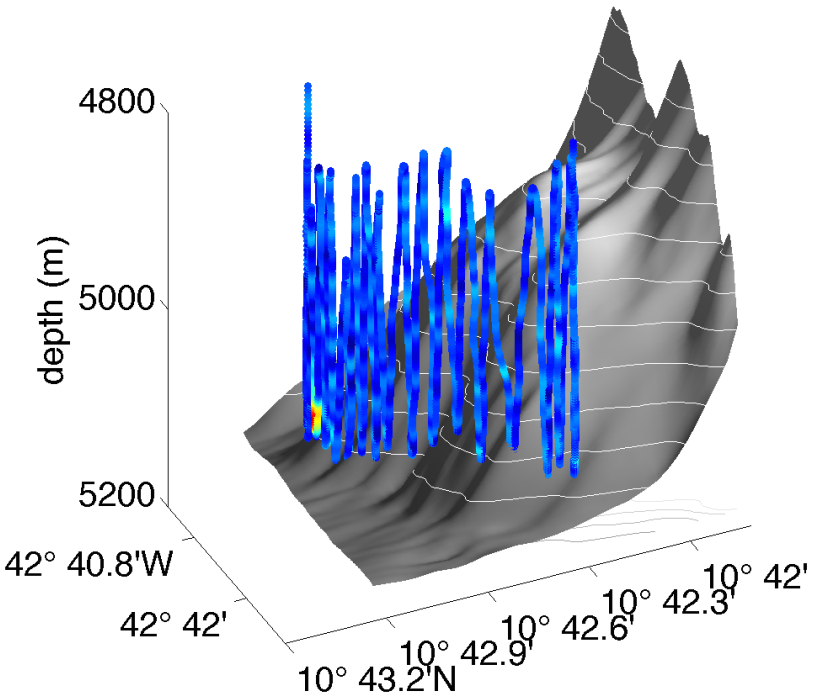

Figure 7-30: Oxidation-reduction potential (Eh) from Tow-Yo CTD deployment at station 8-8. Warm colors indicate Eh anomaly. Grey background represents the seafloor. White lines represent depth

7.4.5 Multibeam Mapping

(N. Augustin, I. Yeo, M. Klischies, D. Metz)

7.4.5.1 Acquisition and Processing

During cruise SO237 extensive multibeam mapping was conducted with the onboard EM122 echosounder system provided by Kongsberg Maritime. The EM122 collects bathymetric data in water depths up to 11,000m with an angular coverage sector of up to 150 degrees (controlled by the operator), a nominal sound frequency of 12 kHz and up to 864 soundings per ping. The system consists of the EM122 transceiver unit, the hydrographic workstation, a motion/heading sensor, a GPS receiver and a sound velocity sensor. Data were acquired using the SIS acquisition software, which output regularly spaced .all files containing the bathymetric and backscatter information. During SO237 the sounding spacing was set to be equiangle (equidistant in the Puerto Rico Trench), meaning data were collected with approximately equal coverage on both port and starboard sides. Sound velocity profiles were extracted from the CTD on the AUV and/or the onboard CTD and were updated at every station (approximately every 4-6° of longitude). After roll, pitch and heading calibration and setting tests during the first transit to define the optimum operating parameters, the majority of surveys were conducted with a symmetrical beam spacing of 60° to both sides, a survey speed of 10 kn and a line spacing of 7nm, giving a typical swath width on the seafloor of around 9nm/17km and yielding bathymetric grids with a final resolution of up to 60m and no gaps. Backscatter data were also logged throughout the cruise and a single small section of water column data in the active transform. In two small areas where the AUV and/or dredge were operating the beam width was narrowed to 45° and the survey speed slowed to 6kn yielding slightly better resolution. During the transits data were recorded but the higher survey speed (12 – 13kn) means data quality is slightly reduced. In the Puerto Rico Trench (PRT) greater water depths required a narrower beam width of 40°/40° yielding a similar typical swath width to earlier surveys of around 11nm/20km.

Post-processing and gridding of data was carried out using the QPS Fledermaus software suite: DMagic and Fledermaus modules for 3D editing and gridding of the data and FMGT for processing and mosaicing the backscatter data. Multibeam data were cleaned manually to remove outliers and then gridded and imported to Global Mapper (Blue Marble), which contained the SO237 GIS project. The final bathymetric maps shown in Figure 7-31 and Figure 7-33 are produced using the texture shading technique (TTS) developed by Leland Brown (2010) merged with minor weighted shaded relief and slope maps to remove any bias associated with the position of a light source. The final grid size of 60 m was chosen to provide the best overview while minimizing artifacts in the outer beams. Smaller grid sizes are possible but roughness in the outer beams is more apparent. Additionally, when data was displayed in Fledermaus a ping appeared to be being ‘dropped’ between data file changes resulting in small (<200 m) data gaps in the gridded datasets. This data is recorded, however SIS does not complete the line during a file change and, as Fledermaus cannot read partial lines, these small data gaps were interpolated for the final grids. Kongsberg can provide a

program to correct this in post processing if required. Backscatter was exported as a single GeoTiff image (Figure 7-32) of all the VEMA survey backscatter (MB01-MB06) and a separate GeoTiff of the Puerto Rico Trench (MB08) area from FMGT at 50m resolution (Figure 7-33). The maps in Figure 7-32 show these data at 100m resolution due to file size restrictions. The raw data, 60m grids of the bathymetric data, geotiffs of the backscatter data as well as .sd files (3D scene files viewable with the QPS iView 4D free software) will be provided to relevant parties after the cruise.

7.4.5.2 Coverage and Geological Description

During SO237 over 111,675 km^2 of the seafloor were imaged at 60m resolution. Just over 94,700 km^2 of this was in the VEMA survey area, 3,225km^2 in the PRT and over 13,750 km^2 of data were collected during the transit between these two survey areas and between the PRT and port in the Dominican Republic.

The VEMA surveys provide a complete, 3 swath wide (approximately 23nm/43 km) transect across the African plate from 25°W to the active spreading centre (Mid-Atlantic Ridge) at 42°W and on the South American plate from the MAR to 48°W. Further, single swath (approximately 9nm/17km wide) data was collected west of this to 50.5°W. The aim of the surveys was to cover the entirety of the VEMA transform fault from the edge of the active transform, already mapped by e.g. Bonatti et al. (2003), east and west to the termination of its topographic expression at 25°W and 50.5°W respectively. Global gravity and bathymetric data (Sandwell et al., 2014) were used to trace the fault off axis. Due to the increased sediment input on the western side of the Atlantic the bathymetric expression of the VEMA is almost non-existent beyond 50.5°W, however on the eastern side it is visible all the way until its intersection with bathymetric features associated with the Cape Verde hotspot. However, as indicated by the global datasets (Sandwell et al., 2014) and now demonstrated by the bathymetric data, the VEMA transform does not take the form of a single fault trace off axis.

Mapping began at the very eastern end of the fossil transform. Picking which fault trace to survey this far away from the site of active movement was difficult as the VEMA appears to be offset at around 34.5°W and, in fact, the area surveyed between 25°W and this point probably covers the trace of a transform parallel with the current VEMA transform, but which dies out at 34.5°W, with the trace of the northern edge of the modern VEMA lying north of the surveyed area and the trace of the southern edge south of it. This pattern of fault traces seem to suggest that the current VEMA transform represents the convergence of two separate transform faults, which progressively migrate towards each other from around 32°W (60 Ma), shortening the spreading segment between them from a length of around 50 km down to nothing by 34.5°W (50 Ma). This shortening is also reflected in the bathymetric expression of the ridge. Until this point the seafloor is characterized by a deep, flat floored valley representing the transform, while the old volcanic seafloor consisting of a series of inward dipping normal faulted blocks, some with recognizable volcanic features. In the shortening segment this regular faulted morphology gives way to more massive, disorganized highs after around 34°W, possibly due to the segment being too short (< 25 km long) to support a magma supply. Other massive highs can be observed throughout the surveyed area but so far

only one, at 29°W, can be positively identified as an oceanic core complex, displaying corrugations on its westward side and a domed profile in cross section. Given the expected sediment cover here (likely to be upwards of 1 km, e.g. Bonatti et al., 2003 and 2005) the fact corrugations are observed is surprising. Even though sedimentation is focused in the valleys and troughs, the sediment cover may be a contributing factor to the low number of core complexes observed in the bathymetric data, although very few of the massive highs displayed a domed profile, the other characteristic feature of a core complex and may instead be inside/outside corner highs, or reflect periods of higher than normal volcanic activity.

The transform itself was surveyed and described by e.g. Cannat et al. (1991), Bonatti et al. (2003) and displays exceptionally steep cliff faces on both the north and south side. The southern uplifted block reaches more than 2000m above the surrounding seafloor and is suggested to be the site of hydrothermal fluid flow (Cannat et al., 1991). No evidence of this is observed in these bathymetric surveys because the resolution is too low. In this area a single swath also covered the southern, active spreading ridge axis of the Mid-Atlantic Ridge. The ridge, marked by inward dipping faults and an increase in depth, appears to be approximately 20 km wide, although the western 10 km of this shows no evidence of volcanic activity despite being almost as deep as the active portion of the axial valley (the eastern side shows bathymetry typical of both flat-topped seamounts and hummocky volcanic terrain).

To the west of the active transform the steep southern ridge of the VEMA disappears at around 45°W and then reappears at 47.5°W before disappearing completely at 50.25°W. Tectonized volcanic terrain is observed on the northern side, with some of the larger ridges crossing the entire flat floor of the axial valley and reaching the southern scarp (for example at 47°W). The undisturbed nature of these contacts makes it hard to distinguish whether the ridge observed in this area lies on the northern or southern side of the transform.

In the PRT two swath widths of data were collected to image the deepest areas of the trough and the base of the scarp to the north, mostly to guide the selection of sample locations. The valley floor is smooth and flat, suggesting it is heavily sedimented, while the small portion of the wall imaged have a typical slope of 10° and show signs of mass wasting in places. The steepest slopes imaged were 60° and likely represent the breakaway of one such event, with a talus ramp at its base.

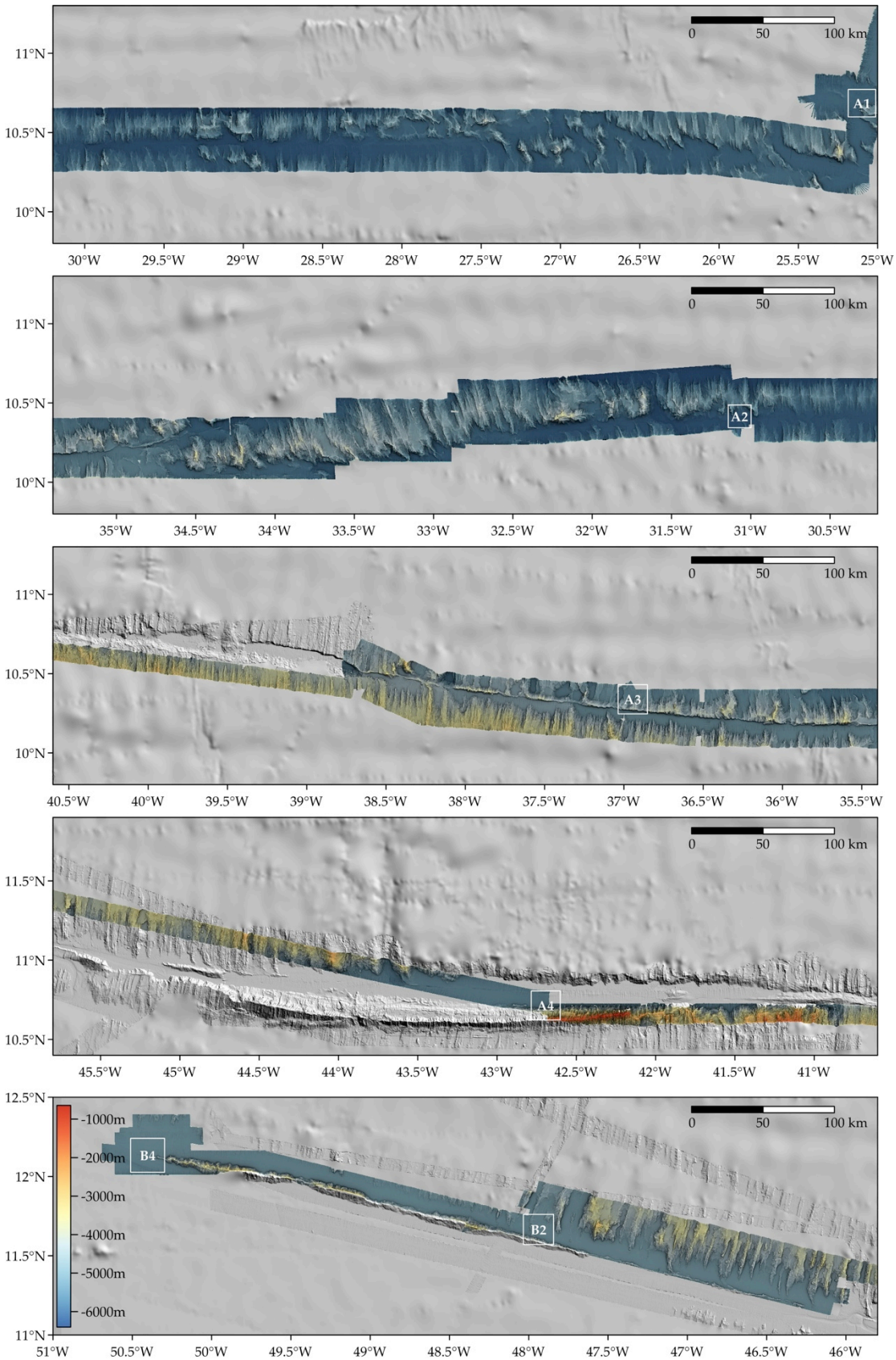

Figure 7-31: Terrain Texture Shaded bathymetry (60m) collected during the VEMA-transform portion of the cruise. Panels more progressively further west. The underlying, low resolution shaded relief is derived from Sandwell (2014). The higher resolution (70m) greyscale bathymetry shown in panels 3, 4 and 5 is provided by the Marine Geoscience Data System: GMRT Map Tool (marine-geo.org).

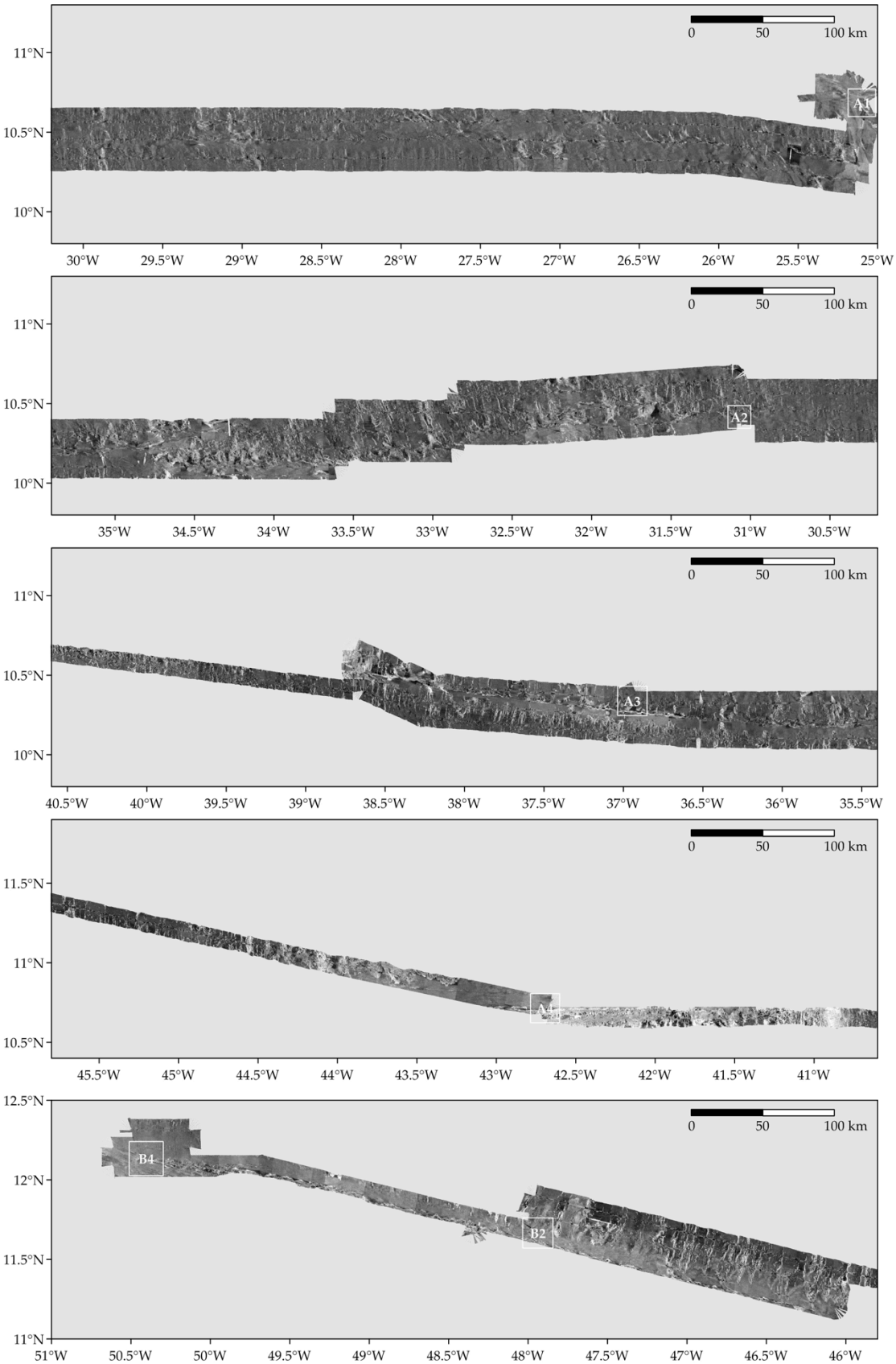

Figure 7-32: Backscatter data from the EM122 multibeam system collected during the VEMA-transform portion of the cruise. Pixel size is 100m and strongly backscattering terrain is shown in lighter colours. Sampling stations are shown by the white boxes.

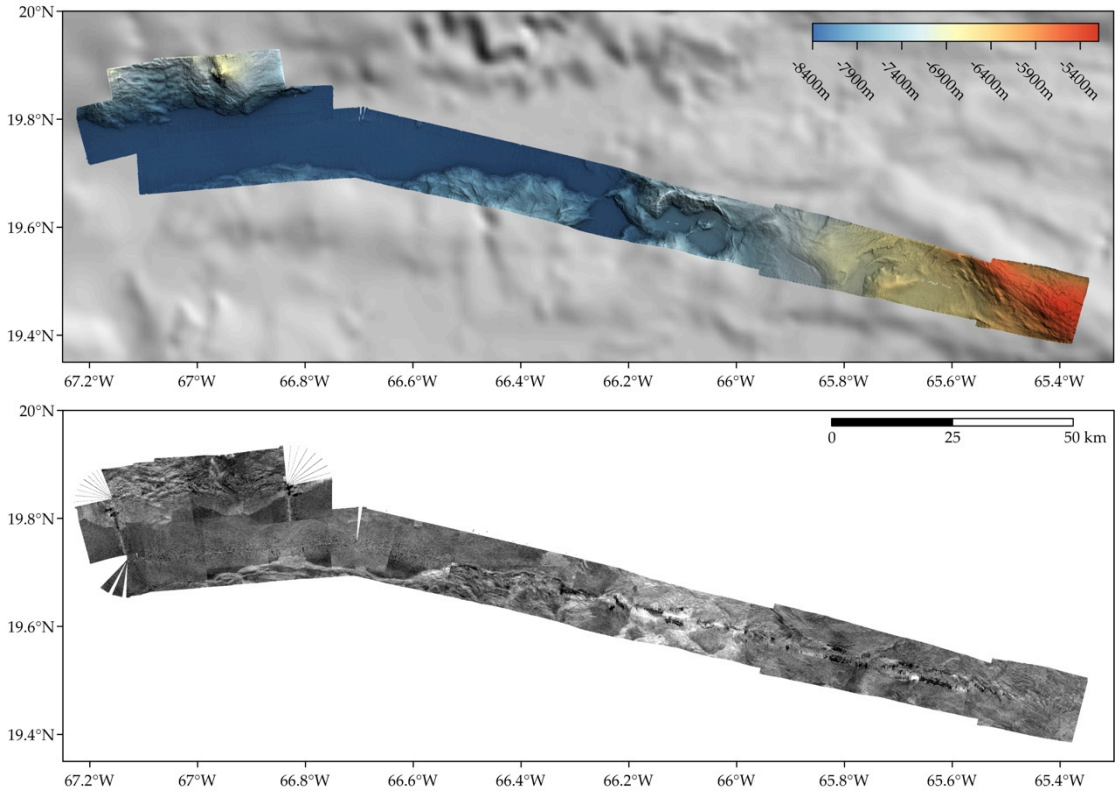

Figure 7-33: Terrain Texture Shaded bathymetry (60m) (top panel) and backscatter data (50m) (bottom panel) collected in the Puerto Rico trench. The underlying, low resolution shaded relief is derived from Sandwell (2014). Strongly backscattering terrain is shown in lighter colours.

7.4.6 AUV Mission Summary

(M. Rothenbeck, A. Steinführer, L. Triebe, E. Wenzlaff)

7.4.6.1 Introduction

The Autonomous Underwater Vehicle (AUV) Abyss (built by HYDROID Inc.) from GEOMAR can be operated in water depths up to 6000 m. The system comprises the AUV itself, a control and workshop container (see Figure 7-34), and a mobile Launch and Recovery System (LARS) with a deployment frame that was installed at the starboard side on the afterdeck of R/V Sonne. The self-contained LARS was developed by WHOI to support ship-based operations so that no Zodiac or crane is required for launch and recovery. The LARS is mounted on steel plates, which are screwed to the deck of the ship. The LARS is configured in a way that the AUV can be deployed over the stern or port/starboard side of the German medium and ocean-going research vessels. The AUV Abyss can be launched and recovered at weather conditions with a swell up to 2.5 m and wind speeds of up to 6 Beaufort. For the recovery the nose float pops off when triggered through an acoustic command. The float and the ca. 19 m recovery line drift away from the vehicle so that a grapnel hook can snag the line. The line is then connected to the LARS winch, and the vehicle is pulled up. Finally, the AUV is brought up on deck and secured in the LARS.

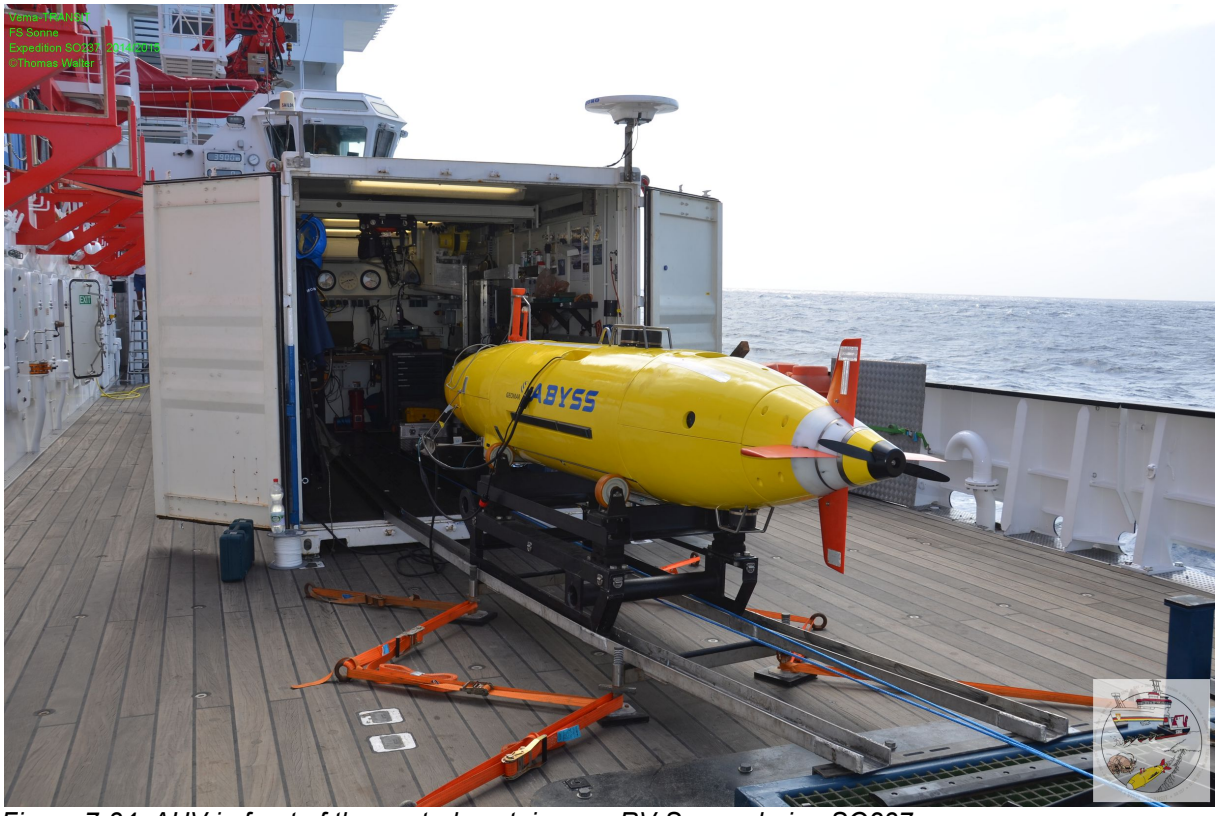

Figure 7-34: AUV in front of the control container on RV Sonne during SO237

During cruise SO237 seven missions were flown by Abyss (Table 7-18). The missions were flown using the multibeam or camera configuration. Primary sensors were the RESON Seabat 7125 (multibeam; 200 kHz; for 4 missions), the electronic still camera (for 3 missions), the Edgetech sidescan sonar (for 3 missions) and the Redox

sensor (Eh; for 6 missions). The microstructure sensor (placed outside the AUV on an outrigger; for 1 mission) was dismounted after the first dive. Detailed descriptions of all dives can be found in Appendix G.

Table 7-18: AUV Mission Statistics for cruise SO237

Station	*Area*	*Dive*	*Date*	*Survey time*	*Mission time*	*Distance travelled*	*Sensors*	*Comment*
2-1	A1	160	Dec. 19	9.7 h	14.6 h	74.7 km	MSS / MB	200 kHz
4-1	A2	161	Dec. 25	-	4.7 h	26.1 km	MB / Eh	Aborted
4-7	A2	162	Dec. 26	12.8 h	15.7 h	87.7 km	MB / Eh	200 kHz
6-2	A3	163	Jan. 01	10.9 h	14.7 h	81.7 km	Camera / SSS / Eh	410 kHz
9-1	B1	164	Jan. 11	11.2 h	14.9 h	83.1 km	MB / Eh	200 kHz
9-6	B1	165	Jan. 12	9.1 h	13.4 h	72.4 km	Camera / SSS / Eh	410 kHz
11-3	B2	166	Jan. 14	16.1 h	20.0 h	111.5 km	Camera / SSS / Eh	120 / 410 kHz
			Total:	**69.8 h**	**98.0 h**	**537.2 km**		

(Survey time = time spent mapping on the seafloor; Mission time = time including descent, survey and ascent phase; Distance travelled = total distance during mission; MSS = Microstructure probe for current measurements; MB = Multibeam Echo Sounder; Eh = Redox Sensor, SSS = Sidescan Sonar)

7.4.6.2 Data Processing

The gathered data from the AUV were processed into a usable format during the cruise. The positional drift of the AUV demands a navigational adjustment to grid either a bathymetric or a sidescan map. The RESON multibeam logs its raw data as *.s7k. The navigation adjustment is done by using MB-Systems (Caress and Chayes 1996, 2008), relative by overlapping swath areas and absolute related to ship-based bathymetry. The re-navigated multibeam data were processed and gridded using QINSy (QPS, Quality Positioning Services BV). Sidescan data were processed using OIC's CleanSweep

The logged images (Tiff format) during missions 163, 165 and 166 already contains the vehicle data like position, time, depth, altitude, pitch, roll etc. During SO237 a software based on C++ was programmed to read out these information and generate a navigation file according a chosen amount of images. The software LAPM[1] tool was used to put the selected images on the vehicle track and merge the image borders. An example of the product is shown in Figure 7-35

[1] Marcon, Y et al. (2013): Large-Area Photo-Mosaicking tool (LAPM tool). doi:10.1594/PANGAEA.808960, Supplement to: Marcon, Yann; Sahling, Heiko; Bohrmann, Gerhard (2013): LAPM: a tool for underwater large-area photo-mosaicking. Geoscientific Instrumentation, Methods and Data Systems, 2(2), 189-198, doi:10.5194/gi-2-189-2013

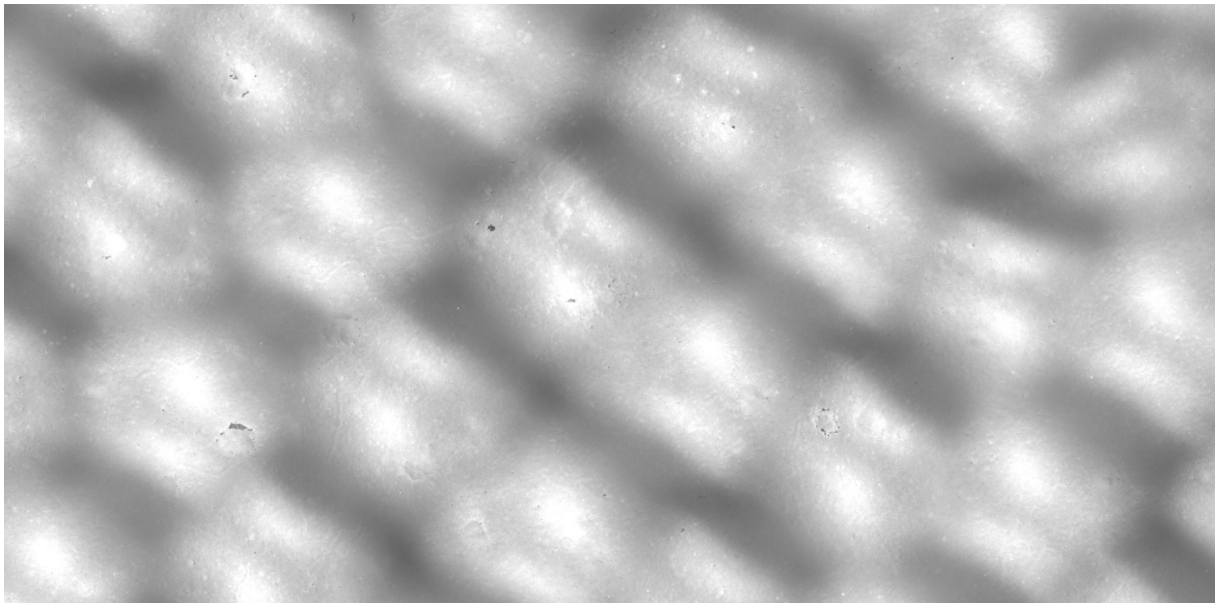

Figure 7-35: Cutout of the photo mosaic dive 165

7.4.7 Preliminary geological description of AUV survey data

(N. Augustin, I. Yeo)

7.4.7.1 Dive Abyss0160 (multibeam)

The dive covers an area of 5.5 km^2 and is divided into two separate geomorphological areas (Figure 11-2). The south is characterised by a platform that lies around 10 m above the fracture zone valley floor. This platform is bounded by a steep edge, which is fairly unstable and appears to be breaking up, depositing large (up to around 70 m in size) blocks on the sedimented valley floor below (Figure 7-36A). At the southernmost extent of the surveyed area the platform first steps and then ramps up, to a height of 35 m above the floor of the valley.

In the northern section (10°43.22'N 25°04.07'W) there is an unusually steep sided, tall cone, reaching around 20 m above the seafloor with a basal diameter of 19 m narrowing to 6 m at the top (Figure 7-36B). The feature is surrounded by scour marks (orientated E – W) and may represent an unusually tall, steep mass-wasted block (although it lies on the furthest northern extent of the debris field associated with the platform edge and doesn't appear to have been smoothed by the currents) or, more likely, something harder than the other blocks imaged, perhaps carbonate associated with fluid seepage or a basement structure.

The rest of the northern area is characteristed by diverse ripple marks, which range from around 20 cm in amplitude to around 60 cm, with a wavelength of between 10 and 25 m (Figure 7-36A). Between 10°43.27'N and 10°43.66'N the area is characterised by strong, E-W orientated, slightly bowed lineations. A number of these lineations are characterised by regularly spaced pits, sometimes elongated along the strike of the feature. These pits are less than a metre deep and range from 20 -50m wide.

7.4.7.2 Dive Abyss0162 (multibeam)

The data cover an area of around 6 km^2, again in a region where a steep slope, associated with the northern edge of what may be a slumping structure reaching several km into the axial valley (see station maps area 2) meets the flat valley floor (see Figure 11-4). The height difference between the top of the slope and the valley floor in the surveyed area is around 90m and the slope is curved, showing typical features of a slumping front, with some mass wasting features and some slope parallel lineations.

The southern section is very flat and has no major features, although small (<50m diameter), pancake like structures (typical height to diameter ratio of 1:100) form a roughly N-S orientated line (Figure 7-36C). No structures are observed in the region of the Eh anomalies detected by the AUV, however the pancake structures have forms similar to mud mounds and may be the product of fluid seepage that is no longer active.

7.4.7.3 Dive Abyss0163 (SSS)

The data cover an area of 4.5 km^2 in a flat area north of the uplifted section of the VEMA and are almost entirely featureless (Figure 11-7). In the eastern corner a few hummocks are observed in the sediment, which are around 40 m in length. The flat area

is characterised by a large number of very small (1 m) holes. These are probably evenly distributed but appear more clearly in the outer beams due to the grazing angle.

7.4.7.4 Dive Abyss0164 (Multibeam)

The data cover an area of 10.7 km^2 and lie12 km north of the uplifted ridge of the VEMA, covering the edge of an unusually long N-S orientated ridge associated with the faulted volcanic terrain observed north and south of the valley (Figure 11-9). The edge of this ridge dominates the NW corner of the survey area, with an elevation difference of 35 m from the top of the ridge to the valley floor. The slope itself, particular in the NW corner, is characterised by parallel channels that cut directly downslope and disappear at the contact with the flat valley floor, suggesting they may no longer be actively forming (Figure 7-36D). The channels themselves are around 1 -2 m deep and range from 15 – 25 m wide. The rest of the valley floor shows some evidence of small cracks in the sediment, although with no preferred orientation, and some small sediment slumping structures from the slope to the west.

7.4.7.5 Dive Abyss0165 (SSS)

Dive Abyss0165 was carried out in the Abyss0164 area, on the edge of the NW slope that showed the channels (see Figure 11-11 and Figure 7-36D). The mosaic covers 0.2 km^2 and was shifted 195 m along a bearing of 113° relative to Abyss0164 in order to match the bathymetry with the SSS information. The NW third of the survey shows the channel structures clearly. Lobate downslope flow features are observed, separated by the channels, giving this area a wavy appearance. This wavy appearance fades out and disappears around 100 m from the contact (Figure 7-36E). The rest of the survey is relatively flat and featureless, with a NE-SW orientation to any fabric observed. There are a few brightly reflecting blocks on the valley floor, which are probably sourced from the higher terrain either east or west of the survey area.

7.4.7.6 Dive Abyss0166 (SSS)

Dive Abyss0166 covers 23 km^2 in the centre of the VEMA transform valley. The same area was covered twice, with 120 kHz sidescan sonar and then a smaller area with 410 kHz sidescan sonar during the photo survey (Figure 11-14 and Figure 11-15). The main features visible in the imagery are a group of NW-SE orientated (294° bearing), small offset, parallel faults in the sediment, which match with a larger scale channel feature in the ships bathymetry (see Figure 3-1, area B2). These faults are spaced between 30 and 300 m apart and cross the entire surveyed area (Figure 7-36F). The photographic survey also imaged them and showed they have very sharp edges and show no sign of erosion or sedimentation. This suggests current tectonic activity on the VEMA transform fault, even 60 Ma away from the spreading axis. The channel is approximately 3 km wide in the ship bathymetry and around 30 m deep. Only the northern edge of this channel is visible in the sidescan imagery. The centre of the channel shows an irregular distribution of channel parallel depressions up to 100 m long and 50 m wide.

The traces of both EBS tracks carried out at this station (Station numbers 11-1 and 11-4) are clearly visible as brightly backscattering lines on the seafloor (Figure 7-36F). The mosaic was shifted 534 m on a bearing of 319° to match the Posidonia positions for these EBS tracks and the ships bathymetry.

In the northern sections of the surveyed area some smaller, channel-parallel cracks are observed again as well as some disorganized sedimentary structure, probably due to erosion of the sediments by currents travelling in an E-W direction. Some small patches of ripple marks, fitting this current direction, are also observed.

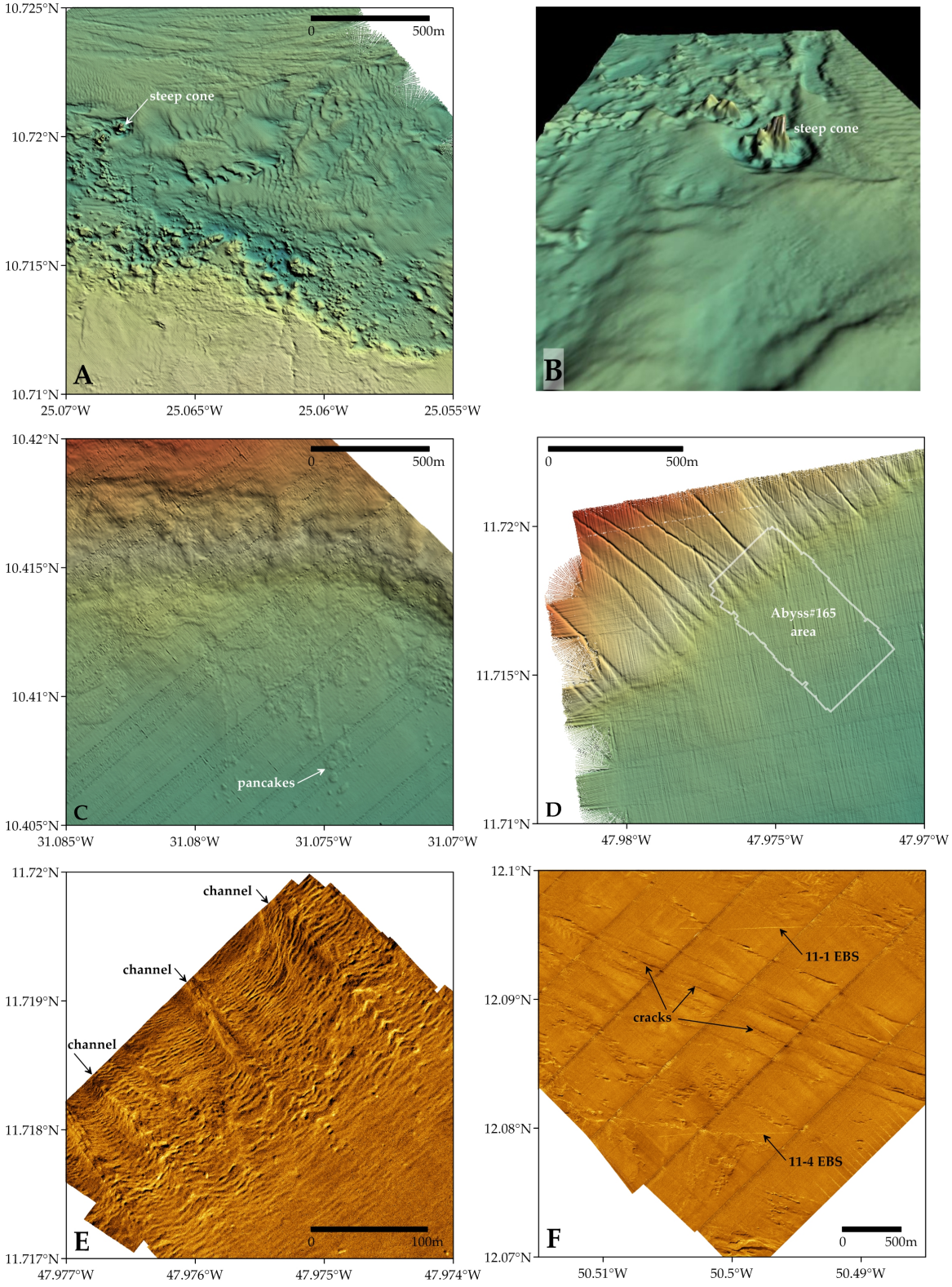

Figure 7-36 (previous page): ***(A)*** *Central area of dive Abyss#160 showing the broken front of the platform meeting the rippled valley floor. The steep sided cone at 10.72°N is also visible. Good examples of the elongated pits are shown in the Northern section.* ***(B)*** *3D view towards the steep sided cone looking west. The imagery is 1.5x vertically exaggerated and surrounded by a clear scour mark at its base.* ***(C)*** *Central area of dive Abyss#162 showing the slope in the north and the small pancake structures highlighted by black arrows.* ***(D)*** *North Western corner of dive Abyss#164 showing clearly the NW-SE striking channel structures on the slope disappearing at the contact with the valley floor. The dive area of Abyss#165 is indicated by the white outline.* ***(E)*** *North western section of dive Abyss#165 showing the channels and lobate downward flow of sediments in 410kHz sidescan data, illuminated from the northwest.* ***(F)*** *The southern corner of dive Abyss#166 showing E-W striking cracks in the sediments (also seen in the photos) and the EBS tracks in 120kHz sidescan sonar data illuminated from the north. The EBS tracks appear as bright lines representing strong backscatter. In all sidescan imagery bright colors represent strongly backscattering terrain.*

8. ACKNOWLEDGEMENTS

We thank Capt. Meyer and his crew for the excellent support during the SO-237 cruise - it was as always a real pleasure to work with them. The cruise was financed through BMBF grant 03G0237A to A. Brandt (travel, transport, consumables) and through internal funds of Geomar (AUV-costs), cruise participation by Alexandra Schönle, Alexandra Jeuck, Dennis Prausse and Hartmut Arndt were supported by a grant from BMBF 03G0237B. The help of the German Embassies in Washington (Frau Weiss) and Santo Domingo (Frau Weber) with acquiring permission to work in the Puerto Rico Trench is gratefully acknowledged.

9. REFERENCES

Adl, S.M., Simpson, A.G.B., Lane, C.E., Lukes, J., Bass, D., Bowser, S.S., Brown, M.W., Burki, F., Dunthorn, M., Hampl, V., Heiss, A., Hoppenrath, M., Lara, E., le Gall, L., Lynn, D.H., McManus, H., Mitchell, E.A.D., Mozley-Stanridge, S.E., Parfrey, L.W., Pawlowski, J., Rueckert, S., Shadwick, L., Schoch, C.L., Smirnov, A., Spiegel, F.W., 2012. The revised classification of eukaryotes. Journal of Eukaryotic Microbiology 59, 429-493.

Allen J A (2008) Bivalvia of the deep Atlanic. Malacologia 50: 57-173

Arístegui J, Gasol JM, Duarte CM, Herndl GJ. (2009). Microbial oceanography of the dark ocean's pelagic realm. Limnol Oceanogr 54: 1501–1529.

Arndt, H., Hausmann, K & Wolf, M. (2003) Deep-sea heterotrophic nanoflagellates of the Eastern Mediterranean Sea: qualitative and quantitative aspects of their pelagic and benthic occurrence. Mar. Ecol. Prog. Ser. 256: 45-56.

Barnett PRO, Watson J, Connelly D (1984). A multiple corer for taking virtually undisturbed samples from shelf, bathyal and abyssal sediments. Oceanol. Acta, 7, 399-408.

Böggemann, M., 2009. Polychaetes (Annelida) of the abyssal SE Atlantic. Org., Divers. & Evol. 9, 251-428.

Bonatti, E., Brunelli, D., Buck, W., Cipriani, A., Fabretti, P., Ferrante, V., Gasperini, L., Ligi, M., 2005. Flexural uplift of a lithospheric slab near the Vema transform (Central Atlantic): Timing and mechanisms. Earth and Planetary Science Letters 240, 642–655. doi:10.1016/j.epsl.2005.10.010

Bonatti, E., Ligi, M., Brunelli, D., Cipriani, A., Fabretti, P., Ferrante, V., Gasperini, L., Ottolini, L., 2003. Mantle thermal pulses below the Mid-Atlantic Ridge and temporal variations in the formation of oceanic lithosphere. Nature 423, 499–505.

Bouchet P, Warén A (1993) Revision of the northeast Atlantic bathyal and abyssal Mesogastropoda. Bolletino Malacologia Supplemento 3: 580-840

Brandt A., Elsner N., Brenke, N., Golovan, O.A., Lavrenteva, A.V., Malyutina, M.V., Riehl, T. (2015): Abyssal macrofauna of the Kuril-Kamchatka Trench area collected by means of a camera-epibenthic sledge (Northwest Pacific). Deep-Sea Research II 111: 175-188. 10.1016/j.dsr2.2014.11.002

Brandt A., Elsner N., Golovan, O., Malyutina, M.V., Riehl, T., Schwabe, E., Würzberg, L., Brenke, N. (2013): Epifauna of the Sea of Japan collected via a new epibenthic sledge equipped with camera and environmental sensor systems. Deep-Sea Research II 86-87: 43-55.

Brandt, A. (2004): New deep-sea species of Macrostylidae (Asellota: Isopoda: Malacostraca) from the Angola Basin off Namibia, South West Africa. Zootaxa 448:1-35.

Brandt, A., (1993). Composition, abundance and diversity of peracarid crustaceans on a transect of the Kolbeinsey-Ridge, north of Iceland. Polar Biol. 13, 565–576.

Brandt, A., (1995). Peracarid fauna (Crustacea, Malacostraca) of the Northeast Water Polynya off Greenland: documenting close benthic-pelagic coupling in the Westwind Trough. Mar. Ecol. Prog. Ser. 121, 39–51.

Brandt, A., (1997a). Abundance, diversity, and community patterns of epi- and benthic-boundary layer Crustacea Peracarida at 75°N of East Greenland. Polar Biol. 17, 159–174.

Brandt, A., Brenke, N., Andres, H.-G., Brix, S., Guerrero-Kommritz, J., Mühlenhardt-Siegel, U., & J.-W. Wägele (2005): Diversity of peracarid crustaceans (Malacostraca) from the abyssal plain of the Angola Basin. Organisms, Diversity and Evolution 5: 105-112.

Brandt, A., Brix, S.B., Held, C, Kihara, T.C. (2014): Molecular differentiation in sympatry despite morphological stasis: deep-sea *Atlantoserolis* Wägele, 1994 and *Glabroserolis* Menzies, 1962 from the south-west Atlantic (Crustacea: Isopoda: Serolidae). Zoological Journal of the Linnean Society 172: 318–359.

Brandt, A., Elsner, N., Malyutina, M.V., Brenke, N., Golovan, O.A., Lavrenteva, A.V., Riehl, T., 2015. Abyssal macrofauna of the Kuril-Kamchatka trench area (northwest pacific) collected by means of a camera-epibenthic sledge. Deep Sea Research Part II: Topical Studies in Oceanography 111, 175–187. doi:10.1016/j.dsr2.2014.11.002

Brandt, A., Gooday, A.J., Brandao, S.N., Brix, S., Brökeland, W., Cedhagen, T., Choudhury, M., Cornelius, N., Danis, B., de Mesel, I., Diaz, R.J., Gillan, D.C., Ebbe, B., Howe, J.A., Janussen, D., Kaiser, S., Linse, K., Malyutina, M.V., Pawlowski, J., Raupach, M.J., Vanreusel, A., 2007. First insights into the biodiversity and biogeography of the Southern Ocean deep sea. Nature 447, 307–311.

Brandt, A., Gooday, A.J., Brix S.B., Brökeland, W., Cedhagen, T., Choudhury, M., Cornelius, N., Danis, B., De Mesel, I., Diaz, R.J., Gillan, D.C., Ebbe, B., Howe, J., Janussen, D., Kaiser, S., Linse, K., Malyutina, M., Brandao, S., Pawlowski, J., Raupach, M., (2007): The Southern Ocean deep sea: first insights into biodiversity and biogeography. Nature 447: 307-311.

Brandt, A., Vassilenko, S., Piepenburg, D., Thurston, M., 1996. The species composition of the peracarid fauna (Crustacea, Malacostraca) of the Northeast Water Polynya (Greenland). Medd. Groenl. Biosci. 44, 1–30.

Brenke, N., 2005. An epibenthic sledge for operations on marine soft bottom and bedrock. Mar. Technol. Soc. J. 39, 13–24.

Brenke, N., Brix, S., and Knuschke, T. (2005) A new deep-sea isopod species from the Angola Basin: Prochelator angolensis sp. nov. (Asellota: Desmosomatidae). Organisms Diversity and Evolution 5: 179-188.

Brix, S. (2007) 'Four new species of Desmosomatidae Sars, 1897 (Crustacea: Isopoda) from the deep sea of the Angola Basin. Marine Biology Research, 3:4, 205 – 230. DOI: 10.1080/17451000701490987

Brix, S., Leese, F., Riehl, T., Kihara, T.C. 2014. A new genus and new species of Desmosomati−dae Sars, 1897 (Isopoda) from the east South−Atlantic abyss described by means of integrative taxonomy. Marine Biodiversity doi:10.1007/s12526−014−0218−3.

Brix, S., Riehl, T., Leese, F. (2011). First genetic data for species of the genus *Haploniscus* Richardson, 1908 (Isopoda: Asellota: Haploniscidae) from neighbouring deep-sea basins in the South Atlantic. Zootaxa 2838: 79–84.

Brökeland, W. 2010. Description of four new species from the *Haploniscus unicornis* Menzies, 1956 complex (Isopoda: Asellota: Haploniscidae). Zootaxa 2536: 1–35.

Brown, L., 2010. A New Technique for Depicting Terrain Relief. Presented at the NACIS, pp. 1–48.

Butler H, Rogerson A (1995) Temporal and spatial abundance of naked amoebae (Gymnamoebae) in marine benthic sediments of the Clyde Sea area, Scotland. J Euk Microbiol 42: 724-730

Cannat M., Mamaloukas-Frangoulis V., Auzende J.-M., Bideau D., Bonatti E., Honnorez J., Lagabrielle Y., Malavieille J. and Mevel C., 1991, A geological cross-section of the Vema fracture zone transverse ridge, Atlantic ocean. *Journal of Geodynamics,* 13, 97-117

Collins; P.C., Croot P., Carlsson J., Colaco A., Grehan A., Hyeong K., Kennedy R., Mohn C., Smith S., Yamamoto H., Rowden A., 2013. A primer for the environmental impact assessment of mining at seafloor massive sulfide deposits. Marine Policy 42, 198-209

Dall WH (1889) Reports of the results of dredging, under the supervision of Alexander Agassiz, in the Gulf of Mexico (1877) and in the Caribean Sea (1879-80) coast survey steamer “Blake”, Lieut-Commander C.D. Sigsbee, U.S.N., and Commander J.R. Bartlett, U.S.N., Commanding. XXIX Report on the Mollusca. Part II Gastropoda and Scaphopoda. Bulletin of the Museum of Comparative Zoology XVIII: 1-492

Dalsgaard J, St. John M, Kattner G, Müller-Navarra D, Hagen W (2003). Fatty acid trophic markers in the pelagic marine environment. Advances in Marine Biology 46, 225–340.

Danovaro R, Gambi C, Dell'Anno A, Corinaldesi C, Fraschetti S, Vanreusel A, Vincx M, Gooday AJ. (2008a). Exponential decline of deep-sea ecosystem functioning linked to benthic biodiversity loss. Curr Biol 18: 1-8.

Danovaro R., Gambi C, Lampadariou N, Tselepides A. (2008b). Deep-sea biodiversity in the Mediterranean Basin: Testing for longitudinal, bathymetric and energetic gradients. Ecography 31: 231–244.

Danovaro, R., Della Croce, N., Dell’Anno, A., Pusceddu, A., 2003. A depocenter of organic matter at 7800 m depth in the SE Pacific Ocean. Deep-Sea Res. I50, 1411–1420.

Danovaro, R., Gambi, C., Croce, N.D., 2002. Meiofauna hotspot in the Atacama Trench, eastern South Pacific Ocean. Deep-Sea Res. I49, 843–857.

Dell’Anno, A. & Danovaro, R. 2005. Extracellular DNA plays a key role in deep-sea ecosystem functioning. Science 309, 2179.

Edgcomb V, Orsi W, Bunge J, Jeon S, Christen R, et al. (2011) Protistan microbial observatory in the Cariaco Basin, Caribbean. I. Pyrosequencing vs Sanger insights into species richness. ISME J 5: 1344-1356.

Edgcomb VP, Kysela DT, Teske A, de Vera Gomez A, Sogin ML. (2002). Benthic eukaryotic diversity in the Guaymas Basin hydrothermal vent environment. Proc Natl Acad Sci U S A 99: 7658-7662.

Edgcomb, V., Orsi, W., Leslin, C., Epstein, S. S., Bunge, J., Jeon, S., Yakimov, M. M., Behnke, A., Stoeck, T., 2009. Protistan community patterns within the brine and halocline of deep hypersaline anoxic basins in the eastern Mediterranean Sea. Extremophiles 13, 151-167.

Enge, A.J., Nomaki, H., Ogawa, N. O., Witte, U., Moeseneder, M.M., Lavik, G., Ohkouchi, N, Kitazato, H., Kucera, M. & Heinz, P. 2011. Response of the benthic foraminiferal community to a simulated short-term phytodetritus pulse in the abyssal North Pacific. Marine Ecology Progress Series 438, 129–142.

Faure, B., Jollivet, D., Tanguy, A., Bonhomme, F., Bierne, N., 2009. Speciation in the Deep Sea: Multi-Locus Analysis of Divergence and Gene Flow between Two Hybridizing Species of Hydrothermal Vent Mussels. PLoS ONE 4, e6485. doi:10.1371/journal.pone.0006485

Fine, M. L. (1970). "Faunal variation on pelagic Sargassum." Marine Biology 7: 112-122.

Fofonoff N.P., Millard R.C., 1983, Algorithms for computation of fundamental properties of seawater, *UNESCO*, Report 44, 15-24

France, S.C., 1994. Genetic population structure and gene flow among deep-sea amphipods, *Abyssorchomene* spp., from six California Continental Borderland basins. Mar. Biol. 118, 67–77. doi:10.1007/BF00699220

Glazier, A.E., Etter, R.J., 2014. Cryptic speciation along a bathymetric gradient. Biol J Linn Soc Lond 113, 897–913. doi:10.1111/bij.12389

Gooday, A.J. 1993. Deep-sea benthic foraminiferal species which exploit phytodetritus: characteristic features and controls on distribution. Marine Micropaleontology 22, 187–205.

Gooday, A.J., Aranda da Silva, A. & Pawlowski, J. 2011. Xenophyophores (Rhizaria, Foraminifera) from the Nazaré Canyon (Portuguese margin, NE Atlantic). Deep Sea Res II 58, 2401–2419.

Gooday, A.J., Rothe, N. & Pearce, R.B. 2013. New and poorly known benthic foraminifera (Protista, Rhizaria) inhabiting the shells of planktonic foraminifera on the bathyal Mid-Atlantic Ridge. Marine Biology Research 9, 447–461.

Grassle, J. F. and L. S. Morse-Porteous (1987). "Macrofaunal colonization of disturbed deep-sea environments and the structure of deep-sea benthic communities." Deep Sea Research 34(12): 1911-1950.

Hausmann, K, Weitere, M., Wolf, M. & Arndt, H. (2002) *Meteora sporadica* gen. nov. et sp. nov. (Protista incertaesedis) - an extraordinary free-living protist from the Mediterranean deep sea. Europ. J. Protistol. 38: 171-177.

Hausmann, K., Selchow, P., Scheckenbach, F., Weitere, M. & Arndt, H. (2006) Cryptic species in a morphospecies complex of heterotrophic flagellates: The case study of *Caecitellus* spp. Acta Protozool. 45: 415-431.

Havermans, C., Sonet, G., d' Udekem d'Acoz, C., Nagy, Z.T., Martin, P., Brix, S., Riehl, T., Agrawal, S., Held, C., 2013. Genetic and morphological divergences in the

cosmopolitan deep-sea amphipod *Eurythenes gryllus* reveal a diverse abyss and a bipolar species. PLoS ONE 8, e74218. doi:10.1371/journal.pone.0074218

Hessler, R.R., Sanders, H.L. 1967. Faunal diversity in the deep sea. Deep-Sea Res 14:65–78.

Huffard, C. L., S. von Thun, A. D. Sherman, K. Sealey and K. L. Smith, Jr. (2014). "Pelagic community change over a 40-year period: temporal and spatial variability." Marine Biology 161(12): 2735-2751.

Itoh, M., Kawamura, K., Kitahashi, T., Kojima, S., Katagiri, H., Shimanaga, M., 2011. Bathymetric patterns of meiofaunal abundance and biomass associated with the Kuril and Ryukyu trenches, western North Pacific Ocean. Deep-Sea Res. I58, 86–97.

Jamieson, A.J., Fujii, T., Mayor, D.J., Solan, M., Priede, I.G., 2010. Hadal trenches: the ecology of the deepest places on Earth.TrendsEcol.Evol. 25, 190–197.

Kaiser, S., Barnes, D.K.A, Linse, K., Brandt, A., 2008. Epibenthic macrofauna associated with the shelf and slope of a young and isolated Southern Ocean island. Antarct. Sci. 20, 281–290.

Laffoley, D. d. A., H. S. J. Roe, M. V. Angel, J. Ardron, N. R. Bates, I. L. Boyd, S. Brooke, K. N. Buck, C. A. Carlson, B. Causey, M. H. Conte, S. Christiansen, J. Cleary, J. Donnelly, S. A. Earle, R. Edwards, K. M. Gjerde, S. J. Giovannoni, S. Gulick, M. Gollock, J. Hallett, P. Halpin, R. Hanel, A. Hemphill, R. J. Johnson, A. H. Knap, M. W. Lomas, S. A. McKenna, M. J. Miller, P. I. Miller, F. W. Ming, R. Moffitt, N. B. Nelson, L. Parson, A. J. Peters, J. Pitt, P. Rouja, J. Roberts, J. Roberts, D. A. Seigel, A. N. S. Siuda, D. K. Steinberg, A. Stevenson, V. R. Sumaila, W. Swartz, S. Thorrold, T. M. Trott and V. Vats (2011). "The protection and management of the Sargasso Sea: The golden floating rainforest of the Atlantic Ocean. Summary Science and supporting evidence case." Sargasso Sea Alliance: 44 pp.

Leal JS (1991) Marine prosobrach gastropods from oceanic islands off Brazil. Backhyus 418pp

Lecroq, B., Lejzerowicz, F., Bachar, D., Christen, R., Esling, P., Baerlocher, L., Østeras, M., Farinelli, L. & Pawlowski, J. 2011. Ultra-deep sequencing of foraminiferal microbarcodes unveils hidden richness of early monothalamous lineages in deep-sea sediments. Proceedings of the National Academy of Sciences 108, 13177–13182.

Lejzerowicz, F., Esling, P. & Pawlowski, J. 2014. Patchiness of deep-sea benthic Foraminifera across the Southern Ocean: insights from high-throughput DNA sequencing. Deep-Sea Res II doi:/10.1016/j.dsr2.2014.07.018.

Lejzerowicz, F., Voltski, I. & Pawlowski, J. 2013. Identifying active foraminifera in the Sea of Japan using metatranscriptomic approach. Deep-Sea Res II 86–87, 214–220.

Lins, L., A. Vanreusel, Van Campenhout, J., Ingels, J., 2013. "Selective settlement of deep-sea canyon nematodes after resuspension — an experimental approach." Journal of Experimental Marine Biology and Ecology 441: 110-116.

McIntyre AD, Warwick RM, 1984. Meiofauna techniques. In: Holme NA, McIntyre AD (eds) Methods for the study of marine benthos. Blackwell, Oxford, pp 217-244.

Moore, D. R. (1963). "Turtle Grass in the Deep Sea." Science, N. S. 139(3560): 1234-1235.

Nitsche, F., Weitere, M., Scheckenbach, F., Hausmann, K., Wylezich, C. & Arndt, H. (2007) Deep sea records of choanoflagellates with a description of two new species. ActaProtozool. 46: 99-106.

Paterson, G.L.J., Glover, A.G., Barrio Froján, C.R.S., Whitaker, A., Budaeva, N., Chimonides, J., Doner, S., 2009. Deep-sea Res II 56, 1739-1746.

Pawlowski, J., Fahrni, J., Lecroq, B., Longet, D., Cornelius, N., Excoffier, L., Cedhagen, T. & Gooday, A.J. 2007. Bipolar gene flow in deep-sea benthic foraminifera. Molecular Ecology 16, 4089–4096.

Pawlowski, J., Fontaine, D., da Silva, A.A., Guiard, J., 2011. Novel lineages of Southern Ocean deep-sea foraminifera revealed by environmental DNA sequencing. Deep Sea Res II 58, 1996–2003.

Pawlowski, J., Holzmann, M., Berney, C., Fahrni, J., Gooday, A.J., Cedhagen, T., Habura, A. & Bowser, S.S. 2003. The evolution of early Foraminifera. Proceedings of the National Academy of Sciences of the United States of America, 100, 11494-11498.

Pedrós-Alió C (2006) Marine microbial diversity: can it be determined? Trends Microbiol 14: 257-263

Post DM (2002). Using stable isotopes to estimate trophic position. Models, methods and assumptions. Ecology 83(3), 703–718.

Priede, I.G. *et al*. 2013. Does presence of a mid-ocean ridge enhance biomass and biodiversity?. PloS one 8, e61550.

Ramirez-Llodra, E., Brandt, A., Danovaro, R., DeMol, B., Escobar, E., German, C.R., Levin, L.A., Martínez Arbizu, P., Menot, L., Buhl-Mortensen, P., Narayanaswamy, B.E., Smith, C.R., Tittensor, D.P., Tyler, P.A., Vanreusel, A., Vecchion, M., 2010. Deep, diverse and definitely different: unique attributes of the world's largest ecosystem. Biogeosciences 7, 2851–2899.

Ratnasingham, S., Hebert, P.D.N., 2007. bold: The Barcode of Life Data System (http://www.barcodinglife.org). Mol. Ecol. Notes 7, 355–364. doi:10.1111/j.1471-8286.2007.01678.x

Raupach, M.J., Malyutina, M., Brandt, A. & Wägele, J. W. (2007): Molecular data reveal a highly diverse species flock within the deep-sea isopod *Betamorpha fusiformis* (Crustacea: Isopoda: Asellota) in the Southern Ocean. DSR II, 54: 1820-1830.

Riehl, T. Brenke, N., Brix, S.B., Driskell, A., Kaiser, S., Brandt, A. (2014): Field and laboratory methods for DNA studies on deep-sea isopod crustaceans. Polish Polar Research 35(2): 203–224.

Salani, F.S., Arndt, H., Hausmann, K., Nitsche, F., Scheckenbach, F., (2012). Analysis of the community structure of abyssal kinetoplastids revealed similar communities at larger spatial scales. ISME Journal 6, 713-723.

Sanders, H.L., Hessler, R.R. 1969. Ecology of the deep-sea benthos. Science (New York) 163:1419.

Sanders, H.L., Hessler, R.R., Hampson, G.R. 1965. An introduction to the study of deep-sea benthic faunal assemblages along the Gay Head- Bermuda transect. Deep Sea Res Oceanogr Abstr 12:845–867.

Sandwell, D. T., R. D. Müller, W. H. F. Smith, E. Garcia, R. Francis, New global marine gravity model from CryoSat-2 and Jason-1 reveals buried tectonic structure, Science, Vol. 346, no. 6205, pp. 65-67, doi: 10.1126/science.1258213, 2014.

Scarabino V, Scarabino F (2011) Then new bathyal and abyssal species of scaphopoda from the Atlantic Ocean. The Nautilus 125: 127-136

Scheckenbach, F., Hausmann, K. Wylezich, C., Weitere, M., & Arndt, H. (2010) Large-scale patterns in biodiversity of microbial eukaryotes from the abyssal sea floor. PNAS 107, 115-120

Scheckenbach, F., Wylezich, C., Mylnikov, A.P. Weitere, M. & Arndt, H. (2006) Molecular comparisons of freshwater and marine isolates of the same morphospecies of heterotrophic flagellates. Appl. Environ. Microbiol. 72: 6638-6643.

Scheckenbach, F., Wylezich, C., Weitere, M., Hausmann, K. & Arndt, H. (2005) Molecular identity of strains of heterotrophic flagellates isolated from surface waters and deep-sea sediments of the South Atlantic based on SSU rDNA. Aquat. Microb. Ecol. 38: 239-247.

Schmidt, C. & Martínez Arbizu, P. (2015). Deep-Sea Unexpectedly higher metazoan meiofauna abundances in the Kuril–Kamchatka Trench compared to the adjacent abyssal plains Research II 111 60–75.

Smith, C. R. and R. R. Hessler (1987). "Colonization and succession in deep-sea ecosystems." Tree 2(12): 359-363.

Stoeck T, Zuendorf A, Breiner HW, Behnke A. (2007). A molecular approach to identify active microbes in environmental eukaryote clone libraries. Microb Ecol 53: 328-339.

Stoner, A. W. and H. S. Greening (1984). "Geographic variation in the macrofaunal associates of pelagic Sargassum and some biogeographic implications." Marine Ecology Progress Series 20: 185-192.

Ullberg, J. and E. Olafsson (2003). "Free-living marine nematodes actively choose habitat when descending from the water column." Marine Ecology-Progress Series 260: 141-149.

van Dover, C. L., 2011. Mining seafloor massive sulphides and biodiversity: what is at risk?: ICES Journal of Marine Science 68 (2), 341-348.

Weis, J. S. (1968). "Fauna associated with pelagic Sargassum in the Gulf Stream." American Midland Naturalist 80(2): 554-558.

Wilson, G.D.F., Hessler, R.R., 1987. Speciation in the deep sea. Annual Reviews in Ecology and Systematics 18, 185–207.

Yeatman, H. C. (1962). "The problem of dispersal of marine littoral copepods in the Atlantic Ocean, including some redescriptions of species." Crustaceana 4(4): 253-272.

10. DATA AND SAMPLE STORAGE AND AVAILABILITY

10.1 Biological samples

(Springer, T., Brandt, A., Brix, S.)

The biological samples of the VEMA-Transit expedition are organized with a digital data management system in MS Access 2010 which includes all the data content produced during the expedition from the MUC and the EBS. The sorting process recorded in the expedition database will be linked to the local database in the home laboratory of the DZMB (German Centre for Marine Biodiversity Research) after our return. In total, we created 1272 datasets on board from sorting 797 single sample jars from 9 stations. The sorting of the ethanol samples from the VEMA fracture zone could be finished (preliminary results are presented in Sections 7.2.3 - 7.2.5), the formalin samples from the VEMA fracture zone and the samples from the Puerto Rico Trench will be sorted at the CeNak, ZMH and in cooperation with the DZMB (German Centre for Marine Biodiversity Research HH and WHV). The complete sorting of samples will be finished most likely in summer 2016. Specimens are available for specialists on request and provided as loan to work with the specimens before they are finally stored in museum collections. The DZMB is the link between the sampling effort on the vessel, the scientists working up the samples and the final storage of specimens in museum collections. After sorting, the samples are housed in the Meteor archives (http://www.material-archiv.de/en/home.html) from where they can be made available to interested individuals at any time.

10.2 Geological Samples

(C. Devey)

All geological samples (dredged rocks, gravity cores) will be placed in the Geomar sample and core repositories. Access to samples in these repositories is protected initially by a moratorium period, after which application can be made to the data management team at Geomar.

10.3 Bathymetric, side-scan and photo data

(C. Devey)

The bathymetric data will be placed in the Geomar data management system to ensure safe archiving. Following interpretation and publication of the data, it will be transferred to a World Data Centre archive most likely linked to the GeoMapApp project via EMODNet. All data from the AUV will be archived by the AUV-Team also in the Geomar data management system. After a moratorium period it will be available from the data management team on request.

11. APPENDICES

A. Station List / Stationsliste

Stat. No.	Date	Time UTC	Latitude	Longitude	Depth [m]	Wire Length [m]	Device	Action
			** Posidonia position*					
1-1	18.12.14	19:56	10°38.06' N	25°03.88' W	4790	4750	CTD + MAPR	Soundvelocity profile
2-1	19.12.14	8:49	10°43.25' N	25°03.88' W	5461	-	AUV	Launch Dive 160
2-2	19.12.14	11:15	10°43.11' N	25°03.88' W	5507	5535	GC + MAPR	On/Off bottom
	19.12.14	11:32	10°43.118' N	25°03.893' W	-	-	Algae	Sampling at sea surface
2-3	19.12.14	15:08	10°43.112' N	25°03.886' W	5498	5561	MUC + MAPR	On/Off bottom
2-4	19.12.14	19:43	10°43.108' N	25°03.888' W	5517	5559	MUC	On/Off bottom
2-5	20.12.14	4:34	10°43.17' N	25°03.88' W	5518	5553	MUC	On/Off bottom
2-6	20.12.14	11:09	*10°42.330' N	*25°05.580' W	5520	8204	EBS	On bottom
2-6	20.12.14	12:18	*10°42.969' N	*25°04.728' W	5520	6568	EBS	Off bottom
2-7	20.12.14	19:50	*10°41.370' N	*25°05.137' W	5514	8200	EBS	On bottom
2-7	20.12.14	21:20	*10°42.287' N	*25°03.952' W	5510	5725	EBS	Off bottom
3-1	21.12.14	3:30	10°39.00' N	25°05.60' W	5144	5195	DS	On bottom
3-1	21.12.14	5:25	10°39.60' N	25°05.30' W	4879	4871	DS	Off bottom
4-1	25.12.14	21:38	10°27.70' N	31°01.60' W	5672	-	AUV	Launch Dive 161
4-2	25.12.14	21:52	10°27.82' N	31°01.64' W	5637	200	Plankton-Net	On depth
4-3	26.12.14	3:06	10°25.11' N	31°04.61' W	5771	5809	MUC	On/Off bottom
4-4	26.12.14	7:24	10°25.12' N	31°04.62' W	5759	5813	MUC + MAPR	On/Off bottom
4-5	26.12.14	11:39	10°25.12' N	31°04.62' W	5767	5814	MUC	On/Off bottom
	26.12.14	12:16	10°25.114' N	31°4.617' W	-	-	Algae	Sampling at sea surface
4-6	26.12.14	17:31	10°24.84' N	31°04.54' W	5805	5857	GC	On/Off bottom
4-7	26.12.14	20:34	10°24.76' N	31°04.53' W	5808	-	AUV	Launch Dive 162
4-8	27.12.14	1:24	*10°24.161' N	*31°06.205' W	5735	8200	EBS	On bottom
4-8	27.12.14	2:46	*10°24.950' N	*31°05.204' W	5725	6080	EBS	Off bottom
4-9	27.12.14	8:33	*10°24.082' N	*31°04.795' W	5735	8200	EBS	On bottom
4-9	27.12.14	10:52	*10°24.589' N	*31°04.247' W	5733	6050	EBS	Off bottom
	28.12.14	16:58	10°24.481' N	31°5.318' W	-	-	Algae	Sampling at sea surface
4-10	28.12.14	17:52	10°27.48' N	31°05.31' W	5814	5857	GC + MAPR	On/Off bottom
4-11	28.12.14	20:11	10°24.48' N	31°05.32' W	5820	300	CTD	Casting Depth of 300 m
5-1	29.12.14	6:15	10°22.515' N	32°12.987' N	5455	5584,3	DS	On bottom
5-1	29.12.14	9:30	10°22.874' N	32°12.755' N	5004	4967	DS	Off bottom
6-1	01.01.15	19:25	10°21.01' N	36°57.58' W	5138	5178	MUC	On/Off bottom
6-2	01.01.15	21:20	10°20.998' N	36°57.616' W	5136	-	AUV	Launch Dive 163
6-3	01.01.15	23:37	10°21.03' N	36°57.59' W	5138	5180	MUC + MAPR	On/Off bottom
6-4	02.01.15	3:30	10°21.03' N	36°57.61' W	5134	5182	MUC + MAPR	On/Off bottom
6-5	02.01.15	7:09	10°21.03' N	36°57.61' W	5137	5178	MUC + MAPR	On/Off bottom
6-6	02.01.15	10:48	10°21.02' N	36°57.60' W	5135	5177	GC + MAPR	On/Off bottom

6-7	02.01.15	17:49	*10°20.659' N	*36°57.010' W	5085	7500	EBS	On bottom
6-7	02.01.15	19:15	*10°21.547' N	*36°55.585' W	5079	5600	EBS	Off bottom
6-8	02.01.15	2:12	*10°21.542' N	*36°57.236' W	5119	7100	EBS	On bottom
6-8	02.01.15	3:20	*10°22.293' N	*36°55.852' W	5127	5400	EBS	Off bottom
7-1	03.01.15	13:17	10°13.62' N	36°31.96' W	5063	5102	DS	On bottom
	03.01.15	14:54	10°14.161' N	36°31.615' W	-	-	Algae	Sampling at sea surface
7-1	03.01.15	15:50	10°13.763' N	36°31.81' W	4760	4490	DS	Off bottom
8-1	06.01.15	05:04	10° 43.60' N	42° 40.99' W	5184	-	AUV	Transponder 1 to water
8-1	06.01.15	05:54	10° 43.58' N	42° 41.92' W	5183	-	AUV	Transponder 2 to water
8-2	06.01.15	8:08	10°43.56' N	42°41.59' W	5183	5239	MUC	On/Off bottom
8-3	06.01.15	11:38	10°43.56' N	42°41.59' W	5182	200	Plankton-Net	At depth
8-4	06.01.15	19:01	10°43.00' N	42°39.91' W	5176	7500	EBS	On bottom
8-4	06.01.15	20:18	10°43.00' N	42°39.73' W	5178	5450	EBS	Off bottom
8-5	06.01.15	0:50	10°43.55' N	42°41.59' W	5183	5243	MUC + MAPR	
8-6	07.01.15	4:37	10°43.54' N	42°41.58' W	5180	5200	MUC	
8-7	07.01.15	8:40	10°44.62' N	42°41.58' W	5185	5226	MUC	
8-8	07.01.15	14:35	*10°42.263' N	*42°42.343' W	5110	5100	CTD + MAPR	Tow-Yo-Start
8-8	07.01.15	20:22	*10°42.792' N	*42°40.264' W	5170	5160	CTD + MAPR	Tow-Yo-End
8-9	08.01.15	0:35	10°43.67' N	42°41.75' W	5141	5206	GC + MAPR	On/Off bottom
8-10	08.01.15	7:10	10°42.58' N	42°40.99' W	5117	5167	MUC	On/Off bottom
8-11	08.01.15	10:49	10°42.59' N	42°40.99' W	5122	5162	MUC	On/Off bottom
8-12	08.01.15	15:13	10°42.79' N	42°41.76' W	5176	5213	GC + MAPR	On/Off bottom
	08.01.15	19:10	10°42.645' N	42°41.893' W	-	-	Algae	Sampling at sea surface
9-1	11.01.15	6:23	11°42.58' N	47°59.07' W	4974	-	AUV	Launch Dive 164
9-2	11.01.15	10:38	*11°40.299' N	*48°00.071' W	4995	7100	EBS	On bottom
9-2	11.01.15	14:45	*11°40.410' N	*47°59.565' W	4986	4870	EBS	Off bottom
9-3	11.01.15	19:34	11°41.37' N	47°57.36' W	4996	5051	MUC + MAPR	On/Off bottom
9-4	11.01.15	0:31	11°41.36' N	47°57.34' W	5000	5050	MUC + MAPR	On/Off bottom
	12.01.15	00:51	11°41.357' N	47°57.334' W	-	-	Algae	Sampling at sea surface
9-5	12.01.15	4:23	11°41.35' N	47°57.36' W	4997	5017	MUC	On/Off bottom
9-6	12.01.15	7:14	11°42.58' N	47°59.07' W	4977	-	AUV	Launch Dive 165
9-7	12.01.15	11:17	11°32.00' N	47°51.64' W	4941	4955	GC + MAPR	On/Off bottom
9-8	12.01.15	17:33	*11°39.014' N	*47°56.168' W	5004	5460	EBS	On bottom
9-8	12.01.15	19:29	*11°39.201' N	*47°54.697' W	5001	5260	EBS	Off bottom
10-1	13.01.15	3:49	11°39.96' N	48°20.89' W	4236	4307	DS	On bottom
10-1	13.01.15	6:10	11°40.44' N	48°19.56' W	3625	3625	DS	Off bottom
11-1	14.01.15	00:00	*12°05.732' N	*50°30.239' W	5093	5721	EBS	On bottom
11-1	14.01.15	10:34	*12°05.727' N	*50°28.922' W	5088	5400	EBS	Off bottom
11-2	14.01.15	11:47	12°05.80' N	50°27.96' W	-	-	Plankton-Net	In Water
11-2	14.01.15	12:23	12°05.92' N	50°28.01' W	-	-	Plankton-Net	On deck
11-3	14.01.15	13:57	12°05.99' N	50°28.4' W	5093	-	AUV	Launch Dive 166
11-4	14.01.15	17:27	*12°04.753' N	*50°30.348' W	5130	5770	EBS	On bottom
11-4	14.01.15	19:03	*12°04.791' N	*50°29.114' W	5108	5460	EBS	Off bottom

11-5	14.01.15	23:19	12°05.40' N	50°26.98' W	5091	5145	MUC	On/Off bottom
11-6	15.01.15	3:03	12°05.42' N	50°26.98' W	5090	5115	MUC	On/Off bottom
11-7	15.01.15	6:38	12°05.40' N	50°26.97' W	5090	5142	MUC	On/Off bottom
	19.01.15	00:54	19°43.400' N	67°8.010' W	-	-	Algae	Sampling at sea surface
12-1	19.01.15	17:15	19°46.01' N	66°49.99' W	8346	8414	MUC + MAPR	On/Off bottom
12-2	19.01.15	23:36	19°46.02' N	66°49.00' W	8337	8428	MUC	On/Off bottom
12-3	20.01.15	6:13	19°46.01' N	66°50.00' W	8336	8404	MUC	On/Off bottom
12-4	20.01.15	12:14	19°50.20' N	66°50.30' W	8323	8404	GC	On/Off bottom
12-5	20.01.15	20:40	19°49.50' N	66°50.97' W	8339	8964	EBS	On bottom
12-5	20.01.15	22:54	19°46.85' N	66°49.99' W	8338	8845	EBS	Off bottom
12-6	21.01.15	07:19	19°48.49' N	66°45.44' W	8340	9470	EBS	On bottom
12-6	21.01.15	08:19	19°48.60' N	66°45.12' W	8336	9208	EBS	Off bottom
12-7	21.01.15	15:58	19° 46.00' N	66° 49.99' W	8338	8407	MUC	On/Off bottom
12-8	21.01.15	21:49	19° 46.00' N	66° 49.99' W	8340	8421	MUC	On/Off bottom
12-9	22.01.15	00:56	19° 46.01' N	66° 49.99' W	8338	200	Plancton-Net	At depth
12-10	22.01.15	05:02	19° 48.81' N	66° 58.39' W	8317	8403	GC	On/Off bottom
13-1	22.01.15	11:57	19°43.809' N	67°09.284' W	8352	8430	MUC	On/Off bottom
13-2	22.01.15	17:56	19°43.812' N	67°09.284' W	8350	8430	MUC	On/Off bottom
13-3	22.01.15	23:26	19°43.817' N	67°09.285' W	8350	8428	MUC	On/Off bottom
13-4	23.01.15	06:47	19°46.73' N	67°06.21' W	8329	9261	EBS	On bottom
13-4	23.01.15	08:07	19°47,13' N	67°05.79' W	8316	9050	EBS	Off bottom
13-5	23.01.15	15:49	19°49.85' N	67°02.91' W	8082	9157	EBS	On bottom
13-5	23.01.15	16:52	19°50.14' N	67°02.60' W	8043	8853	EBS	Off bottom
13-6	23.01.15	23:45	19°48.63' N	66°58.43' W	8322	8399	GC	On/Off bottom
14-1	24.01.15	18:42	*19°00.760' N	*67°10.219' W	4552	5111	EBS	On bottom
14-1	24.01.15	19:55	*19°01.373' N	*67°09.776' W	4552	5156	EBS	Off bottom
14-2	25.01.15	0:34	*19°03.044' N	*67°08.650' W	4930	5490	EBS	On bottom
14-2	25.01.15	1:57	*19°03.877' N	*67°08.100' W	4925	5181	EBS	Off bottom
14-3	25.01.15	6:11	19°04.68' N	67°07.77' W	4925	4996	MUC	On/Off bottom
14-4	25.01.15	9:38	19°04.66' N	67°07.75' W	4925	4969	MUC	On/Off bottom
14-5	25.01.15	13:00	19°04.66' N	67°07.76' W	4925	4992	MUC	On/Off bottom

EBS - Epibenthos-Sled
MUC - Multicorer
GC - Gravity Corer (5m)
MAPR - Miniature Autonomous Plume Recorders
AUV - Autonomous Underwater Vehicle (ABYSS, Geomar)
DS - Chain bag dredge

B. Descriptions of dredged samples

Rock Descriptions. Fg= fine grain, vfg= very fine grain, cpx= clinopyroxene, Mn= Manganese.

Station	Date	Depth (m)	Sample Number	Rock Description
3-1	21-12-2014	5143.5-4879.4	SO237-3-1	Mn-nodule: subrounded, smooth surface. Mn crust has minor damage, and is a thin and dark layer. Interior is unknown (weight of nodule suggests carbonate interior). 55-60 mm in diameter.
3-1	21-12-2014	5143.5-4879.4	SO237-3-2	Mn-nodule: 75 x 44 mm, subrounded, minor damage to crust but interior is still unknown. Minor sediment on surface of sample (white particle on the surface). Surface is easily scratched.
3-1	21-12-2014	5143.5-4879.4	SO237-3-3	Mn-nodule: 79 x 59 mm, irregular in shape, some holes (can see through the sample, however the holes have been coated with Mn as well). Interior is unknown, however weight suggests carbonate. White fg mud on surface of nodule.
3-1	21-12-2014	5143.5-4879.4	SO237-3-4	Mn-nodule: 66 x 55 mm, irregular in shape and broken on one edge of sample. Interior is a light pink-orange coloured carbonate. Crust thickness is 4 mm. Hard to scratch surface, no individual grains of carbonate is visible. Veins of Mn in the carbonate, outlining the tracts of previous organisms.
3-1	21-12-2014	5143.5-4879.4	SO237-3-5	Mn-nodule: 65 x 53 mm. Minor vfg clay on surface of nodule. No damage to crust, interior unknown. Surface easily scratched, subrounded in shape ad surface is relatively smooth.

3-1	21-12-2014	5143.5-4879.4	SO237-3-6	Mn nodule: 59 x 45 mm. Subrounded to irregular in shape. Mn crust is 3 mm in thickness. Crust is broken on edge of sample. Light pink carbonate inside with no visible grains. Mn veining
3-1	21-12-2014	5143.5-4879.4	SO237-3-7	Mn-nodule: 58 x 47 mm. Small piece broken off of edge of sample. Crust is ~1mm thick. Rough surface and easily scratched. Fg clay on surface (white in colour). Sample is subrounded
3-1	21-12-2014	5143.5-4879.4	SO237-3-8	Mn-nodule: 60 x 49 mm. Subrounded in shape and smooth on the surface. Minor damage tot he crust, but the interior is still unknown (weight suggests carbonate). Some fg clay on surface, and easily scratched.
3-1	21-12-2014	5143.5-4879.4	SO237-3-9	Mn-nodule: 77 x 65 mm, irregular in shape but smooth on the surface. Minor damage to crust but the interior is unknown. Clay present on the surface.
3-1	21-12-2014	5143.5-4879.4	SO237-3-10	Mn-nodule: 77 x 60 mm. Subrouded with rough surface. Irregularities on the surface (small bumps). Interior composition is unknown, and minor fg clay is present on the surface.
3-1	21-12-2014	5143.5-4879.4	SO237-3-11	Mn-nodule: 98 x 72 mm. Rounded (looks like a potato). Rough surface, minor damage but interior composition is still unknown. Pink and white vfg clay on the surface of the nodule. Too fg to differentiate the mineralogy.
3-1	21-12-2014	5143.5-4879.4	SO237-3-12	Mn-nodule: 126 x 171 mm. Irregular in shape and flat. Rough surface with holes (but not vesicles). Small piece broken, carbonate inside. Fg clay on surface (white and pink in colour). Thickness of crust 3 mm. Minor pockets of clay on the surface.

3-1	21-12-2014	5143.5-4879.4	SO237-3-13	Fragment of Mn-crust (possibly minor pillow basalt attached). ~18 mm thick and 112 x 70 mm. Layering observed of varying thickness. Honeycomb texture on small surface of one layer. Thin layer of sediment, fg, light pink to orange in colour.
3-1	21-12-2014	5143.5-4879.4	SO237-3-14	Brown, vfg (no crystals observed on the surface). Composition unknown. Very thin dark brown crust on surface, assumed to be Mn. Some vesicles, <1%. Easy to scratch the thin Mn crust. The main component of sample is hard to scratch. After CUT: relatively fresh vesicular basalt. A thin alteration around the sample is evident by a change is colour, ~ 3mm thick, and goes around ~1/2 of the sample. Phenocrysts of clinopyroxene and olivine appear to have been altered to a secondary phase (unknown)
3-1	21-12-2014	5143.5-4879.4	SO237-3-15	Mn-nodule fragment: 160 x 126 mm. Crust thickness = 9 mm in upper section and 4 mm in lower section. This provides an up direction, as the thin side will have been on the seafloor. Smooth surface. Interior is a fine grain mud, very soft, vfg, with ~15% Mn veining.
3-1	21-12-2014	5143.5-4879.4	SO237-3-16	Mn-nodule fragment: 150 x 100 mm. Lot's of Mn veins and Mn coated tracts of previous organisms. Tubes ~6 mm, up to 15 mm, in diameter. Smooth surface with some bumps. Lot's of tubes lined with Mn. Fg clay, pink, no discernable grains.

3-1	21-12-2014	5143.5-4879.4	SO237-3-17	Mn-crust: interior is a soft mud/carbonate. Mn crust is ~4 mm, 220 x 140 mm. No observable layering in the crust. Glass MAY be present.
3-1	21-12-2014	5143.5-4879.4	SO237-3-18	Mn-nodule: 195 x 160 mm. Relatively flat, black, smooth. A dark black layer on top of a dark brown layer. Dark brown is slightly harder to scratch. Carbonate with fragments of light green/yellow fg hard pieces (~1 cm^3, possibly highly altered basalt). After CUT: History of rock formation was visible. 1. Pillow basalt broke and fragmented. 2. Alteration of pillow basalt fragments by alteration rims caused by several million years of interaction with fluids. No protolith remains, yellow/brown, easy to scratch. 3. Sediments from the basalts cemented the fragments together. 4. Mn event occurred depositing a thin crust. 5. Tectonic activity broke up the crust and moved some basalt fragments. 6. Carbonate formation and Mn crust was the final stage.
3-1	21-12-2014	5143.5-4879.4	SO237-3-19	Mn-nodule: rounded, rough surface. Interior unknown as it is all covered in Mn. 105 x 84 mm.
3-1	21-12-2014	5143.5-4879.4	SO237-3-20	Flat Mn-nodule: 236 x 200 mm, much heavier than other nodules. Same black surface as others, relatively smooth, overlying a dark brown crust. Some sediment remains on surface, vfg.
3-1	21-12-2014	5143.5-4879.4	SO237-3-21	Mn-crust fragment: 241 x 181 x 94 mm. Very heavy, rough surface,

				fragment of carbonate present on the surface (~ 2 cm^3)
3-1	21-12-2014	5143.5-4879.4	SO237-3-22	Large sample has been broken into several pieces and stored in 3 separate bags labelled 22 a/b/c. Carbonate fragments present of varying levels of hardness. Some pieces are lightly iridescent (possibly glass fragments). Some samples have been cut and show interesting features.

5-1	29-12-2014	5537.2-5004.7	Refer to Appendix C.	**BASALT:** Samples of lavas and sheeted dikes have been collected. However exact locations cannot be determined, so they have all been classified as basalts. The samples are variable in the modal abundance of phenocrysts and vesicles, but mineralogically appear to be similar to one another. Phenocrysts range in abundance from 5-45%, range in size from <1-4mm, and are variably altered. Secondary mineralogy is difficult to determine, but the primary phases appear to include olivine, clinopyroxene, and plagioclase. Most vesicles are in-filled with a secondary phase, possibly zeolites that are either red or white in colour. Most often the basalt samples are badly altered and now have a red colouring, however a few samples do show areas where fresh basalt may still be present (dark grey in colour. Further analysis by thin section will be needed to understand exactly what minerals are present and to what degree these samples have been altered.

5-1	29-12-2014	5537.2-5004.7	Refer to Appendix C.	**GABBRO:** One large sample was collected of a heavily altered gabbro. Almost no primary minerals remain (from initial observations). Large crystals, up to 5 cm in length, have been altered to an unknown secondary phase (red in colour, crystalline, and hard). Further analysis on land is required to understand the secondary mineralogy. Two small samples of gabbro (1 may not be gabbro, but hard to differentiate at this time). These are coarse grained, heavily altered samples. One sample (SO237-5-46) has distinct crystals, possibly clinopyroxene and plagioclase, however the degree of alteration is unknown. All gabbros collected need to be made into thin sections and analyzed further.
5-1	29-12-2014	5537.2-5004.7	Refer to Appendix C.	**SEDIMENTARY:** SO237-5-22 sandstone with sharp contact between a fg sand (<1/8 mm in size) and a coarse grain sand (varies between ½ - 2 mm in size). Red/orange in colour, no structures visible. SO237-5-17 siltstone, still slightly rough so not a mudstone, grey/tan in colour with fine interlayered beds of black organic matter. No visible structures (e.g. Waves, burrows, etc.).
5-1	29-12-2014	5537.2-5004.7	Refer to Appendix C.	**BRECCIA:** SO237-5-2 mudstone matrix, clast supported breccia. Fragments of basalt, carbonate, and sandstone range in size from 1-30 mm. Mn-crust on the surface, 2mm thick. SO237-5-40 green mudstone matrix, clast supported breccia. Clasts range from 1-40 mm and are composed of highly altered basalt and sandstone. Thin Mn-crust on surface, 2-3 mm in thickness.

5-1	29-12-2014	5537.2-5004.7	Refer to Appendix C.	**MN-CRUST/NODULES/CARBONATES:** **A** few samples of Mn-crust were collected. Fine grain, black, light in weight. Some show layering, but not a significant amount. SO237-5-10 Mn-nodule had a fragment of basalt as a nucleus, but some carbonate. Crust was ~7mm thick. 1 bag is labelled Mn-nodules and contains a variety of nodules, some heavier than others. SO237-5-49 was a large Mn-nodule with carbonate in the center. Only a couple fragments were catalogued due to the original size of the nodule (35 cm in diameter).
7-1	03-01-2015	5063-4760	SO237-7-1	-Highly altered basalt, possibly an altered pillow (slight glassy appearance to the surface of the sample). -Distinct rim of alteration around the top edge of the sample (parallel to the glass). -Phenocrysts are variably altered (most to zeolites, very soft, white and red in colour). -Sample is heavily fractured, which is why it is so altered.
7-1	03-01-2015	5063-4760	SO237-7-2	-Vfg basalt. -Only a few phenocrysts present (~1% modal abundance). -Sample is relatively fresh (especially compared to dredge 2, SO237-5). -Some fracturing visible. -Secondary mineralogy is difficult to differentiate, possibly zeolites (soft and variable colours), nothing suggesting chlorite or amphibole. -Initial observations suggest that cpx has been predominantly altered (however thin section will be needed to confirm).

7-1	03-01-2015	5063-4760	SO237-7-3	-Fg basalt. -Phenocrysts present, ranging from 1-3mm (plagioclase and clinopyroxene, but further analysis needs to be conducted). Variably altered, and not abundant in the sample (<5% modal abundance). -Only sample collected with breccia and Mn-crust on the surface. The breccia is clast supported, with fragments of highly altered basalt. -Few phenocrysts present of unknown secondary phase (primary may be clinopyroxene). -Center of sample is brown in colour, but only the center. Reason unknown.
7-1	03-01-2015	5063-4760	SO237-7-4	-Fg basalt, similar to sample SO237-7-5. -Less fractured than SO237-7-5, most fractures in filled with vfg unknown mineral, hard to scratch. -Distinct alteration rim all around the edge. -~5% vesicles (in filled) and 25% phenocrysts. -Phenocrysts are variably altered and range in size from <1-4 mm. -the secondary phases present are unknown, and further analysis with thin sections is required.
7-1	03-01-2015	5063-4760	SO237-7-5	-Fg basalt. -Abundant phenocrysts (25% modal abundance) of plagioclase and clinopyroxene, with varying degrees of alteration. Range in size from <1 mm to 5 mm. -A few in filled vesicles present (red and white zeolites, soft to scratch). -Sample is heavily fractured, in filled with unknown precipitated minerals (too fine grain to observe, and hard to scratch). Some fractures are in filled with red mud, very soft.
8-5	07-01-2015	5176	SO237-8-1-GC5	Serpentinite fragments collected from the gravity corer. The gravity corer returned back empty except for 5 rock fragments. They are pebble size (~1-2

				cm) and highly magnetic (except for one sample). Dark grey/green/black in colour.
9-2	11-01-2015	5050-4925	SO237-9-EBS1-1	Mn-nodules: 100's of Mn-nodules were collected during an EBS deployment. They vary in size (3-15 cm in diameter) and weight, however every sample that was cut was an actual Mn-nodule (was not full of carbonate). The nucleus of each nodule varies from sediment to carbonate. Some samples the nucleus is unknown due to the size of the material (too small to determine). One sample cut had a piece of basalt (~2 cm in size) as the nucleus.
9-2	11-01-2015	5050-4925	SO237-9-EBS2-1	Mn-crusts: thin crust (broken into pieces) was collected during EBS 2 deployment. ~0.8cm in thickness, dark grey in colour. One side is oxidized (red in colour) possibly suggesting that side was lying directly on the sediment.

C. Dredge Station 5-1 Sample numbers and storage locations

Sample Number	Rock Type	Box #
SO237-5-1	basalt	1
SO237-5-2	basalt	1
SO237-5-3	basalt	2
SO237-5-4	Mn-crust	1
SO237-5-5	basalt	2
SO237-5-6	basalt	1
SO237-5-7	basalt	2
SO237-5-8	basalt	2
SO237-5-9	basalt	2
SO237-5-10	Mn-crust	1
SO237-5-11	basalt	1
SO237-5-12	basalt	2
SO237-5-13	basalt	2
SO237-5-14	basalt	2
SO237-5-15	basalt	1
SO237-5-16	basalt	1
SO237-5-17	sandstone	1
SO237-5-18	basalt	2
SO237-5-19	basalt	1
SO237-5-20	basalt	2
SO237-5-21	basalt	2
SO237-5-22	sandstone	1
SO237-5-23	basalt	2
SO237-5-24	basalt	2
SO237-5-25	basalt	1
SO237-5-26	basalt	2
SO237-5-27	basalt	2
SO237-5-28	basalt	2
SO237-5-29	basalt	2
SO237-5-30	basalt	2
SO237-5-31	basalt	1
SO237-5-32	basalt	2
SO237-5-33	Mn-nodule	2
SO237-5-34	basalt	1
SO237-5-35	basalt	2
SO237-5-36	basalt	2
SO237-5-37	basalt	2
SO237-5-38	basalt	1
SO237-5-39	basalt	1
SO237-5-40	basalt	1

SO237-5-41	basalt	1
SO237-5-42	basalt	1
SO237-5-43	basalt	2
SO237-5-44	basalt	2
SO237-5-45	breccia	1
SO237-5-46	breccia	1
SO237-5-47	carbonate	1
SO237-5-48	gabbro	4
SO237-5-49	large Mn-nodule/carbonate	1

D. Dredge sample photos

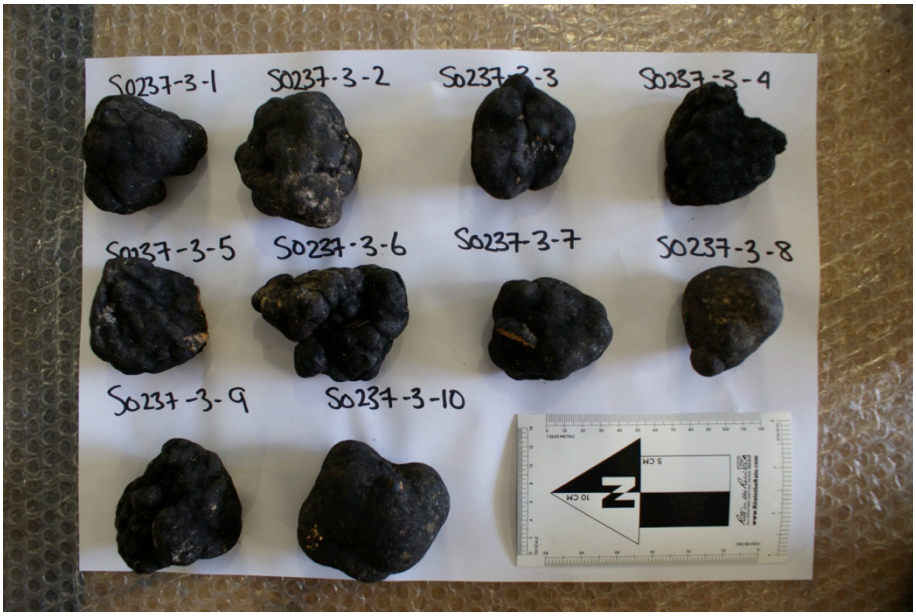

Figure D-1: Samples SO237-3-1 to 10 of Mn-nodules filled with carbonate from station 3-1.

Figure D-2: SO237-3-15, piece of a large Mn-nodule. Filled with pink carbonates and covered in ~1 cm of Mn. Black colouring on the pink carbonate is residue from the Mn. Sample from station 3-1.

Figure D-3: Sample SO237-5-15. Representative sample of fresh basalt from station 5-1.

Figure D-4: Sample SO237-5-19. Representative sample of basalt from station 5-1. Basalt has become altered, slightly red in colour and the phenocrysts have been >70% altered to a secondary phase.

Figure D-5: Sample SO237-7-4 from station 7-1. Fresh basalt, most samples were equally as fresh.

Figure D-6: Samples SO237-9-EBS1-4, 5, 6, and 9. Representative samples of the Mn-nodules collected during EBS deployment 1 at station 9.

Figure D-7: Sample SO237-9-EBS2-1. Mn-crusts collected during EBS deployment 2 and station 9. The red oxidization may suggest that side of the crusts was on the sediment surface.

E. List of water bottles closed during CTD casts

Station 1-1	
Bottle number	**Depth (m)**
1	4750
2	4749
3	4749
4	4750
5	4751
6	4751
7	4750
8	4749
9	4749
10	4750
11	4751
12	998
13	997
14	250
15	249
16	21
17	20
18	12
19	11
20	10
21	10
22	9
23	6
Station 4-11	
Bottle number	**Depth (m)**
1 – 24	12
Station 8-8	
Bottle number	**Depth (m)**
1	5127
2	5126
3	5127
4	5129
5	5130
6	5129
7	5127
8	5127
9	5127
10	5128
11	5129
12	5128
13	5128
14	5129
15	18
16	19
17	19

18	19
19	18
20	18
21	18
22	18
23	19
24	18

F. Morphospecies and their to date sorted abundances per EBS deployment along the Vema Transform transect. Stations marked with * are incomplete.

Class	Morphospecies	02_06*	02_07	04_08	04_09*	06_07*	06_08*	08_04*	09_02	09_08*	11_01	11_04*
Caudofoveata												
	Caudofoveata sp. 1	1										
	Caudofoveata sp. 2	2	6	15	3							
	Caudofoveata sp. 3		5		1	4	2					
Solenogastres												
	Solenogastres sp. 1		3			1	3		3	3		
	Solenogastres sp. 2		2	1	2	2	5			3	1	3
	Solenogastres sp. 3			2	1					2		
	Solenogastres sp. 4			2								
Scaphopoda												
	Siphonodentaliidae sp. 1			18	9		1	3		1		
	Siphonodentaliidae sp. 2			2		3					1	
	Pulseliidae sp.		7	85	27	2	1	1			1	
	Dentaliidae sp.			62	4	7						
Gastropoda												
	Mesogastropoda sp. 1	1										
	cf. Scaphandridae sp.			2								
	Mesogastropoda sp. 2			1		3						
	cf. Brookula sp.									1		
	Buccinoidea sp.											
	cf. Epitoniidae sp.							1				
	Rissoidea sp.								1			1
	cf. Trochoidea sp.									1		
Bivalvia												
	cf. *Neionella* sp	2		12		1	1			1	1	
	Ledella sp.			21		1		1		9	3	
	Yoldiella sp.				1	2				1		
	Malletia sp.			12	10	8	9	26	1	3	1	1
	Silicula sp.			5		5	1					
	Limopsis sp.		1									
	Dacrydium sp.	2	4	2	1	11	11	8	1		1	
	Limatula sp.					2		4		3	1	3
	cf. *Cyclopecten* sp. 1	1										
	cf. *Cyclopecten* sp. 2						1					
	Thyasiridae sp.								1			
	cf. Tellinidae sp.		1			3				1		
	Kelliella sp.	3	2	1	2	3	2	1				
	Cuspidaria sp. 1	1	5	1		3	3			1	1	
	Cuspidaria sp. 2										1	
	Cuspidaria sp. 3		3			5	7					
	SUM (Specimens)	13	39	244	61	66	47	45	7	30	12	8
	SUM (Morphospecies)	8	11	17	11	20	13	8	5	13	10	4

G. AUV Abyss Mission Summaries

Station 2-1 / Dive Abyss0160 / Area A1
Date: 19th Dec. 2014 Launch: 08:35 UTC Recovery: 02:00 UTC
Survey time: 9.7 hours Distance travelled: 74.4 km
Sensors: Multibeam Sonar 200 kHz, Microstructure Probe (MSS)

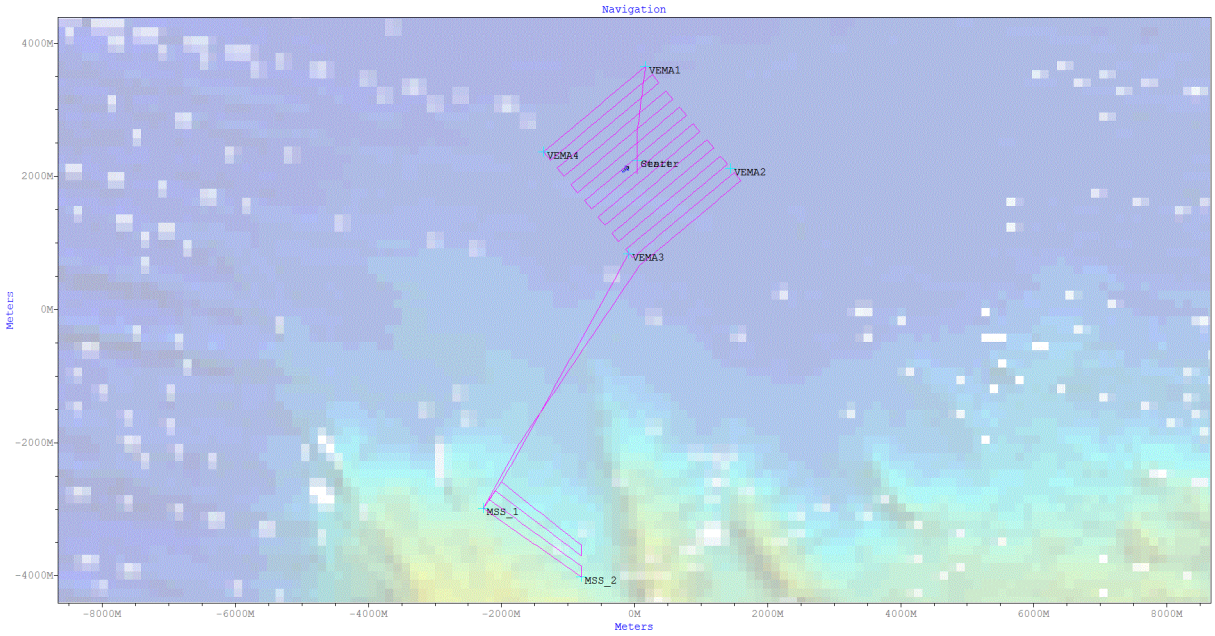

Figure 11-1: Dive plan of mission 160

Mission 160 was the only mission with mounted MSS and was planned in two separate phases (Figure 11-1). The northern survey pattern was to map (multibeam 200 kHz; range 200 m; line spacing 160 m; coverage 1km^2/hour) the sedimented area where the following ship-based sampling should be done. The southern pattern was prepared for MSS data. It was planned in two four-leg-surveys lying upon another with fixed depth instead of bottom following with a set altitude. The lower survey pattern additionally was used to map (multibeam 200 kHz; range 200 m, see Figure 11-2) and was flown in depths between 5020 and 5120 m. The multibeam wasn't logging during the higher survey pattern where the vehicle flew between 5240 and 5340 m depth.

One of the two housing of the MSS were leaking though the whole mission. The replay of the dive showed a ground fault of 100% just after the descent phase. The 100% pointed on a short circuit between the full battery-power and the ground.

The vehicle recovery was done during the night. While trying to grab the rope of the recovery float the vehicle came to close to the stern and was undertowed under the stern. It took several approaches and at least one hour to retrieve the vehicle. The vehicle lost the nose segment, the security guard of the antenna and the top transducers were bent and the MSS including their outrigger were damaged seriously. The lose outrigger damaged parts of the coating of the new nose foam segment. A general check-out showed no impairment of function.

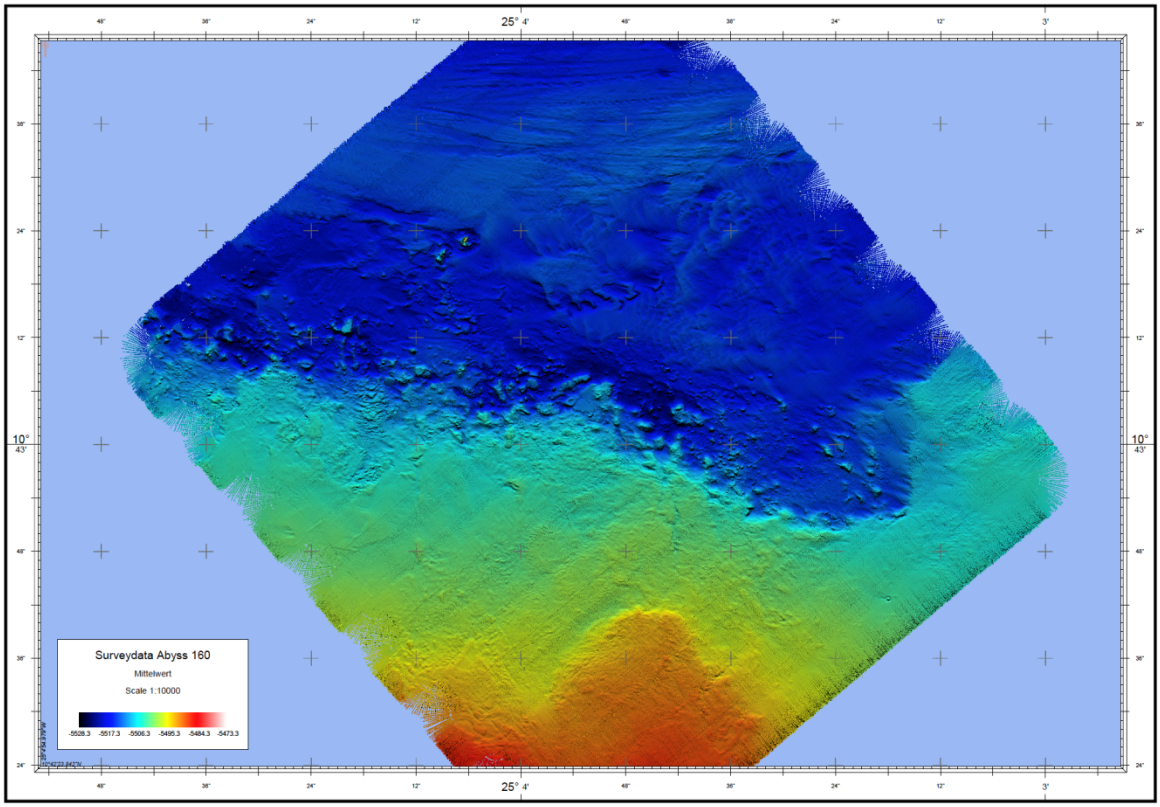

Figure 11-2: Bathymetric map of the survey pattern in the valley

Station 4-1 / Dive Abyss0161 / Area A2

Date: 25th Dec. 2014 Launch: 22:25 UTC Recovery: 15:01 UTC
Survey time: - hours Distance travelled: 26.1 km

Mission 161 aborted just before the vehicle reached the programmed depth after the descent phase. The vehicle could not reach a sufficient pitch to achieve a vertical speed that was needed to finish the descend phase within the time-out-window. The reason was probably a combination of a too lightweight nose and not enough propeller revolution.

The planned mission 161 was repeated in dive 162.

Station 4-7 / Dive Abyss0162 / Area A2

Date: 26th Dec. 2014 Launch: 20:20 UTC Recovery: 15:27 UTC
Survey time: 12.8 hours Distance travelled: 87.7 km
Sensors: Multibeam Sonar 200 kHz, Redox sensor

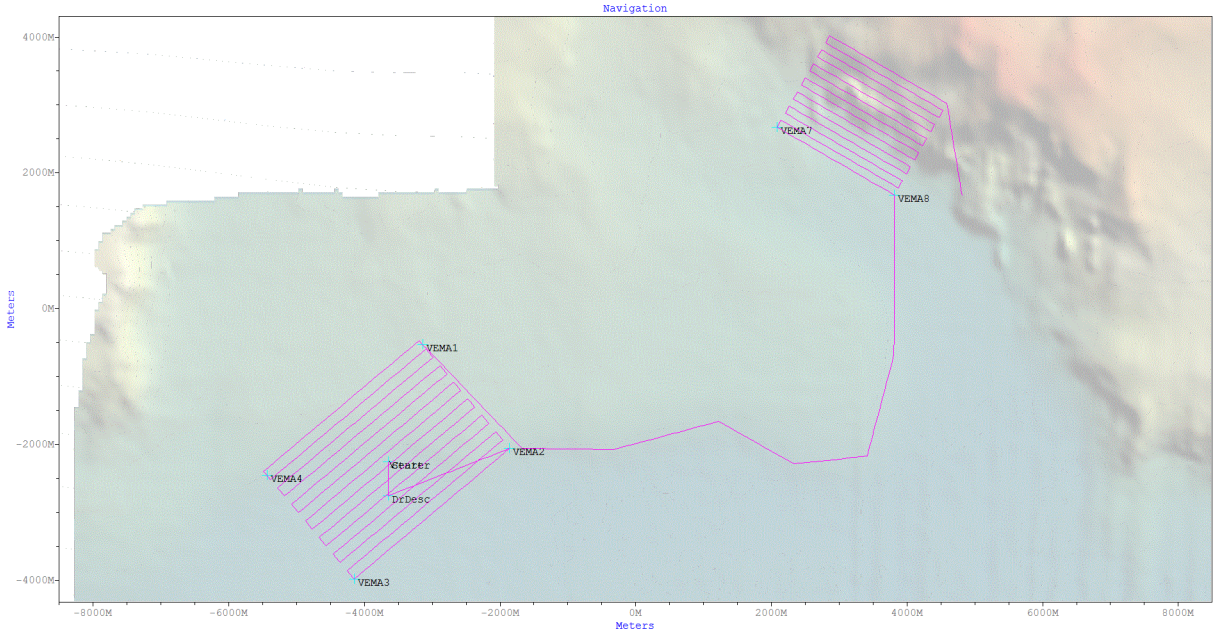

Figure 11-3: Dive plan of mission 162

Mission 162 (see Figure 11-3) was to map the sedimented plain in the first phase, where the ship-based sampling took place, and should find the transition between valley floor and slope structure in an area north-east of the first one in the last phase. On the transit to the second survey pattern the vehicle followed a border that could be seen in the ship-based map. The chosen multibeam settings for all phases including transit were almost identical (range 220 m, altitude 80 m, line spacing 160 m). During the survey pattern above the slope a line spacing of 120 m were set to make sure a sufficient overlap. The logged multibeam raw data were noisier than in dive 160, probably caused by the differences in the sediment structure. The vehicle achieve an average coverage of 1 km^2/hour.

The mapping survey above the slope couldn't be finish since the battery reached a capacity of less than 5% and the vehicle aborted the mission and came up. The maps generated are shown in Figure 11-4 and Figure 11-5.

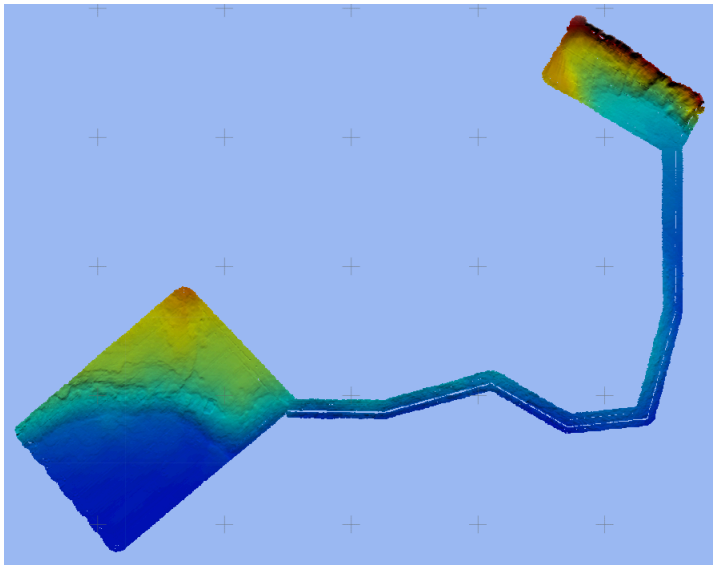

Figure 11-4: Bathymetric map of dive 162

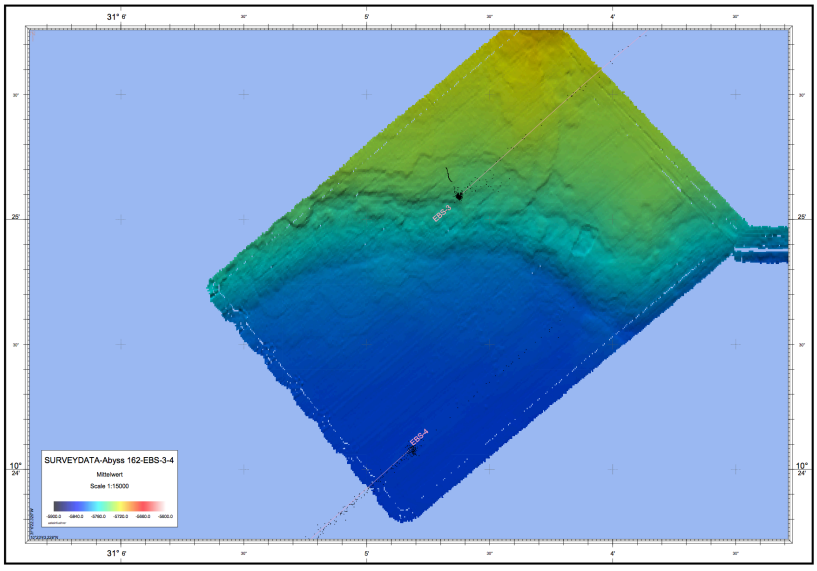

Figure 11-5: Map of the sedimented valley

Station 6-2 / Dive Abyss0163 / Area A3

Date: 1st Jan. 2015 Launch: 21:05 UTC Recovery: 14:02 UTC
Survey time: 10.9 hours Distance travelled: 81.7 km
Sensors: Sidescan Sonar 410 kHz, Electronic Still Camera, Redox sensor

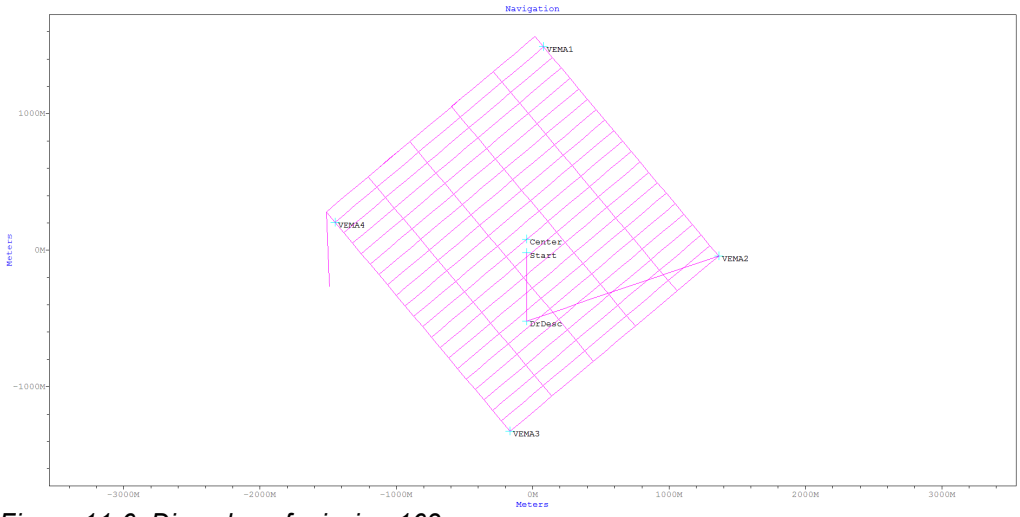

Figure 11-6: Dive plan of mission 163

Mission 163 was the first dive in camera configuration (9230 images) and consisted of 2 altitude layers on top of each other (see Figure 11-6). The first part of the dive was flown on an altitude of 10 meters to gather sidescan data and images of the seafloor. The survey pattern was built mainly for the high-frequency sidescan map (line spacing: 100 m; sidescan range: 100 m). That is why the images have no across-track overlap mosaic (seafloor representation on images: 7x7 meters). The higher survey pattern proceeded on a fix altitude of 40 meters with a corresponding sidescan range of 400 meters and a line spacing between the northwest bound legs of as well 400 meters. The mission itself proceeded without unforeseen occurrences. The ship-based monitoring station (via Acomms bottle and Shipboard Console) couldn't receive messages from the vehicle due to a battery issue on the modem board.

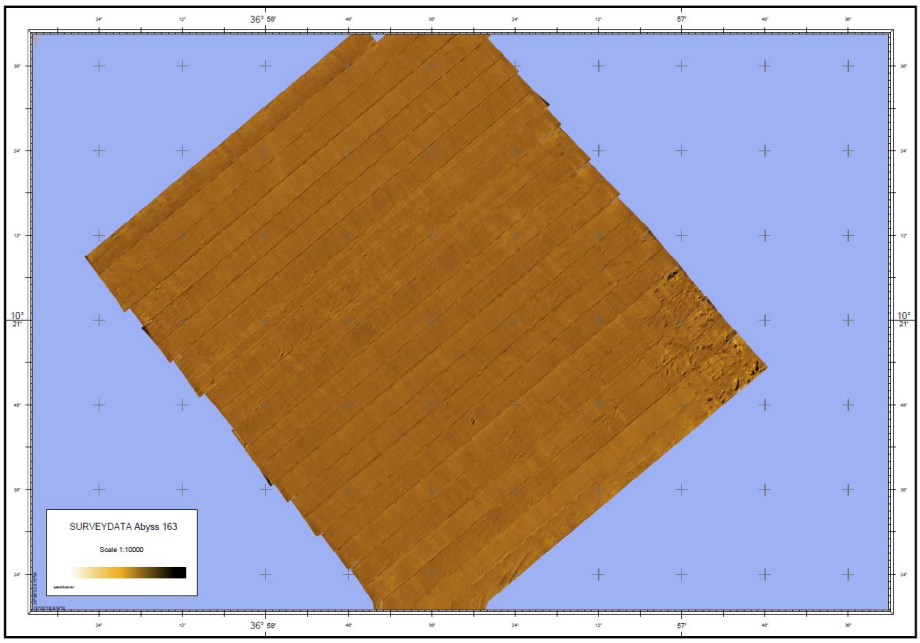

Figure 11-7: Sidescan map of mission 163 (coverage 0.5 km^2/h at the given range and line spacing)

Station 9-1 / Dive Abyss0164 / Area B1

Date: 11th Jan. 2015 Launch: 06:23 UTC Recovery: 22:18 UTC
Survey time: 11.2 hours Distance travelled: 83.1 km
Sensors: Multibeam Sonar 200 kHz, Redox sensor

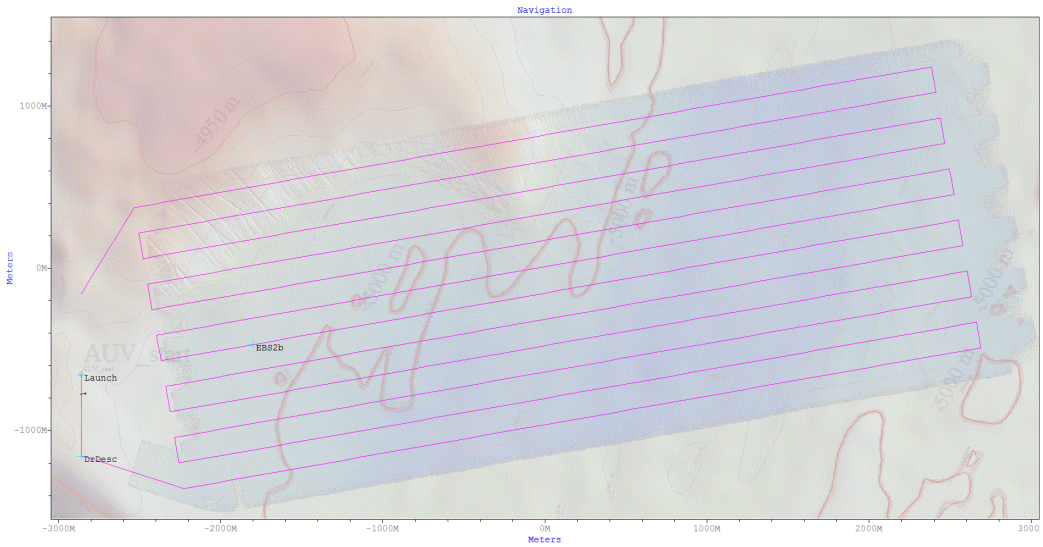

Figure 11-8: Dive plan of mission 164 based on the ships bathymetry

Mission 164 (see Figure 11-8) was to map the area of the Epibenthos Sledge (EBS) that should be deployed just after the AUV launch. Later the EBS track were moved southwards of the AUV working area that means outside of the resulting map. The mission was flown on an altitude of 80 meters with the usual 3 knots. The range of the multibeam was set to 200 m with 160 m (line spacing) between each of the 12 legs. The raw data were noisier than usual that probably was caused by the USBL (every 10 seconds). The map is shown in Figure 11-9. The mission itself proceeded without unforeseen occurrences.

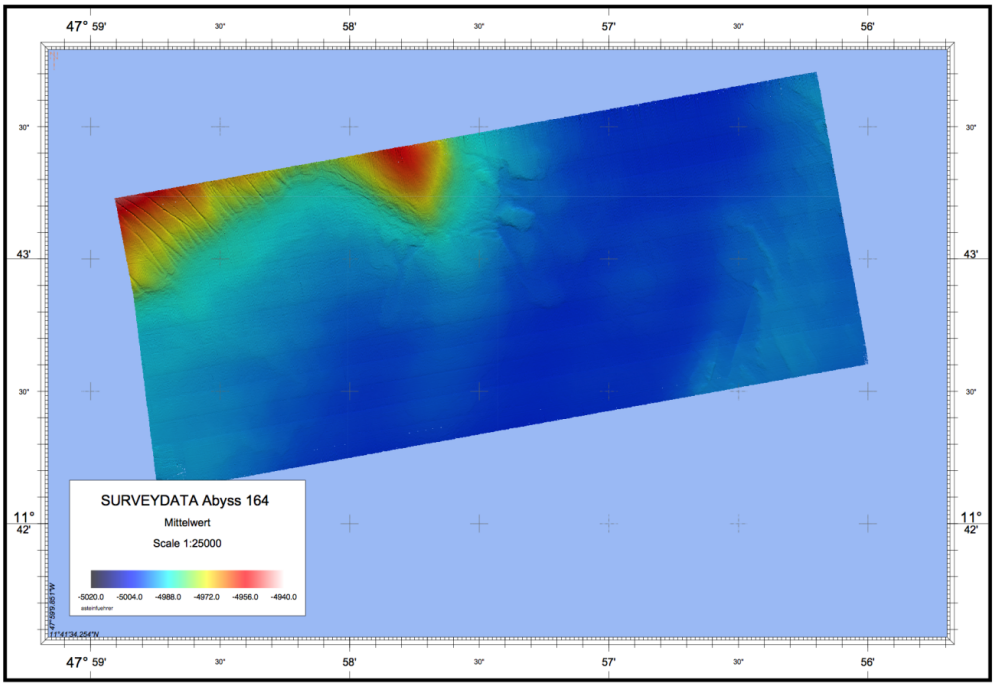

Figure 11-9: AUV bathymetry (200 kHz) of dive 164

Station 9-6 / Dive Abyss0165 / Area B1

Date: 12th Jan. 2015 Launch: 07:14 UTC Recovery: 23:01 UTC
Survey time: 9.1 hours Distance travelled: 72.4 km
Sensors: Sidescan Sonar 410 kHz, Electronic Still Camera, Redox sensor

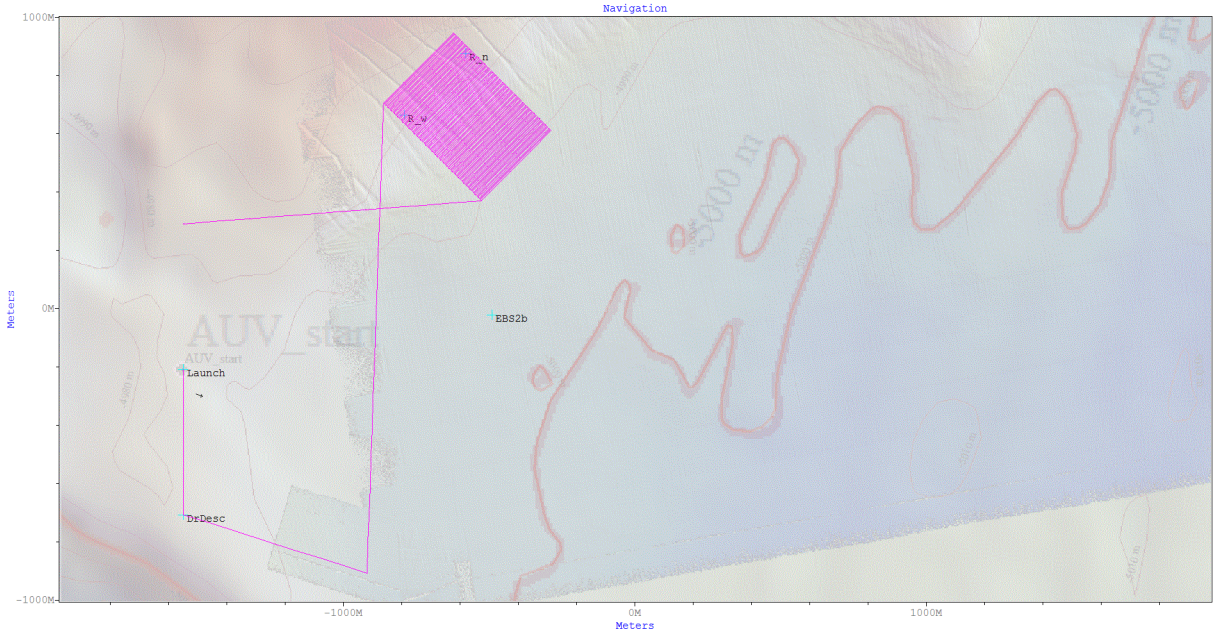

Figure 11-10: Dive plan of mission 165 based on the ships and AUV bathymetry

During dive 165 (Figure 11-10) the vehicle did a photo survey (9580 images) within the map done on dive 164 (Figure 11-9). Simultaneously the sidescan was recording (410 kHz; Range 100m; altitude 10m, results shown in Figure 11-11). The line spacing was set to 4 m to achieve a sufficient overlap for the photo mosaic (seafloor representation on images: 7x7 meters). Launch and surface position were the same as for dive 164. The mission proceeded without unforeseen occurrences. The mission was to gather details about the stream channels which can be seen in the AUV-based map of dive 164 (NW corner of Figure 11-9). The Redox data set showed anomalies on several positions (Figure 11-12 and Figure 11-13).

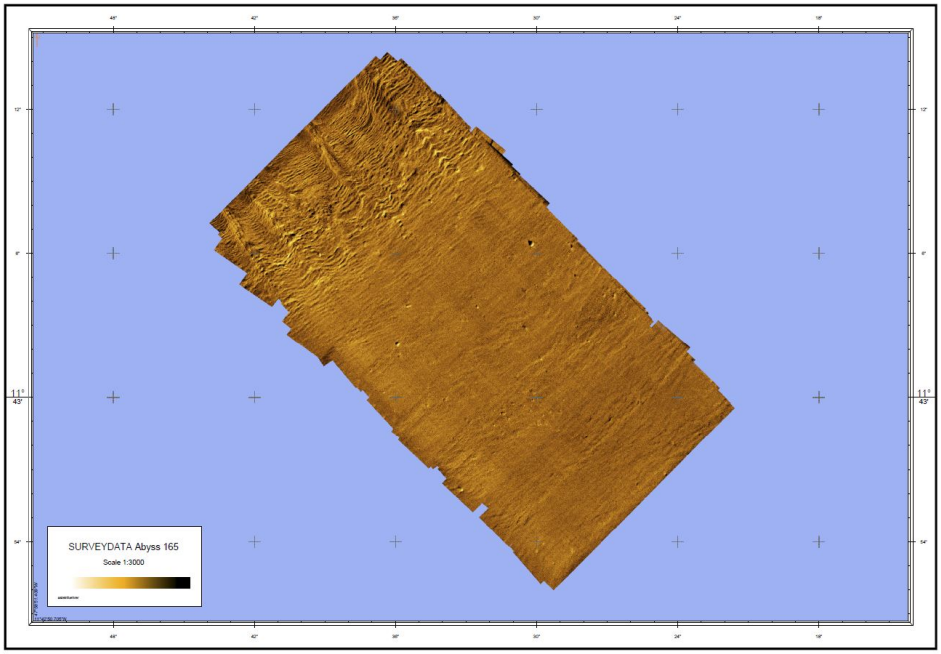

Figure 11-11: Sidescan map (410 kHz) of the surveyed area 165

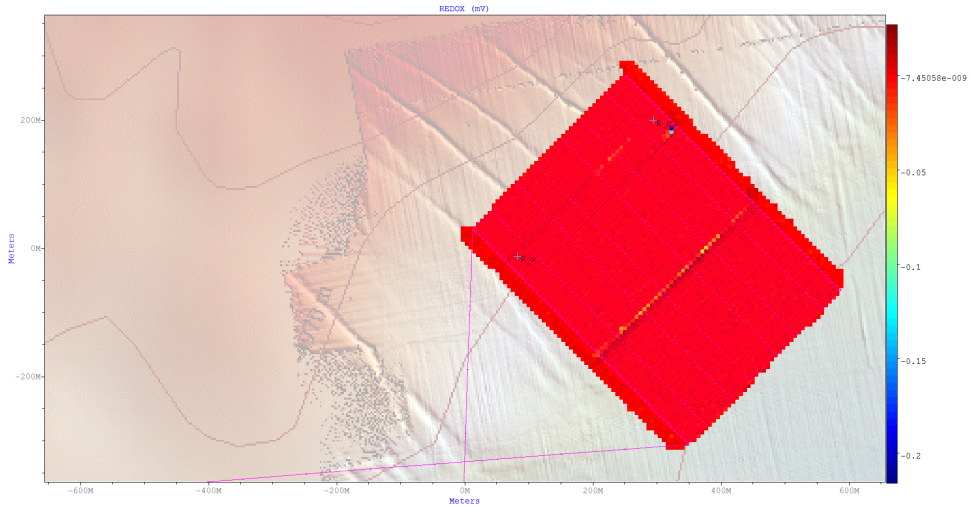

Figure 11-12: Redox anomalies were logged on several legs (red - no anomaly)

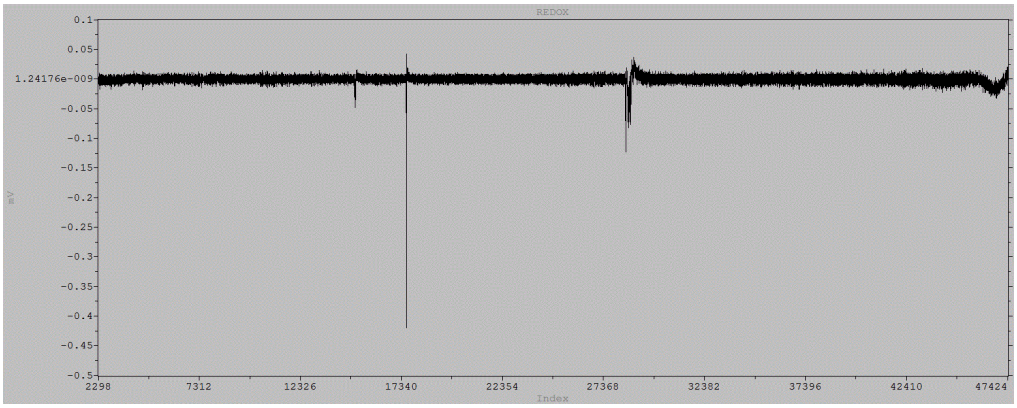

Figure 11-13: Redox data plotted against Mission Time (Linear Plot)

Station 11-3 / Dive Abyss0166 / Area B2

Date: 14th/15th Jan. 2015Launch: 13:57 UTC Recovery: 11:40 UTC
Survey time: 16.1 hours Distance travelled: 111.5 km
Sensors: Sidecan Sonar 120/410 kHz, Electronic Still Camera, Redox sensor

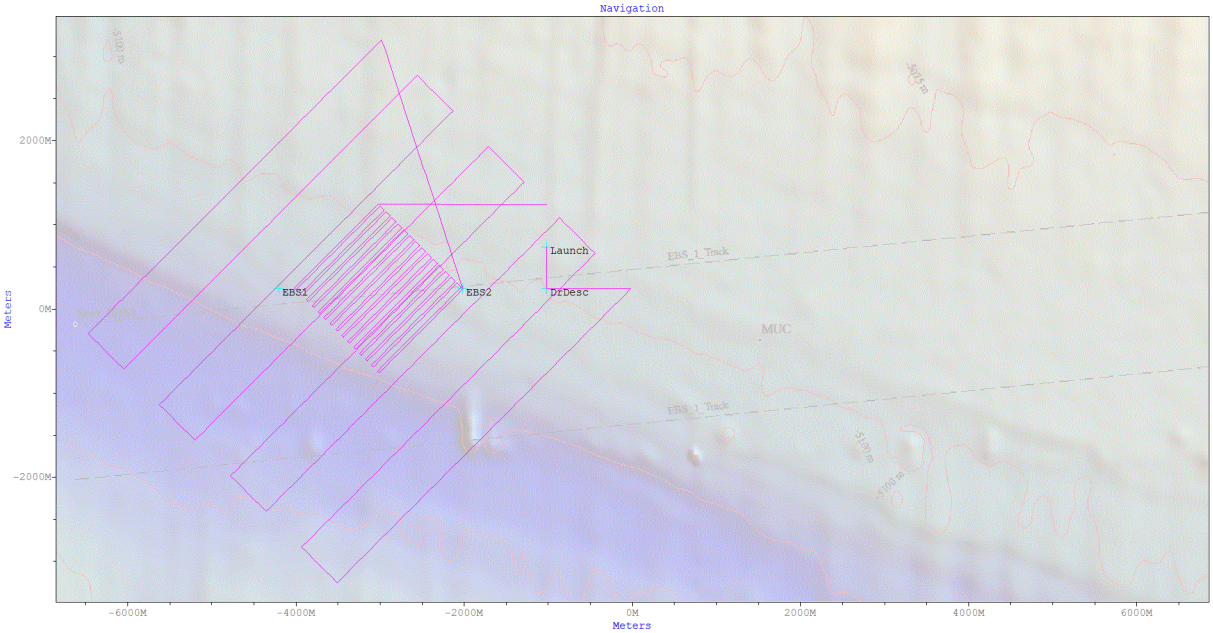

Figure 11-14: Dive plan of mission 166 based on the ships bathymetry

Mission 166 was the only AUV dive in area B2 and was started just after the EBS deployment. The dive was planned in two separate phases (Figure 11-14). At first 8 bottom following legs at an altitude of 60 meters using 120 kHz sidescan (Range: 600 meters, for results see Figure 11-15). Simultaneously to the first part of the dive the Epibenthos sledge (EBS) was towed on the southern track as shown in Figure 11-14. For the second step the vehicle reduced the altitude to 10 meters and changed the sidescan frequency to 410 kHz (Range: alternating 30/70 meters). While diving in phase two the vehicle was to map the area by using sidescan and camera (8140 images) where the first EBS was towed through - the EBS-track was indeed intercepted at several places (see, e.g., Figure 11-16).

The AUV lost bottom lock on leg 14 and 15 of the small survey pattern (leg 1 is the most south-east leg) due to a DVL failure. That meant during this time neither images nor sidescan data were recorded. The vehicle reset the DVL and it slowly came back to the programmed altitude. After this break the dive proceeded as planned and reached the surface position. While the vehicle were ascending an abort happened due to a battery capacity less than 5 %.

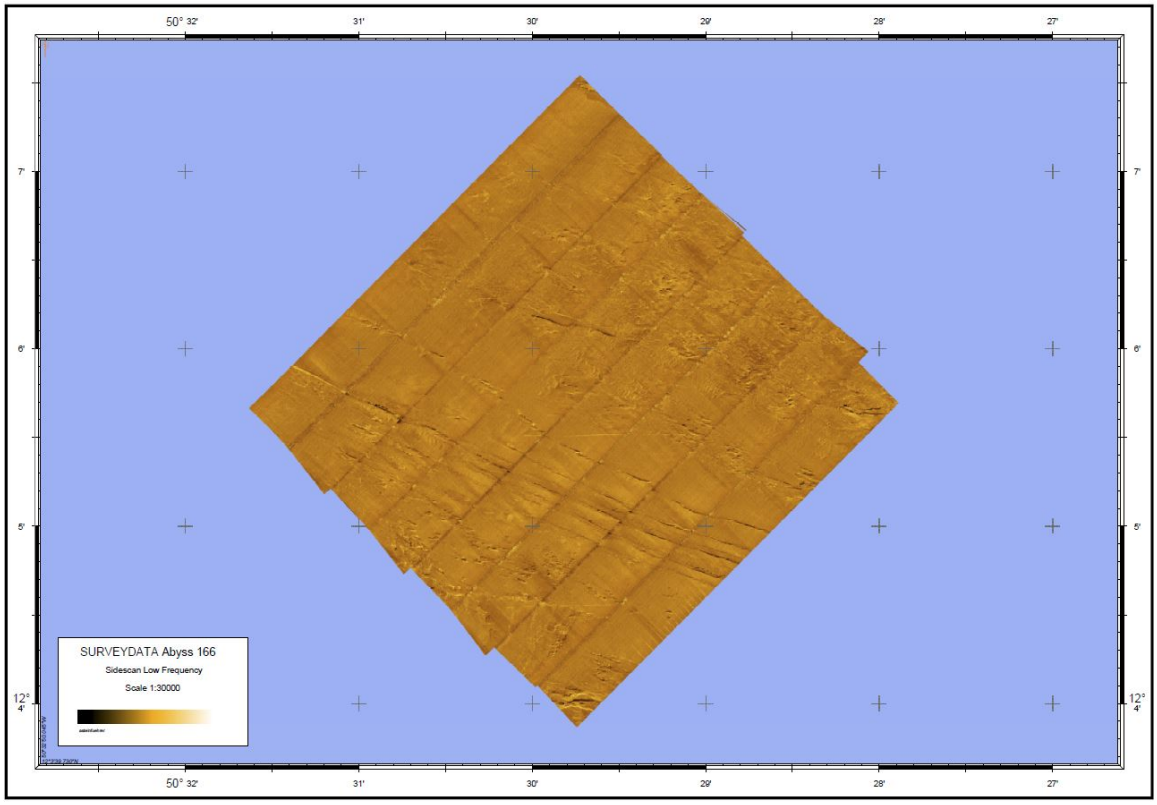

Figure 11-15: Sidescan Map (120 kHz) of the survey area dive 166

Figure 11-16: Image 2618 of AUV dive 166 with track of the Epibenthos sledge (EBS)

GEOMAR
Helmholtz-Zentrum für Ozeanforschung Kiel

GEOMAR Reports

No.	Title
1	FS POSEIDON Fahrtbericht / Cruise Report POS421, 08. – 18.11.2011, Kiel - Las Palmas, Ed.: T.J. Müller, 26 pp, DOI: 10.3289/GEOMAR_REP_NS_1_2012
2	Nitrous Oxide Time Series Measurements off Peru – A Collaboration between SFB 754 and IMARPE –, Annual Report 2011, Eds.: Baustian, T., M. Graco, H.W. Bange, G. Flores, J. Ledesma, M. Sarmiento, V. Leon, C. Robles, O. Moron, 20 pp, DOI: 10.3289/GEOMAR_REP_NS_2_2012
3	FS POSEIDON Fahrtbericht / Cruise Report POS427 – Fluid emissions from mud volcanoes, cold seeps and fluid circulation at the Don-_Kuban deep sea fan (Kerch peninsula, Crimea, Black Sea) – 23.02. – 19.03.2012, Burgas, Bulgaria - Heraklion, Greece, Ed.: J. Bialas, 32 pp, DOI: 10.3289/GEOMAR_REP_NS_3_2012
4	RV CELTIC EXPLORER EUROFLEETS Cruise Report, CE12010 – ECO2@NorthSea, 20.07. – 06.08.2012, Bremerhaven – Hamburg, Eds.: P. Linke et al., 65 pp, DOI: 10.3289/GEOMAR_REP_NS_4_2012
5	RV PELAGIA Fahrtbericht / Cruise Report 64PE350/64PE351 – JEDDAH-TRANSECT -, 08.03. – 05.04.2012, Jeddah – Jeddah, 06.04 - 22.04.2012, Jeddah – Duba, Eds.: M. Schmidt, R. Al-Farawati, A. Al-Aidaroos, B. Kürten and the shipboard scientific party, 154 pp, DOI: 10.3289/GEOMAR_REP_NS_5_2013
6	RV SONNE Fahrtbericht / Cruise Report SO225 - MANIHIKI II Leg 2 The Manihiki Plateau - Origin, Structure and Effects of Oceanic Plateaus and Pleistocene Dynamic of the West Pacific Warm Water Pool, 19.11.2012 - 06.01.2013 Suva / Fiji – Auckland / New Zealand, Eds.: R. Werner, D. Nürnberg, and F. Hauff and the shipboard scientific party, 176 pp, DOI: 10.3289/GEOMAR_REP_NS_6_2013
7	RV SONNE Fahrtbericht / Cruise Report SO226 – CHRIMP CHatham RIse Methane Pockmarks, 07.01. - 06.02.2013 / Auckland – Lyttleton & 07.02. – 01.03.2013 / Lyttleton – Wellington, Eds.: Jörg Bialas / Ingo Klaucke / Jasmin Mögeltönder, 126 pp, DOI: 10.3289/GEOMAR_REP_NS_7_2013
8	The SUGAR Toolbox - A library of numerical algorithms and data for modelling of gas hydrate systems and marine environments, Eds.: Elke Kossel, Nikolaus Bigalke, Elena Piñero, Matthias Haeckel, 168 pp, DOI: 10.3289/GEOMAR_REP_NS_8_2013
9	RV ALKOR Fahrtbericht / Cruise Report AL412, 22.03.-08.04.2013, Kiel – Kiel. Eds: Peter Linke and the shipboard scientific party, 38 pp, DOI: 10.3289/GEOMAR_REP_NS_9_2013
10	Literaturrecherche, Aus- und Bewertung der Datenbasis zur Meerforelle (*Salmo trutta trutta L.*) Grundlage für ein Projekt zur Optimierung des Meerforellenmanagements in Schleswig-Holstein. Eds.: Christoph Petereit, Thorsten Reusch, Jan Dierking, Albrecht Hahn, 158 pp, DOI: 10.3289/GEOMAR_REP_NS_10_2013
11	RV SONNE Fahrtbericht / Cruise Report SO227 TAIFLUX, 02.04. – 02.05.2013, Kaohsiung – Kaohsiung (Taiwan), Christian Berndt, 105 pp, DOI: 10.3289/GEOMAR_REP_NS_11_2013

GEOMAR
Helmholtz-Zentrum für Ozeanforschung Kiel

No.	Title
12	RV SONNE Fahrtbericht / Cruise Report SO218 SHIVA (Stratospheric Ozone: Halogens in a Varying Atmosphere), 15.-29.11.2011, Singapore - Manila, Philippines, Part 1: SO218- SHIVA Summary Report (in German), Part 2: SO218- SHIVA English reports of participating groups, Eds.: Birgit Quack & Kirstin Krüger, 119 pp, DOI: 10.3289/GEOMAR_REP_NS_12_2013
13	KIEL276 Time Series Data from Moored Current Meters. Madeira Abyssal Plain, 33°N, 22°W, 5285 m water depth, March 1980 – April 2011. Background Information and Data Compilation. Eds.: Thomas J. Müller and Joanna J. Waniek, 239 pp, DOI: 10.3289/GEOMAR_REP_NS_13_2013
14	RV POSEIDON Fahrtbericht / Cruise Report POS457: ICELAND HAZARDS Volcanic Risks from Iceland and Climate Change:The Late Quaternary to Anthropogene Development Reykjavík / Iceland – Galway / Ireland, 7.-22. August 2013. Eds.: Reinhard Werner, Dirk Nürnberg and the shipboard scientific party, 88 pp, DOI: 10.3289/GEOMAR_REP_NS_14_2014
15	RV MARIA S. MERIAN Fahrtbericht / Cruise Report MSM-34 / 1 & 2, SUGAR Site, Varna – Varna, 06.12.13 – 16.01.14. Eds: Jörg Bialas, Ingo Klaucke, Matthias Haeckel, 111 pp, DOI: 10.3289/GEOMAR_REP_NS_15_2014
16	RV POSEIDON Fahrtbericht / Cruise Report POS 442, "AUVinTYS" High-resolution geological investigations of hydrothermal sites in the Tyrrhenian Sea using the AUV "Abyss", 31.10. – 09.11.12, Messina – Messina, Ed.: Sven Petersen, 32 pp, DOI: 10.3289/GEOMAR_REP_NS_16_2014
17	RV SONNE, Fahrtbericht / Cruise Report, SO 234/1, "SPACES": Science or the Assessment of Complex Earth System Processes, 22.06. – 06.07.2014, Walvis Bay / Namibia - Durban / South Africa, Eds.: Reinhard Werner and Hans-Joachim Wagner and the shipbord scientific party, 44 pp, DOI: 10.3289/GEOMAR_REP_NS_17_2014
18	RV POSEIDON Fahrtbericht / Cruise Report POS 453 & 458, "COMM3D", Crustal Structure and Ocean Mixing observed with 3D Seismic Measurements, 20.05. – 12.06.2013 (POS453), Galway, Ireland – Vigo, Portugal, 24.09. – 17.10.2013 (POS458), Vigo, Portugal – Vigo, Portugal, Eds.: Cord Papenberg and Dirk Klaeschen, 66 pp, DOI: 10.3289/GEOMAR_REP_NS_18_2014
19	RV POSEIDON, Fahrtbericht / Cruise Report, POS469, "PANAREA", 02. – 22.05.2014, (Bari, Italy – Malaga, Spain) & Panarea shallow-water diving campaign, 10. – 19.05.2014, Ed.: Peter Linke, 55 pp, DOI: 10.3289/GEOMAR_REP_NS_19_2014
20	RV SONNE Fahrtbericht / Cruise Report SO234-2, 08.-20.07.2014, Durban, South Africa - Port Louis, Mauritius, Eds.: Kirstin Krüger, Birgit Quack and Christa Marandino, 95 pp, DOI: 10.3289/GEOMAR_REP_NS_20_2014
21	RV SONNE Fahrtbericht / Cruise Report SO235, 23.07.-07.08.2014, Port Louis, Mauritius to Malé, Maldives, Eds.: Kirstin Krüger, Birgit Quack and Christa Marandino, 76 pp, DOI: 10.3289/GEOMAR_REP_NS_21_2014

GEOMAR
Helmholtz-Zentrum für Ozeanforschung Kiel

No.	Title
22	RV SONNE Fahrtbericht / Cruise Report SO233 WALVIS II, 14.05-21.06.2014, Cape Town, South Africa - Walvis Bay, Namibia, Eds.: Kaj Hoernle, Reinhard Werner, and Carsten Luter, 153 pp, DOI: 10.3289/GEOMAR_REP_NS_22_2014

For GEOMAR Reports, please visit:
https://oceanrep.geomar.de/view/series/GEOMAR_Report.html

Reports of the former IFM-GEOMAR series can be found under:
https://oceanrep.geomar.de/view/series/IFM-GEOMAR_Report.html

GEOMAR
Helmholtz-Zentrum für Ozeanforschung Kiel

Das GEOMAR Helmholtz-Zentrum für Ozeanforschung Kiel
ist Mitglied der Helmholtz-Gemeinschaft
Deutscher Forschungszentren e.V.

The GEOMAR Helmholtz Centre for Ocean Research Kiel
is a member of the Helmholtz Association of
German Research Centres

Helmholtz-Zentrum für Ozeanforschung Kiel / Helmholtz Centre for Ocean Research Kiel
GEOMAR
Dienstgebäude Westufer / West Shore Building
Düsternbrooker Weg 20
D-24105 Kiel
Germany

Helmholtz-Zentrum für Ozeanforschung Kiel / Helmholtz Centre for Ocean Research Kiel
GEOMAR
Dienstgebäude Ostufer / East Shore Building
Wischhofstr. 1-3
D-24148 Kiel
Germany

Tel.: +49 431 600-0
Fax: +49 431 600-2805
www.geomar.de